

**SURFACTANT-MEDIATED ELECTRIC CHARGING
PHENOMENA IN NONPOLAR DISPERSIONS**

A Dissertation
Presented to
The Academic Faculty

by

Joohyung Lee

In Partial Fulfillment
of the Requirements for the Degree
Doctor of Philosophy in the
School of Chemical & Biomolecular Engineering

Georgia Institute of Technology
December 2015

COPYRIGHT © 2015 BY JOOHYUNG LEE

**SURFACTANT-MEDIATED ELECTRIC CHARGING
PHENOMENA IN NONPOLAR DISPERSIONS**

Approved by:

Dr. Sven H. Behrens, Advisor
School of Chemical & Biomolecular
Engineering
Georgia Institute of Technology

Dr. Yulin Deng
School of Chemical & Biomolecular
Engineering
Georgia Institute of Technology

Dr. J. Carson Meredith
School of Chemical & Biomolecular
Engineering
Georgia Institute of Technology

Dr. Hang Lu
School of Chemical & Biomolecular
Engineering
Georgia Institute of Technology

Dr. Alberto Fernandez-Nieves
School of Physics
Georgia Institute of Technology

Date Approved: Nov. 6, 2015

To Giyoung,

ACKNOWLEDGEMENTS

Without the enormous supports from these people, I would never have finished this tough marathon.

Above all, I would like to express my greatest appreciation to my thesis advisor Dr. Sven Behrens. As I mentioned at the final defense, he is the best scientist I know, and also, the best human being I know. It's been an honour and a privilege working for him over the past four and a half years. Perhaps, I will never be able to work with a person like him.

I sincerely thank my committee members, Dr. Yulin Deng, Dr. J. Carson Meredith, Dr. Hang Lu, and Dr. Alberto Fernandez-Nieves, for their valuable and encouraging comments on this research.

I am grateful to my collaborators: Dr. Zhang-Lin Zhou in Hewlett Packard Laboratory, for his initial help on setting up the organic synthesis lab; John Hyatt in Dr. Fernandez-Nieves lab, for his 3D Cross-Correlation DLS measurement; Benjamin Yezer in Dr. Dennis Prieve lab (Carnegie Mellon University) for his EIS measurement; Guillermo Alas in Dr. Collard lab, for his help on surfactant hydrogenation; Kathy Huggins, for her help on all administration works.

I am also very grateful to my past and current lab mates: Dr. Qiong Guo, Dr. Hongzhi Wang, Dr. Abiola Shitta, Joanna Tsao, Yi Zhang, Songcheng Wang, Xiaotang (Tony) Du, Katie Ohnemus, and Ruiyang Zhao, for their continuous supports. Wish you the very best of luck.

Many thanks to the Korean Chemical Engineering Student Association. I apologize I am not able to mention every single name. All the fun time will be missed.
다들 잘 되서 다시 만나자구. ㅎㅎ.

I thank my parents for their endless encouragement and prayer. I have always leaned on you, from childhood until now, no matter how far apart. Thank you very much for being there. Please feel free to be proud of your son, a Ph.D.

Finally, I thank my wife Giyoung Kim for *everything*. The conclusion of this thesis is that I could not do anything without her. Therefore, I dedicate this thesis to her.

지영아! 정말 고맙다. 이 200 페이지의 종이 뭉치를 들춰 볼 날이 얼마나 되겠냐만은 그래도 흘러간 노래를 들으면 예전 생각이 나는 것처럼 가끔 몇 페이지를 만지작 거리면서 우리가 이 곳에서 함께한 시간을 떠올릴 수 있다면 그걸로 정말 좋을 것 같다. 사랑해! 앞으로도 잘 살자.

TABLE OF CONTENTS

	Page
ACKNOWLEDGEMENTS	iv
LIST OF TABLES	x
LIST OF FIGURES	xi
SUMMARY	xviii
<u>CHAPTER</u>	
1 INTRODUCTION	1
1.1. Background	1
1.2. Motivation and Objectives	2
1.3. Thesis Outline	4
1.4. References	5
2 CHARACTERIZING THE ACID/BASE BEHAVIOR OF OIL-SOLUBLE SURFACTANTS AT THE INTERFACE OF NONPOLAR SOLVENTS WITH A POLAR PHASE	9
2.1. Introduction	9
2.2. Methods and Materials	13
2.2.1. Application of the van Oss-Chaudhury-Good (vOCG) Model	13
2.2.2. Surfactant Synthesis and Purification	18
2.2.3. Interfacial Tensiometry	21
2.2.4. Computational Tools	21
2.2.5. Quartz Crystal Microbalance (QCM)	21
2.3. Results and Discussions	23
2.3.1. Determination of Component Parameters for Nonpolar Samples	23

2.3.2. Component Parameters of Pure Hexane	25
2.3.3. Lewis Acid/Base Behavior of Surfactant Solutions in Contact with a Polar Phase	26
2.4. Conclusion	38
2.5. References	39
3 INVESTIGATION OF PARTICLE CHARGING WITH SYSTEMATIC VARIATION OF SURFACTANT CHEMISTRY	43
3.1. Introduction	43
3.2. Materials and Methods	45
3.2.1. Surfactant Synthesis and Purification	45
3.2.2. Preparation of Particle Dispersions (“Solvent Swap”)	46
3.2.3. Electrophoresis	46
3.2.4. Dynamic Light Scattering	47
3.2.5. Karl Fischer Titration	47
3.2.6. Conductivity	48
3.3. Results and Discussions	48
3.3.1. Electrophoretic Particle Mobility	48
3.3.2. Interpretation in Terms of Acid-Base Interaction between Particles and Surfactants	53
3.3.3. Interpretation in Terms of Inverse Micellar Ion Adsorption	58
3.3.4. Surface Charging of the PMMA Particles	71
3.4. Conclusion	75
3.5. References	76
4 INVESTIGATION OF PARTICLE CHARGING WITH SYSTEMATIC VARIATION OF SURFACE PROPERTIES	81

4.1. Introduction	81
4.2. Materials and Methods	83
4.2.1. Custom and Commercial Surfactants	83
4.2.2. Nonpolar Dispersions	83
4.2.3. Electrophoresis	84
4.2.4. Quartz Crystal Microbalance (QCM)	85
4.2.5. Karl Fischer Titration	86
4.3. Results and Discussions	86
4.3.1. Surface Charging Correlated to the Type of “Particle Bulk”	86
4.3.2. Preferential Adsorption of Inverse Micellar Ions	102
4.3.3. Ionization of Specific “Surface Functionality”	107
4.4. Conclusion	115
4.5. References	117
5 ATYPICAL IONIZATION PROCESSES OF OIL-BORNE AMPHIPHILES	122
5.1. Overview	122
5.2. “Ionization” of “Nonionic” Surfactants	122
5.2.1. Polarity of Surfactant Moieties	123
5.2.2. Electric Charging of O/W Interfaces Mediated by the Nonionic Surfactant	124
5.2.3. Electric Charging of W/O Interfaces Mediated by the Nonionic Surfactant	126
5.3. Surface Charging by Preferential Adsorption of Micelle “Ions”	131
5.3.1. Polarity of the Silica Particle Surface	133
5.3.2. Surface Charging of the Silica Particles	138

5.4. Charging Agent “Amphiphiles” Other than the Molecular Surfactants	141
5.4.1. Oil-Dispersible “Janus” Particles	142
5.4.2. Particle Synthesis via a Two-Step Seeded Emulsion Polymerization	143
5.4.3. Oil-Dispersibility of the Particles with a Co-Polymeric Hydrophobic Bulb	146
5.4.4. Interfacial Activity of the Oil-Borne Particles with Water (Hydrophilicity)	149
5.4.5. Electric Charging of a Nonpolar Solvent Containing the Amphiphilic Particles	153
5.5. References	158
6 CONCLUDING REMARKS	164

LIST OF TABLES

	Page
Table 2.1: Known surface energy component parameters of polar reference liquids (in mJ/m^2).	17
Table 2.2: Measured interfacial tensions of pure hexane with four polar reference liquids (in mJ/m^2). Here the reported error margin is the experimental standard deviation over four measurements.	25
Table 2.3: Inferred surface energy component parameters for hexane based on the best fit solution to the over-determined equation set (Eq. 2.4) with interfacial tension data from the four reference liquids (in mJ/m^2). The literature values are also shown. ^{21,28}	26
Table 2.4: Measured interfacial tensions of OLOA11000/hexane solution using four polar reference liquids.	37
Table 2.5: Inferred parameters of OLOA11000/hexane solution and comparison of the calculated and measured interfacial tension between OLOA11000/hexane solution and formamide.	37
Table 3.1: Acid (γ_s^+) and base γ_s^- parameters of the solid PMMA, measured for films cast from our PMMA particles ¹⁷ and adopted from the literature. ^{27,29}	55
Table 4.1: Surface energy components γ_s^{LW} , γ_s^+ , and γ_s^- , of solid polymer surfaces (in mJ/m^2). ¹	97
Table 5.1: Acid (γ_s^+) and base (γ_s^-) parameters of the solid silica surface (in mJ/m^2). ⁴⁰	135
Table 5.2: Solvodynamic diameter of the oil-borne particles in hexane measured by DLS.	148

LIST OF FIGURES

	Page
Figure 2.1: Interface between drop of hexane-based surfactant solution (20 mM PIBS-C) with a reference liquid (ethylene glycol), the tension of which is obtained by droplet shape analysis.	16
Figure 2.2: Complete spreading of a hexane droplet on a PMMA surface with a surface energy of 38.8 mJ/m^2 . ^{10,19}	18
Figure 2.3: Scheme of three polyisobutylene succinimide (PIBS) polyamine surfactants synthesized by coupling polyisobutylene succinic anhydride (PIBSA) and a series of polyamines.	19
Figure 2.4: Measured interfacial tensions of PIBS/hexane solutions with water, shown as a function of surfactant concentration (in mJ/m^2). Interfacial tensions of pure hexane are indicated with the red-dotted lines for comparison.	27
Figure 2.5: Measured interfacial tensions of PIBS/hexane solutions with ethylene glycol, shown as a function of surfactant concentration (in mJ/m^2). Interfacial tensions of pure hexane are indicated with the red-dotted lines for comparison.	27
Figure 2.6: Measured interfacial tensions of PIBS/hexane solutions with dimethyl sulfoxide, shown as a function of surfactant concentration (in mJ/m^2). Interfacial tensions of pure hexane are indicated with the red-dotted lines for comparison.	28
Figure 2.7: Measured interfacial tensions of PIBS/hexane solutions with glycol, shown as a function of surfactant concentration (in mJ/m^2). Interfacial tensions of pure hexane are indicated with the red-dotted lines for comparison.	28
Figure 2.8: Inferred Lifshitz-van der Waals parameters γ_L^{LW} of PIBS/hexane solutions, shown as a function of surfactant concentration (in mJ/m^2). Literature parameters for pure hexane are indicated with the red-dotted lines for comparison.	30
Figure 2.9: Inferred acidity parameters γ_L^+ of PIBS/hexane solutions, shown as a function of surfactant concentration (in mJ/m^2). Literature parameters for pure hexane are indicated with the red-dotted lines for comparison.	30
Figure 2.10: Inferred basicity parameters γ_L^- of PIBS/hexane solutions, shown as a function of surfactant concentration (in mJ/m^2). Literature parameters for pure hexane are indicated with the red-dotted lines for comparison.	31

- Figure 2.11: The resonance frequency shift of polymer-coated quartz crystal microbalances in response to the change in surfactant mass coupled to the surfaces; data for a PS surface is shown in green, data for a PMMA surface in black. 32
- Figure 3.1: The field dependent electrophoretic mobility of the charged PMMA particle in hexane-based dispersions of the surfactant PIBS-C in the range of applied field strength between 2.5 kV/m to 50 kV/m. 50
- Figure 3.2: The zero-field electrophoretic mobility of the charged PMMA particle in hexane-based dispersions of the surfactant PIBS-C, represented as a function of surfactant concentration. 50
- Figure 3.3: The field dependent electrophoretic mobility of the charged PMMA particle in hexane-based dispersions of the surfactant PIBS-O in the range of applied field strength between 2.5 kV/m to 50 kV/m. 51
- Figure 3.4: The zero-field electrophoretic mobility of the charged PMMA particle in hexane-based dispersions of the surfactant PIBS-O, represented as a function of surfactant concentration. 51
- Figure 3.5: The zero-field electrophoretic mobility of the charged PMMA particle in hexane-based dispersions of the surfactant PIBS-N, represented as a function of surfactant concentration. 52
- Figure 3.6: The zero-field electrophoretic mobility of the charged PMMA particle in hexane-based dispersions of the surfactant PIBS-N, represented as a function of surfactant concentration. 52
- Figure 3.7: The zero-field electrophoretic mobility of the charged PMMA particle in hexane-based dispersions of the three PIBS surfactants, represented as a function of surfactant concentration. 53
- Figure 3.8: The polar (acid-base) work of adhesion between the solid PMMA surface (S) and the liquid surfactant solutions (L_1), which roughly equals the interaction energy (per unit area) of the solid's basic and the liquid's acidic moieties (favoring positive surface charging). The contribution of solid acid – liquid base interaction (which favors negative surface charging) is negligible according to the negligibly low surface acid parameter (Table 3.1). 58
- Figure 3.9: The field dependent electrophoretic mobility in the particle-free, hexane-based solutions of the surfactant PIBS-C. 61
- Figure 3.10: The field dependent electrophoretic mobility in the particle-free, hexane-based solutions of the surfactant PIBS-O. 61
- Figure 3.11: The field dependent electrophoretic mobility in the particle-free, hexane-based solutions of the surfactant PIBS-N. 62

- Figure 3.12: Hypothetical mechanisms for the creation of micellar ions with a significant size asymmetry, consisting of the (i) intra-micellar acid-base interaction between the surfactant (Lewis base) and water (Lewis acid) and (ii) inter-micellar exchange of surfactant molecules. 63
- Figure 3.13: The total acid-base work of adhesion between the water surface (L_2) and surfactant solutions (L_1). 66
- Figure 3.14: The adduct formation energy of the water surface's basic (electron donor or proton acceptor) sites with the surfactant solutions' acidic (electron acceptor or proton donor) sites. 66
- Figure 3.15: The adduct formation energy of the water surface's acidic (electron acceptor or proton donor) sites with the surfactant solutions' basic (electron donor or proton acceptor) sites. 67
- Figure 3.16: Water content in the three PIBS surfactant solutions as a function of surfactant concentration. The dashed red line indicates the water content of pure hexane. 68
- Figure 3.17: Electric conductivity in the three types of PIBS surfactant solutions 69
- Figure 3.18: Surface charging of a hydrophobic particle via preferential adsorption of size-asymmetric micellar ions in case of a small size asymmetry. Dots on the surface represent lone electron pairs 74
- Figure 3.19: Surface charging of a hydrophobic particle via preferential adsorption of size-asymmetric micellar ions in case of a large size asymmetry. Dots on the surface represent lone electron pairs 74
- Figure 4.1: The field dependent electrophoretic mobility of the charged PMMA-sulfate particle in hexane-based dispersions of the surfactant PIBS-N in the range of applied field strength between 2.5 kV/m to 50 kV/m. 88
- Figure 4.2: The zero-field electrophoretic mobility of the charged PMMA-sulfate particle in hexane-based dispersions of the surfactant PIBS-N, represented as a function of surfactant concentration. 88
- Figure 4.3: The field dependent electrophoretic mobility of the charged PS-sulfate particle in hexane-based dispersions of the surfactant PIBS-N in the range of applied field strength between 2.5 kV/m to 50 kV/m. 89
- Figure 4.4: The zero-field electrophoretic mobility of the charged PS-sulfate particle in hexane-based dispersions of the surfactant PIBS-N, represented as a function of surfactant concentration. 89

- Figure 4.5: The field dependent electrophoretic mobility of the charged PS-carboxyl particle in hexane-based dispersions of the surfactant PIBS-N in the range of applied field strength between 2.5 kV/m to 50 kV/m. 90
- Figure 4.6: The zero-field electrophoretic mobility of the charged PS-carboxyl particle in hexane-based dispersions of the surfactant PIBS-N, represented as a function of surfactant concentration. 90
- Figure 4.7: The field dependent electrophoretic mobility of the charged PS-amidine particle in hexane-based dispersions of the surfactant PIBS-N in the range of applied field strength between 2.5 kV/m to 50 kV/m. 91
- Figure 4.8: The zero-field electrophoretic mobility of the charged PS-amidine particle in hexane-based dispersions of the surfactant PIBS-N, represented as a function of surfactant concentration. 91
- Figure 4.9: The zero-field electrophoretic mobility of the charged polymer particles in hexane-based dispersions of the surfactant PIBS-N, represented as a function of surfactant concentration. 92
- Figure 4.10: The electrophoretic mobility of the charged polymer particles in aqueous NaCl solutions, represented as a function of NaCl concentration. 92
- Figure 4.11: The shift in resonance frequency (Δf) of quartz crystal microbalances coated with polymer surfaces, in response to the surfactant adsorption (mass increase) to the surfaces. 95
- Figure 4.12: The adduct formation energy of the solid surfaces' acidic (electron acceptor or proton donor) sites with the surfactant solutions' basic (electron donor or proton acceptor) sites. 100
- Figure 4.13: The adduct formation energy of the solid surfaces' basic (electron donor or proton acceptor) sites with the surfactant solutions' acidic (electron acceptor or proton donor) sites. 100
- Figure 4.14: Schemes of multiple surface charging pathways which determine the *net* surface charge of colloidal particles in nonpolar dispersions: i) direct acid-base (donor-acceptor) interaction of particle bulk with surfactants, ii) preferential adsorption of inverse micellar ions (formed in the liquid bulk by intra-micellar acid-base interaction of moisture and surfactants), and iii) ionization of surface functionality promoted by excess moisture. 101
- Figure 4.15: The field dependent electrophoretic mobility of the charged PMMA-sulfate particle in hexane-based dispersions of the surfactant OLOA11000 in the range of applied field strength between 2.5 kV/m to 50 kV/m. 108

Figure 4.16: The zero-field electrophoretic mobility of the charged PMMA-sulfate particle in hexane-based dispersions of the surfactant OLOA11000, represented as a function of surfactant concentration.	108
Figure 4.17: The field dependent electrophoretic mobility of the charged PS-sulfate particle in hexane-based dispersions of the surfactant OLOA11000 in the range of applied field strength between 2.5 kV/m to 50 kV/m.	109
Figure 4.18: The zero-field electrophoretic mobility of the charged PS-sulfate particle in hexane-based dispersions of the surfactant OLOA11000, represented as a function of surfactant concentration.	109
Figure 4.19: The field dependent electrophoretic mobility of the charged PS-carboxyl particle in hexane-based dispersions of the surfactant OLOA11000 in the range of applied field strength between 2.5 kV/m to 50 kV/m.	110
Figure 4.20: The zero-field electrophoretic mobility of the charged PS-carboxyl particle in hexane-based dispersions of the surfactant OLOA11000, represented as a function of surfactant concentration.	110
Figure 4.21: The field dependent electrophoretic mobility of the charged PS-amidine particle in hexane-based dispersions of the surfactant OLOA11000 in the range of applied field strength between 2.5 kV/m to 50 kV/m.	111
Figure 4.22: The zero-field electrophoretic mobility of the charged PS-amidine particle in hexane-based dispersions of the surfactant OLOA11000, represented as a function of surfactant concentration.	111
Figure 4.23: The zero-field electrophoretic mobility of the charged polymer particles in hexane-based dispersions of the surfactant OLOA11000, represented as a function of surfactant concentration.	112
Figure 4.24: Water content in hexane solutions of the surfactant OLOA11000 and custom surfactant PIBS-N.	113
Figure 5.1: Electrophoretic mobility of the o/w emulsion droplets, stabilized by the surfactant PIBS-C, in a range of pH values.	125
Figure 5.2: Schemes of the o/w emulsion droplets, positively charged by the surfactant PIBS-C “pinned” at the o/w interfaces.	125
Figure 5.3: The field dependent electrophoretic mobility in the water-saturated PIBS-C/hexane solutions.	129
Figure 5.4: Schemes of the oppositely charged w/o emulsion droplets, created by i) intramicellar donor-acceptor interaction between water and surfactant polar moieties and ii) inter-micellar exchange of surfactant molecules	129

- Figure 5.5: Electric conductivity of “dry” and “wet” hexane solutions of the surfactant PIBS-C, represented as a function of surfactant concentration. The inset shows a magnified plot for the dry solutions. 131
- Figure 5.6: Electrophoretic mobility of the silica particles in aqueous phases in a range of pH values. 134
- Figure 5.7: Schemes of the charged silica particles with hydroxyl functional groups effectively solvated and ionized in aqueous phases. 134
- Figure 5.8: The adduct formation energy of the solid surfaces’ acidic (electron acceptor or proton donor) sites with the surfactant solutions’ basic (electron donor or proton acceptor) sites. 137
- Figure 5.9: The adduct formation energy of the solid surfaces’ basic (electron donor or proton acceptor) sites with the surfactant solutions’ acidic (electron acceptor or proton donor) sites. 137
- Figure 5.10: The field dependent electrophoretic mobility of the charged silica particles in hexane-based dispersions of the surfactant PIBS-C, in the range of applied field strength between 2.5 kV/m to 50 kV/m. 138
- Figure 5.11: The zero-field electrophoretic mobility of the charged silica particles in hexane-based dispersions of the surfactant PIBS-C, represented as a function of surfactant concentration. 139
- Figure 5.12: Schemes of the charged silica particles in nonpolar dispersions containing the surfactant PIBS-C. No evidence found for direct charge transfer polar interaction between the particle (bulk and functional groups) and surfactant. 139
- Figure 5.13: Oil-dispersible Janus snowman particles consisting of poly(St-co-TMSPA) (hydrophilic) and poly (St-co-IDMA) (hydrophobic) surfaces. The particles were deposited on the glass slide from a 20 ppm hexane dispersion and sputter-coated with small gold/palladium particles for SEM imaging. The (larger) hydrophobic lobes, which presumably swell in the alkane solution, are harder to discern in the images because of their weak contrast. The insets show examples of two associated snowman particles with their hydrophilic heads in contact. The scale bar represents a 100 nm. 146
- Figure 5.14: (A) Pure (linear) PS particles failing to disperse in hexane. (B) Lipophilic Janus snowman particles dispersed in hexane. (C) Lipophilic Janus snowman particles failing to disperse in water. 147
- Figure 5.15: Time-dependent interfacial tension of water with hexane-based dispersions of Janus snowman particles. 150

Figure 5.16: Equilibrium interfacial tension of water with hexane-based dispersions of Janus snowman particles (plateau values from Figure 5.15, represented as a function of particle concentration).	150
Figure 5.17: Formation of a water-in-oil (w/o) emulsion using oil-borne Janus snowman particles. Left: Water phase dyed with Rhodamine B (0.01 wt. %) and hexane based particle dispersion (white) prior to homogenization; Right: w/o emulsion with sedimented water droplets	151
Figure 5.18: Stable emulsions produced at different pH with the Janus snowman particles	152
Figure 5.19: Electric conductivity of hexane involving Janus snowman particles, as a function of particle concentration (in pS/m).	153
Figure 5.20: Moisture content in hexane involving Janus snowman particles, as a function of particle concentration (in ppm).	155
Figure 5.21: Nyquist plot of impedance data for the dodecane sample containing the Janus snowman particles. The data was taken at frequencies from 10^3 Hz to 10^2 Hz.	157
Figure 5.22: Semi-log Bode plot of the real impedance.	157
Figure 5.23: Semi-log Bode plot of the imaginary impedance.	158

SUMMARY

Electric charging of colloidal particles in nonpolar solvents plays a crucial role for many industrial applications and products, including rubbers, engine oils, toners, or electronic displays. Although disfavored by the low solvent permittivity, particle charging can be induced by added surfactants, even nonionic ones, but the underlying mechanism is poorly understood, and neither the magnitude nor the sign of charge can generally be predicted from the particle and surfactant properties.

The aim of this thesis is to achieve a better understanding on surfactant-mediated particle charging mechanisms in nonpolar dispersions, using a series of highly systematic approaches. We develop a method of characterizing the Lewis acid/base behavior of oil-borne surfactants, by which we can predict the propensity of charge transfer in polar interactions of the surfactants with other polar components in nonpolar media and examine some traditional speculations where surface charging was attributed to the direct polar interaction of the surfactants with particle surfaces. We synthesize and purify a series of custom surfactants under subtle variations of the chemical structure, and employ these surfactants as surface charging agents of several colloidal particles with well-defined surface polarity. We experimentally represent that surface charging is not likely a consequence of the single type of polar interaction between surfactant moieties and surface functional groups, disproving the past hypotheses, but a consequence of interplays between multiple charging pathways. In mechanistic interpretation of surface charging phenomena in these well-defined nonpolar systems, we prove that the ionization of surfactants is more preferred in the nonpolar liquid bulk via their polar interaction with

oil-borne moisture, the third component, than at the particle surfaces via such interaction with surface moieties. We suggest that the inverse micellar ions, created by this surfactant-moisture polar interaction, can influence net surface charging significantly, as another (ionic) acids and bases adsorbing to the surfaces asymmetrically. We also claim that the asymmetric adsorption state may not only be determined by the surface's chemical preference for a certain sign of micelle ions in terms of ion-dipole interaction, but also by the size asymmetry between the oppositely charged micellar ions in terms of minimizing the translational entropy loss associated with confining the continuous phase-soluble adsorbates. We show that the ionization of surface functional groups, which has been traditionally suggested as the only surface charging pathway, may only play a role as a contribution to net surface charging in the case where the surface is sufficiently wet by local aqueous bulk. Finally, we develop a new type of solid particle amphiphile promoting the electric conduction of nonpolar media, as an alternative to the molecular charging agent surfactants, based on the knowledge we gain from the prior mechanistic investigations.

We expect both the general methodology we employ to solve the problem, and mechanistic insights we gain on particle charging phenomena to be useful references to investigate and formulate more complicated nonpolar dispersions in practical applications. We also expect our prototype solid particle charging agent amphiphile to be further developed by tailoring their chemical and physical properties on demand, which may be potentially useful for developing new types of electrorheological fluids or lab-on-chip devices.

CHAPTER 1

INTRODUCTION

1.1. Background

Electric charging is common in aqueous environments and interfacial charges play an important role in the stabilization of multiphase systems such as colloidal dispersions¹ and emulsions.² On the other hand, purely nonpolar media such as saturated hydrocarbons are often considered charge-free because of the high energetic cost for separating the oppositely charged counter-ions in such media of low dielectric permittivity ϵ_r .³ The difficulty of charge separation in nonpolar media can be appreciated by considering the Bjerrum length λ_B , the distance between two oppositely charged monovalent ions below which the Coulombic attraction exceeds the thermal energy unit $k_B T$, given by

$$\lambda_B = \frac{e^2}{4\pi\epsilon_r\epsilon_0 k_B T}, \quad (1.1)$$

where e is the elementary charge, ϵ_0 is the electric permittivity in vacuum, k_B is the Boltzmann constant, and T is temperature.⁴ In contrast to water ($\epsilon_r \sim 80$, $\lambda_B \sim 0.7$ nm), nonpolar liquids ($\epsilon_r \sim 2$, $\lambda_B \sim 28$ nm) have a Bjerrum length well above the typical size of ions⁴ and thus strongly disfavor charging processes.

Despite the difficulty associated with the energetic cost, however, oil-soluble surfactants have often been reported to promote electric charging in nonpolar media.⁵⁻⁶ They are believed to do so by incorporating single ions in the polar core of surfactant

inverse micelles, which reduces the cost of charging (ionic Born energy) by increasing the dielectric constant of the ions' local environment.⁵⁻¹¹ Interestingly, ionic head-group moieties are not required for surfactants to cause electric charging; several studies have shown that nonionic surfactants, too, can increase the electric conductivity in nonpolar media dramatically.⁸⁻¹² Statistical equilibrium fluctuation theory has been used to explain inverse micelle charging in terms of charge fluctuations around a zero mean,¹³⁻¹⁶ but yields no insights into the charging pathway.

Similarly, it is known that surfactants can also promote surface charging of the colloidal particles in nonpolar dispersions by stabilizing the counter-ions in the nonpolar liquid,^{5-7,10,17-29} and this phenomenon has practical benefits, *e. g.* in electrophoretic image displays,³⁰⁻³⁴ printing toners,³⁵⁻³⁷ electrorheological fluids,³⁸ some drug delivery systems,³⁹⁻⁴⁰ detergents,³ or for asphaltene stability in crude oil.⁴¹⁻⁴² The underlying mechanisms of the particle charging, however, are not yet understood, although different hypotheses exist.⁵⁻⁶ – the details of the proposed hypotheses will be discussed in later chapters of this thesis.

1.2. Motivation and Objectives

A low level understanding of particle charging mechanisms in nonpolar dispersions has led to practical problems in industry with respect to developing advanced devices and troubleshooting malfunctions. To achieve a better mechanistic understanding on these phenomena, therefore, is not only desirable for scientific interest, but also important in industrial applications. We believe that progress towards that goal will depend on experimental data in which relevant physicochemical parameters are clearly *defined*, precisely *controlled*, and systematically *varied*. We point out that many past studies investigating particle charging phenomena in nonpolar dispersions lack either

aspect. As a consequence, their largely speculative mechanistic insights sometimes led to significantly misleading “general” conclusions which are not applicable at all to interpreting completely different systems from their own.

The primary objective of this thesis will be to achieve a better understanding on surfactant-mediated particle charging mechanisms in nonpolar dispersions, using a series of highly systematic approaches. Specifically, three outstanding problems will be systematically addressed throughout the thesis to obtain meaningful mechanistic insights.

- (i) There is no generally accepted way of estimating the polar (acid-base or donor-acceptor) interaction of surfactants with solid surfaces,⁴³ although such interaction has often been speculated to be the origin of surface charging in nonpolar media.¹⁷⁻²²
- (ii) Most past studies have focused on only few commercial surfactants with vastly different chemical structures.^{5-6,34} The direct comparison of such widely dissimilar systems provides little help in identifying the influence of individual material properties on the observed charging phenomena. Moreover, the commercial products often exist as mixtures of several derivatives and even contain unknown impurities.^{34,44-45} Investigation of charging mechanisms mediated by such poorly defined proprietary materials is extremely challenging.
- (iii) Choices of model colloids were not highly systematic for investigation of surface charging mechanisms in many past studies. Surfaces were often not “pristine”, containing some grafted steric stabilizers,^{7,10,25-26} the influence of which on surface charging is not obvious. “Defining” the surfaces’ polarity (likely relevant to their charging properties) was not attempted in many cases, and some quantitative parameters characterizing the surfaces’ polarity were not compatible with their interaction partners, surfactants.⁴³

The second minor objective of this thesis will be to develop another interesting amphiphilic material which mimics the small molecular surfactants as a charging agent in nonpolar media, based on some knowledge gained from our investigations with molecular surfactants.

1.3. Thesis Outline

In Chapter 2, a pragmatic way of characterizing the Lewis acid/base behavior of oil-soluble non-ionic surfactants will be proposed to address the outstanding problem (*i*). A combination of surface thermodynamic theory and experimental interfacial tension measurements allows for semi-quantitative estimation of acid/base behavior of oil-soluble surfactants which is effective at the interface of nonpolar solvents with a polar phase.

In Chapter 3, we investigate the surface charging of a model colloid in hexane-based solutions of a series of surfactants under *subtle* structural variations. This is an attempt to address the outstanding problem (*ii*). We precisely vary the surfactant chemistry, regarding it as a relevant system parameter, by replacing only a single electronegative atom located at a fixed position within the polar head-group. Interpretation of the observed charging phenomena, along with thorough characterization of respective system parameters, reveals the importance of inverse micelle ion adsorption in surface charging, in contrast to the traditional belief that surface charging would be mainly caused by direct charge transfer between the surface and the adsorbed (electrically) neutral surfactants. We also discuss an elusive role of moisture which not only participates in generation of micellar ions but also influences the asymmetric adsorption state of the oppositely charged micellar ions.

In Chapter 4, we investigate the surface charging of a series of polymer particles under systematic variations of their surface properties in nonpolar solutions, in an attempt to address the outstanding problem (iii). First, we vary the type of primary particle phase (“particle bulk”), and secondly, vary the specific surface functional groups. Careful interpretation of the observed charging phenomena leads to a major conclusion that surfactant-mediated particle charging in nonpolar dispersions is essentially a consequence of interplays between multiple charging pathways, not regulated by a single rule.

In Chapter 5, some in-depth discussions will be represented on atypical ionization processes of the proposed mechanistic schemes, with additional experimental supports. Also, an atypical oil-borne charging agent “amphiphile”, developed based on our knowledge gained from prior mechanistic investigations with small molecular surfactants, will be introduced.

In Chapter 6, the primary contributions of this thesis research will be summarized and some concluding remarks will be given.

1.4. References

1. Russel, W. B.; Saville, D. A.; Schowalter, W. R. *Colloidal Dispersions*; Cambridge University Press; Cambridge, 1989.
2. Marinova, K. G.; Alargova, R. G.; Denkov, N. D.; Velev, O. D.; Petsev, D. N.; Ivanov, I. B.; Borwankar, R. P. Charging of Oil-Water Interfaces Due to Spontaneous Adsorption of Hydroxyl Ions. *Langmuir* **1996**, *12*, 2045-2051.
3. Van der Hoeven, P. C.; Lyklema, J. Electrostatic Stabilization in Non-Aqueous Media. *Adv. Colloid Interface Sci.* **1992**, *42*, 205-277.
4. Israelachvili, J. N. *Intermolecular and Surface Forces*, 3rd ed.; Academic Press; Oxford, 2011.
5. Morrison, I. D. Electric Charges in Nonaqueous Media. *Colloids Surf., A* **1993**, *71*, 1-37.

6. Smith, G. N.; Eastoe, J. Controlling Colloid Charge in Nonpolar Liquids with Surfactants. *Phys. Chem. Chem. Phys.* **2013**, *15*, 424-439.
7. Hsu, M. F.; Dufresne, E. R.; Weitz, D. Z. Charge Stabilization in Nonpolar Solvents. *Langmuir* **2005**, *21*, 4881-4887.
8. Kim, J.; Anderson, J. L.; Garoff, S.; Schlangen, L. J. M. Ionic Conduction and Electrode Polarization in a Doped Nonpolar Liquid. *Langmuir* **2005**, *21*, 8620-8629.
9. Strubbe, F.; Verschueren, A. R. M.; Schlangen, L. J. M.; Beunis, F.; Neyts, K. J. Generation Current of Charged Micelles in Nonaqueous Liquids: Measurements and Simulations. *J. Colloid Interface Sci.* **2006**, *300*, 396-403.
10. Roberts, G. S.; Sanchez, R.; Kemp, R.; Wood, T.; Barlett, P. Electrostatic Charging of Nonpolar Colloids by Reverse Micelles. *Langmuir* **2008**, *24*, 6530-6541.
11. Guo, Q.; Singh, V.; Behrens, S. H. Electric Charging in Nonpolar Liquids Because of Nonionizable Surfactants. *Langmuir* **2010**, *26*, 3203-3207.
12. Dukhin, A. S.; Dukhin, S. S. How Non-Ionic "Electrically Neutral" Surfactants Enhance Electrical Conductivity and Ion Stability in Non-Polar Liquids. *Electrophoresis* **2005**, *26*, 2149-2153.
13. Eicke, H. F.; Borkovec, M.; Das-Gupta, B. J. Conductivity of Water-In-Oil Microemulsions: A Quantitative Charge Fluctuation Model. *J. Phys. Chem.* **1989**, *93*, 314-317.
14. Hall, D. G. Conductivity of Microemulsions: An Improved Charge Fluctuation Model. *J. Phys. Chem.* **1990**, *94*, 429-430.
15. Kallay, N.; Chittofrati, A. Conductivity of Microemulsions: Refinement of Charge Fluctuation Model. *J. Phys. Chem.* **1990**, *94*, 4755-4756.
16. Kallay, N.; Tomic, M.; Chittofrati, A. Conductivity of Water-In-Oil Microemulsions: Comparison of the Boltzmann Statistics and the Charge Fluctuation Model. *Colloid Polym. Sci.* **1992**, *270*, 194-196.
17. Fowkes, F. M.; Jinnai, H.; Mostafa, M. A.; Anderson, F. W.; Moore, R. J. Mechanism of Electric Charging of Particles in Nonaqueous Liquids. *ACS Symposium Series* **1982**, *200*, 307-324.
18. Fowkes, F. M.; Pugh, R. J. Steric and Electrostatic Contributions to the Colloidal Properties of Nonaqueous Dispersions. *ACS Symposium Series* **1984**, *240*, 331-354.
19. Poovadorom, S.; Berg, J. C. Effect of Particle and Surfactant Acid-Base Properties on Charging of Colloids in Apolar Media. *J. Colloid Interface Sci.* **2010**, *346*, 370-377.
20. Gacek, M.; Brooks, G.; Berg, J. C. Characterization of Mineral Oxide Charging in Apolar Media. *Langmuir* **2012**, *28*, 3032-3036.

21. Gacek, M. M.; Berg, J. C. Investigation of Surfactant Mediated Acid-Base Charging of Mineral Oxide Particles Dispersed in Apolar Systems. *Langmuir* **2012**, *28*, 17841-17845.
22. Gacek, M. M.; Berg, J. C. Effect of Surfactant Hydrophile-Lipophile Balance (HLB) Value on Mineral Oxide Charge in Apolar Media. *J. Colloid Interface Sci.* **2015**, *449*, 192-197.
23. Kitahara, A.; Satoh, T.; Kawasaki, S.; Kon-No, K. Specific Adsorption of Surfactants Containing Mn or Co on Polymer Particles Revealed by Zeta-Potential in Cyclohexane. *J. Colloid Interface Sci.* **1982**, *86*, 105-110.
24. Smith, P. G.; Patel, M. N.; Kim, J.; Milner, T. E.; Johnston, K. P. Effect of Surface Hydrophilicity on Charging Mechanism of Colloids in Low-Permittivity Solvents. *J. Phys. Chem. C* **2007**, *111*, 840-848.
25. Kemp, R.; Sanchez, R.; Mutch, K. J.; Bartlett, P. Nanoparticle Charge Control in Nonpolar Liquids: Insights from Small-Angle Neutron Scattering and Microelectrophoresis. *Langmuir* **2010**, *26*, 6967-6976.
26. Smith, G. N.; Alexander, S.; Brown, P.; Gillespie, D. A. J.; Grillo, I.; Heenan, R. K.; James, C.; Kemp, R.; Rogers, S. E.; Eastoe, J. Interaction between Surfactants and Colloidal Latexes in Nonpolar Solvents Studied Using Contrast-Variation Small-Angle Neutron Scattering. *Langmuir* **2014**, *30*, 3422-3431.
27. Smith, G. N.; Grillo, I.; Rogers, S. E.; Eastoe, J. Surfactants with Colloids: Adsorption or Absorption? *J. Colloid Interface Sci.* **2015**, *449*, 205-214.
28. Espinosa, C.E.; Guo, Q.; Singh, V.; Behrens, S. H. Particle Charging and Charge Screening in Nonpolar Dispersions with Nonionic Surfactants. *Langmuir* **2010**, *26*, 16941-16948.
29. Guo, Q.; Lee, J.; Singh, V.; Behrens, S. H. Surfactant Mediated Charging of Polymer Particles in a Nonpolar Liquid. *J. Colloid Interface Sci.* **2013**, *392*, 83-89.
30. Comiskey, B.; Alvert, J. D.; Yoshizawa, H.; Jacobson, J. An Electrophoretic Ink for All-Printed Reflective Electronic Displays. *Nature* **1998**, *394*, 253-255.
31. Chen, Y.; Au, J.; Kazlas, P.; Ritenour, A.; Gates, H.; McCreary, M. Flexible Active-Matrix Electronic Ink Display. *Nature* **2003**, *423*, 136-136.
32. Verschueren, A. R.M.; Stofmeel, L. W. G.; Baesjou, P. J.; van Delden, M. H. W. M.; Lenssen, K. M. H.; Mueller, M.; Oversluizen, G.; van Glabbeek, J. J.; Osenga, J. T. M.; Schuurbiens, R. M. Optical Performance of In-Plane Electrophoretic Color E-Paper. *J. Soc. Inf. Disp.* **2010**, *18*, 1-7.
33. Heikenfeld, J.; Drzaic, P.; Yeo, J.-S.; Koch, T. Review Paper: A Critical Review of the Present and Future Prospects for Electronic Paper. *J. Soc. Inf. Disp.* **2011**, *19*, 129-156.

34. Parent, M. E.; Yang, J.; Jeon, Y.; Toney, M. F.; Zhou, Z.-L.; Henze, D. Influence of Surfactant Structure on Reverse Micelle Size and Charge for Nonpolar Electrophoretic Inks. *Langmuir* **2011**, *27*, 11845-11851.
35. Pearlstine, K.; Page, L.; Elsayed, L. Mechanism of Electric Charging of Toner Particles in Nonaqueous Liquid with Carboxylic Acid Charge Additives. *J. Imaging Sci.* **1991**, *35*, 55-58.
36. Jenkins, P.; Basu, S.; Keir, R. I.; Ralston, J.; Thomas, J. C.; Wolffenbuttel, B. M. A. The Electrochemistry of Nonaqueous Copper Phthalocyanine Dispersions in the Presence of a Metal Soap Surfactant: A Simple Equilibrium Site Binding Model. *J. Colloid Interface Sci.* **1999**, *211*, 252-263.
37. Gacek, M. M.; Berg J. C. Effect of Synergists on Organic Pigment Particle Charging in Apolar Media. *Electrophoresis* **2014**, *0*, 1-7.
38. Hao, T. Electrorheological Fluids. *Advanced Materials* **2001**, *13*, 1847-1857.
39. Jones, S. A.; Martin, G. P.; Brown, M. B. Manipulation of Beclomethasone-Hydrofluoroalkane Interactions Using Biocompatible Macromolecules. *J. Pharm. Sci.* **2006**, *95*, 1060-1074.
40. Rosenholm, J. B. Solvent and Surfactant Induced Interactions in Drug Dispersions. *Colloids Surf., A* **2010**, *354*, 197-204.
41. Leon, O.; Rogel, E.; Espidel, J.; Torres, G. Asphaltenes: Structural Characterization, Self-Association, and Stability Behavior. *Energy & Fuels* **2000**, *14*, 6-10.
42. Gonzelez, G.; Neves, G. B. M.; Saraiva, S. M.; Lucas, E. F.; Sousa, M. A. Electrokinetic Characterization of Asphaltenes and the Asphaltenes-Resins Interaction. *Energy & Fuels* **2003**, *17*, 879-886.
43. Lee, J.; Zhou, Z.-L.; Behrens, S. H. Characterizing the Acid/Base Behavior of Oil-Soluble Surfactants at the Interface of Nonpolar Solvents with a Polar Phase. *J. Phys. Chem. B* **2015**, *119*, 6628-6637.
44. Dukhin, A.; Parlia, S. Ions, Ion Pairs and Inverse Micelles in Non-Polar Media. *Curr. Opin. Colloid Interface Sci.* **2013**, *18*, 93-115.
45. De. T. K.; Maitra, A. Solution Behaviour of Aerosol OT in Non-Polar Solvents. *Adv. Colloid Interface Sci.* **1995**, *59*, 95-193.

CHAPTER 2

CHARACTERIZING THE ACID/BASE BEHAVIOR OF OIL-SOLUBLE SURFACTANTS AT THE INTERFACE OF NONPOLAR SOLVENTS WITH A POLAR PHASE

2.1. Introduction

Oil-soluble nonionic surfactants are commonly used in various industrial applications and in academic research.¹⁻¹⁷ In contrast to *ionic* surfactants, the oil-soluble nonionic amphiphiles do not readily partition into a contacting aqueous phase, which often makes them more efficient emulsifiers. Since they also tend to be less irritant to the human skin than ionic surfactants,¹ some nonionic surfactants such as sorbitan esters (Span) have been used extensively as emulsifiers in cosmetic formulations and in household products. Other nonionic surfactants such as polyisobutylene succinimide (PIBS) have long been used as additives in the oil industry, to prevent the aggregation of ultrafine carbon black particles formed in engine oil during engine operation,²⁻⁵ or to control the asphaltene deposition during petroleum handling.⁶ Recently, oil-soluble nonionic surfactants have been employed as electric charging agents⁷⁻¹³ with applications *e.g.* in the development of electrophoretic inks for electronic image displays or toners for electrostatic lithographic printers.⁷ These applications have also sparked interest in scientific investigations of these surfactants' interfacial behavior.^{5,14-15}

In the absence of dissociable moieties, the head-group polarity of nonionic surfactants is often a critical factor for their application. When interacting with a

contacting polar phase, the head-group of an oil-borne surfactant may exhibit (Lewis) acid and base behavior, acting as a proton (or electron) donor or acceptor. In applications to engine oils, for example, carbon-based acids generated by oxidative degradation of hydrocarbon-based oils are neutralized by adding “basic” PIBS surfactants as lubricant additives.³ Similarly, acid/base complexes of nonionic surfactants have been suggested as a key element in the removal of thin oil slicks from water surfaces.¹⁶ Recently, studies on particle charging in nonpolar dispersions suggested that nonionic surfactants can undergo acid-base interaction in contact with a particle surface, and play an important role in determining the sign and magnitude of the particle surface charge.¹⁰⁻¹³ The ability to describe the strength of such acid-base interaction quantitatively would provide practical benefits for formulation efforts and help gain insights into the poorly understood electric charging phenomena in nonpolar systems.¹⁷⁻¹⁸

The donor/acceptor properties of most cationic, anionic or zwitterionic surfactants are predictable based on their chemical structure, and characterization methods using various titration techniques are well established.¹⁵ For nonionic surfactants, however, the situation is less clear, given the lack of a dissociable moiety obviously responsible for charging, and numerous factors, including resonance, electronegativity, induction by neighboring groups or molecular orbital hybridization, potentially affecting the net acidity and basicity of the surfactant molecules.²⁰ Depending on the molecular composition, it is possible for a surfactant to possess both acid and base character, to be only acidic or only basic, or to possess neither attribute.²⁰⁻²³ Common techniques used for the characterization of acidity/basicity of nonionic surfactants are based on potentiometric titration, the detailed procedures of which are described in the American

Society for Testing and Materials (ASTM) standards.²⁴⁻²⁵ According to ASTM standards, the acidity of an oil product is defined by “the acid number”, which represents the amount of potassium hydroxide (KOH) required to neutralize a gram of sample in a specified titration medium, a mixture of water, anhydrous propan-2-ol, and toluene.²⁴ Similarly, the basicity of an oil product is defined as “the base number”, which represents the amount of a specific acid to neutralize a gram of sample, where the quantity of the required acid is expressed as the equivalent amount of KOH per gram of sample, but in a completely different titration medium, an anhydrous mixture of chlorobenzene and glacial acetic acid.²⁵

Since it is well known that the acidity and basicity of organic species can be severely affected by the solvating performance of the medium,²⁰ and the acid number and base number are determined in *different* titration media, it should not be assumed that these numbers accurately describe the surfactant’s acid and base characteristics in the *same* medium, especially if that medium is quite different from both reference media. Nor can measurements probing the behavior of surfactant dissolved in a liquid *bulk* be expected to reflect the acid-base interaction of surfactant adsorbed at an *interface*. As if this was not reason enough for concern, the potentiometric titration is sensitive to proton transfer and may reveal only the acid/base strength of the material in the *Brønsted* sense, while it is the *Lewis* acid/base properties of nonionic surfactants that are believed critical for their affinity to polar phases. Moreover, the acid and base numbers based on ASTM standards are not compatible with common acid/base metrics for solid surfaces or polar liquids, such as pKa,^{14,20} point of zero charge (PZC),¹²⁻¹³ or surface energy components.²¹⁻²³ Solid surfaces and polar liquids, however, are likely donor-acceptor interaction

partners for oil-borne surfactants, and there seems little hope for a better understanding of these interactions without a common framework for describing the acid/base properties of the interacting species. Lastly, the standard protocols pose a number of practical challenges arising from the complexity of experimental setups and procedures, the use of toxic titration agents, and the requirement of a large amount of sample.

In the present Chapter, we propose a simple method of characterizing the effective Lewis acid/base behavior of oil-soluble nonionic surfactants from a nonpolar oil phase at interfaces with a more polar second phase – in terms of parameters also used to characterize solid and liquid interaction partners. The procedure of the proposed method includes (a) measuring the interfacial tensions of surfactant/alkane solutions with a diverse series of polar reference liquids of known Lewis acid/base parameters, and (b) substituting the measured interfacial energy in a set of equations adopted from a thermodynamic surface energy component model to obtain Lewis acid/base parameters that reflect the net interfacial behavior of the nonpolar surfactant solution when in contact with a more polar phase. The surface energy component model inspiring our approach has been proposed by van Oss and co-workers;²¹⁻²³ details of this model will be reviewed in the following section. Using the proposed method, the amphoteric properties (independent acidity/basicity) of oil-soluble surfactants can be examined for a unified set of contacting reference liquids in a semi-quantitative manner. The method directly probes the behavior of interfacially adsorbed surfactants, and the inferred parameters are compatible with known component parameters of various condensed phases; they are therefore expected to provide insights into physicochemical phenomena achieved by donor-acceptor interactions of surfactants at the interfaces of nonpolar oil phases. Finally,

the proposed method has the benefit of using as experimental input only tensiometry data obtainable via simple measurements that require only small amounts of samples, a key advantage when working with limited resources such as expensive, custom-synthesized surfactant. We test the proposed method by employing a series of well-purified PIBS analogs with small structural variations, and show some exemplary applications of the inferred parameters. Important limitations of the suggested method are also discussed.

2.2. Methods and Materials

2.2.1. Application of the van Oss-Chaudhury-Good (vOCG) Model

There have been many approaches to measuring the acidity and basicity of condensed phases.^{12-14,19-25} Here, we adopt the thermodynamic surface energy component model suggested by van Oss, Chaudhury, and Good (vOCG)²¹⁻²³ to estimate the acidity and basicity of oil-borne nonionic surfactants. Despite some past criticism,²⁶ it is among the most popular models for describing the polar and apolar contributions to the work of adhesion between condensed phases, and has been widely used in the field of adhesion science.^{19,27}

According to the model, the total work of adhesion (W_{12}) between the phase 1 and 2 can be defined as a sum of a Lifshitz-van der Waals contribution (W_{12}^{LW}) and an acid/base contribution (W_{12}^{AB}),

$$W_{12} = W_{12}^{LW} + W_{12}^{AB}, \quad (2.1)$$

where the Lifshitz-van der Waals (LW) contribution is often dominated by the London dispersion interaction of fluctuating and induced dipoles, and the acid/base (AB) contribution includes all donor-acceptor interactions in the Lewis sense.²¹ Surface charge or covalent bonding effects are not considered here, as they do not affect the investigation of energy components for nonionic surfactants.

The model employs three energy component parameters, a Lifshitz-van der Waals parameter γ_i^{LW} , an acidity parameter γ_i^+ , and a basicity parameter γ_i^- to describe the material properties of liquid or solid phases, and combinations of such parameters for two adhering phases determine the apolar/polar work of adhesion via

$$W_{12}^{LW} = -2(\gamma_1^{LW} \gamma_2^{LW})^{1/2} \quad (2.2)$$

$$W_{12}^{AB} = -2(\gamma_1^+ \gamma_2^-)^{1/2} - 2(\gamma_1^- \gamma_2^+)^{1/2}, \quad (2.3)$$

where the negative sign indicates the attraction according to the thermodynamic convention.²¹ Together with well-known summation relations between the work of adhesion (W_{12}) and the interfacial tension between two phases (γ_{12}),²¹ equations 2.1 through 2.3 lead to the following expression for the experimentally accessible interfacial tension $\gamma_{L_1 L_2}$ between two liquids L_1 and L_2 ,

$$\gamma_{L_1 L_2} = [(\gamma_{L_1}^{LW})^{1/2} - (\gamma_{L_2}^{LW})^{1/2}]^2 + 2[(\gamma_{L_1}^+)^{1/2} - (\gamma_{L_2}^+)^{1/2}][(\gamma_{L_1}^-)^{1/2} - (\gamma_{L_2}^-)^{1/2}], \quad (2.4)$$

which is a function of the three energy components parameters. This expression (Eq. 2.4) permits to infer the unknown energy components, $\gamma_{L_1}^{LW}$, $\gamma_{L_1}^+$, and $\gamma_{L_1}^-$, for a target liquid

phase L_1 by measuring its interfacial tensions $\gamma_{L_1L_2}$ with a series of immiscible reference liquids L_2 whose energy components, $\gamma_{L_2}^{LW}$, $\gamma_{L_2}^+$, and $\gamma_{L_2}^-$, are known.

To infer (and compare) the Lewis acid/base properties of interfacially adsorbed surfactants from a nonpolar oil phase in a *semi-quantitative* manner, we measure the interfacial tensions $\gamma_{L_1L_2}$ (Figure 2.1) of alkane-based surfactants solution L_1 with a series of “polar” reference liquids L_2 (Table 2.1). These interfacial tensions obviously differ from the interfacial tension of the reference liquids with the pure, surfactant-free oil (dielectric permittivity $\epsilon_r \approx 2$, $\gamma_{alkanes}^+ = 0 = \gamma_{alkanes}^-$) in a manner that reflects the interfacial adsorption of the surfactant and depends on the acid/base character of its polar head-group. From the series of interfacial tensions $\gamma_{L_1L_2}$ as experimental input and the known surface energy components $\gamma_{L_2}^{LW}$, $\gamma_{L_2}^+$, and $\gamma_{L_2}^-$ of the polar reference liquids, we can formally calculate the parameters $\gamma_{L_1}^{LW}$, $\gamma_{L_1}^+$, and $\gamma_{L_1}^-$ for the nonpolar surfactant solutions, using equation 2.4. It is important to note that these parameters should not be interpreted as “surface energy components” in the usual sense: they represent no intrinsic *property* of the solution or of the surfactant alone, but serve as indicators of a certain *behavior* displayed upon solution contact with a second phase; as such they are neither independent of the surfactant concentration nor of the polarity of the partner phase. In contact with a nonpolar contacting phase such as a gas, for instance, the surfactant would be depleted from the interface, not adsorbed to it, and therefore have a very different effect on the interfacial tension. We propose that the “solution parameters” $\gamma_{L_1}^{LW}$, $\gamma_{L_1}^+$, and $\gamma_{L_1}^-$ obtained from measurements against a set of polar reference liquids are nonetheless

useful in gauging the effective acid-base interaction of the same surfactant solution with another *polar* phase. This interaction is “effective” precisely because it relies on the adaptive behavior of the adsorbing surfactants. It is the result of a net tendency of displaying acidic and basic moieties that depends not only on those polar surfactant head-group moieties themselves, but also on the nonpolar portion of the molecule through its influence on the molecule’s solubility in the oil and steric effects in the adsorbed layer. The key idea then is to use the adaptive character of solutions to infer the net acid/base effects of the surfactant. Arguably it is this net effect which is of primary practical interest for many applications in which nonionic surfactants are used as additives for nonpolar solvents, and the inferred parameters allow us to compare the relative Lewis donor/acceptor strength of different surfactants under the given constraints (nonpolar solvent in contact with a more polar phase in which the surfactant is insoluble).

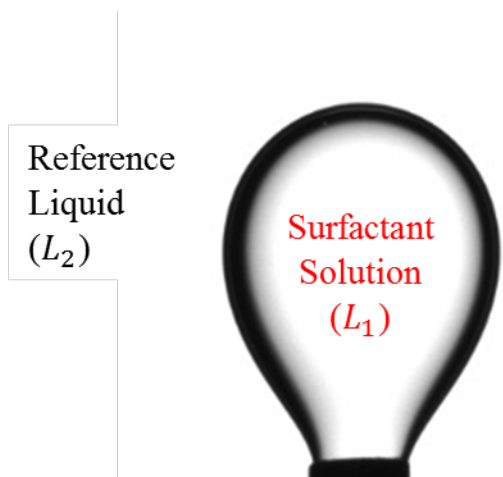


Figure 2.1. Interface between drop of hexane-based surfactant solution (20 mM PIBS-C) with a reference liquid (ethylene glycol), the tension of which is obtained by droplet shape analysis.

Table 2.1. Known surface energy component parameters of polar reference liquids (in mJ/m^2).

Polar Reference Liquid	γ_{L_2}	$\gamma_{L_2}^{LW}$	$\gamma_{L_2}^+$	$\gamma_{L_2}^-$	$\gamma_{L_2}^- / \gamma_{L_2}^+$
Water (W) ^{23,28}	72.8	21.8	25.5	25.5	1
Ethylene Glycol (E) ^{23,28}	48	29	1.92	47	24.5
Dimethyl Sulfoxide (D) ¹⁹	44	36	0.5	32	64
Glycerol (G) ^{23,28}	64	34	3.92	57.4	14.6

In principle, the measurement of contact angle on reference solid surfaces might seem like an alternative way of evaluating the vOCG parameters of the sample liquid. In practice, however, this method is impractical for nonpolar surfactant solutions because of their low surface tension: most solid surfaces have surface tensions on the order of 40 mJ/m^2 ,²³ and oil-based liquids often spread completely on the surface without a measurable contact angle (Figure 2.2). Three-phase contact angle measurements involving a solid surface and a second liquid could avoid such complete spreading, but would add undesirable complexity in allowing for surfactant assembly at multiple interfaces. Moreover, surface roughness can further influence contact angles in a way that makes it difficult to extract reliable information about acid/base properties. We therefore consider the interfacial tension between solutions of nonionic surfactant in nonpolar oils and polar reference liquids a far more promising way to characterize the effective acid/base behavior of the surfactant solutions.



Figure 2.2. Complete spreading of a hexane droplet on a PMMA surface with a surface energy of 38.8 mJ/m^2 .^{10,19}

2.2.2. Surfactant Synthesis and Purification

The surfactants used to test the proposed method are examples of PIBS polyamine surfactants. Industrial mixture of these surfactants have been used as lubricant additives in the oil industry for decades,^{4-5,7} as well as electric charging agents.^{7,11,13,17-18} The synthesis and purification of our PIBS polyamine surfactants, with which the investigation of surface charging mechanisms will be carried out in the rest of this thesis, were done following procedures described by Parent and co-workers.⁷ Three types of PIBS analogs, PIBS-C, PIBS-N, and PIBS-O, were synthesized by coupling polyisobutylene succinic anhydride (PIBSA) and different polyamines (Figure 2.3). A commercial PIBSA named OLOA15500 ($M_w \sim 1000 \text{ g/mol}$) was obtained from Chevron Oronite, polyamine N,N-diethylpentane-1,5-diamine (97%, $M_w \sim 158.2 \text{ g/mol}$) was purchased from Matrix Scientific, N,N-diethyldiethylenetriamine (98%, $M_w \sim 159.3$

g/mol) from Sigma Aldrich, and [2-(2-aminoethoxy)ethyl]diethylamine (95%, $M_w \sim 160.3$ g/mol) from Ukrorgsyntez Ltd. (Ukraine). In the synthesis of each surfactant type, an equimolar mixture of PIBSA and the polyamine were dissolved in m-xylene (>99%, Sigma-Aldrich) and placed into a round-bottom flask equipped with a Dean-Stark apparatus to remove water generated during the reaction. The solution was heated in a paraffin oil bath at 190 °C and refluxed for 20 hours. After the reaction, the solution was cooled down to room temperature. Finally, the m-xylene was removed via distillation at 200 °C.

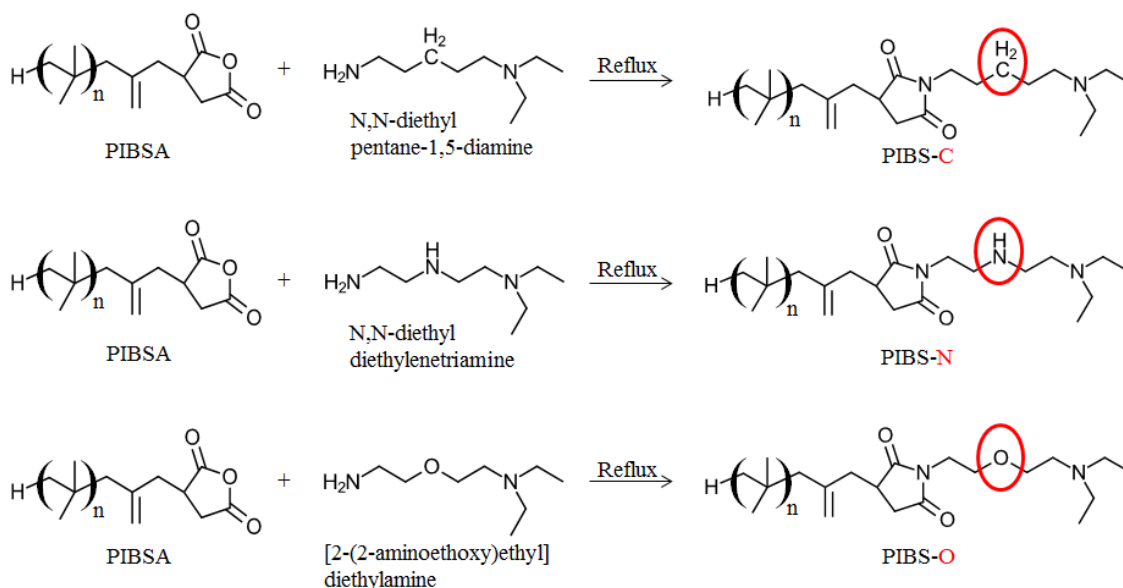


Figure 2.3. Scheme of three polyisobutylene succinimide (PIBS) polyamine surfactants synthesized by coupling polyisobutylene succinic anhydride (PBISA) and a series of polyamines.

The resulting products were further purified by flash chromatography to remove impurities. Silica gel (pore size 60 Å, 70 – 230 mesh, 63 – 200 μm, Sigma-Aldrich), as

the stationary phase, was packed in a 2 (I.D.) × 18 (E.L.) inch gravity column. Before loading the synthesis products, the silica gel column was pre-treated with Lewis base by flowing a 20:1 hexane (>98.5%, VWR) / triethylamine (>99.5%, Sigma Aldrich) mixture to avoid the irreversible binding of basic surfactant molecules on the acidic silica gel surfaces. The synthesis products were then loaded in the column, and passed through the silica gel using 20:1 chloroform (>99.8%, VWR) / ethanol anhydrous (>99.5% 200 proof, Sigma Aldrich) mixture as the eluent. An impurity with low polarity was eluted at the very early stage of column chromatography. The exact chemical identity of this impurity was not investigated, but Shen⁴ plausibly assumed a similar low-polar impurity of PIBSA to be unreacted polyisobutylene (PIB). The target PIBS surfactants eluted later from the column, and were collected separately. The eluent solvent mixture was evaporated in a rotary evaporator at 45 °C with vacuum pressure ~160 mmHg for 3 hours. Purified surfactants were then dissolved in an apolar oil (hexane, >98.5%, $\epsilon_r = 1.89$, VWR) at a concentration of 150 mM and were filtered through an alumina based membrane (pore size 0.02 μm , Whatman[®] Anotop[®] 10 syringe filter) to remove any large impurities introduced during the sample preparation. Finally, the filtered PIBS/hexane solutions were diluted to four different concentrations, 2 mM, 5 mM, 10 mM and 20 mM, at which interfacial tension measurements were carried out.

We also employed a commercial charging agent product, OLOA11000. This proprietary material is known as a mixture of several PIBS derivatives and mineral oils but the exact chemical composition is poorly defined.^{7,17} The material was received from Chevron Oronite and used without further purification.

2.2.3. Interfacial Tensiometry

Interfacial tensions of PIBS/hexane solutions with a series of polar reference liquids were measured to estimate the surfactant acid/base properties. Measurements were carried out with video image edge tracing (ramé-hart goniometer, model-250), where the interfacial tension is calculated based on the pendant drop shape of surfactant solutions at an inverted steel needle submerged in reference liquids (Figure 2.1). The interfacial tension was investigated at four surfactant concentrations, 2, 5, 10, and 20 mM, where the critical micelle concentration (CMC) was around ~2 mM as determined by dynamic light scattering (DLS).⁸ Polar reference liquids used in this study include 1) ultrapure water with a resistivity of 18.2 M Ω ·cm (Barnstead), 2) ethylene glycol (>99.8% Sigma-Aldrich), 3) dimethyl sulfoxide (>99.9%, Sigma-Aldrich), and 4) glycerol (>99.5%, Sigma-Aldrich). The surface energy component parameters of these reference liquids are listed in Table 2.1. The measured interfacial tensions were averaged over 4 independent measurements.

2.2.4. Computational Tools

Numerical least square solutions for an excess number of reference liquids were obtained by using the MATLAB 7.14.0.739 (The MathWorks, Inc.) optimization package.

2.2.5. Quartz Crystal Microbalance (QCM)

We performed the quartz crystal microbalance (QCM) experiment to show the difference in surfactant adsorption to polymeric surfaces with different acid/base

parameters. In preparation of the polymeric surfaces, bare gold crystals purchased from Biolin Scientific were cleaned by following a series of procedures: they were treated in a UV/ozone system for 10 minutes, soaked in a 5:1:1 mixture of DI water, ammonia (25%, Merck), and hydrogen peroxide (30%, Merck) for 10 minutes at 75 °C, rinsed with DI water, dried with nitrogen gas, and finally treated in the UV/ozone system for another 10 min. The cleaned gold crystals were spin-coated with thin polymer films, using 1 wt.% chloroform solutions of two polymeric materials, poly(methyl methacrylate) (PMMA) and poly(styrene) (PS), obtained by dissolution of dried polymer particles (PMMA, Bangs Laboratories, catalog #PP04N and PS, Life Technologies, catalog # C37274). The spin-coated crystal was heated to 80 °C in the oven for 30 minutes and then allowed to cool to room temperature. The QCM experiments were carried out using the commercial Q-Sense E4 system (Biolin Scientific). The fundamental (resonance) frequency of the polymer-coated crystal under alternating electric fields was initially obtained without adsorbed surfactant, and then the crystal was exposed to a parallel flow of the surfactant solution with a rate of 200 $\mu\text{L}/\text{min}$ to monitor the frequency shift (Δf), which is proportional to the change in mass coupled to the surface.²⁹ Before exposure to the surfactant solution, the surface was flushed with the background solvent, pure hexane, at least for 30 min to obtain a stable baseline. Once the stable baseline was established, the surfactant solution was injected to the system and the frequency change of the crystal due to the surfactant adsorption was monitored for 45 min. The crystal surface was then again flushed with pure hexane and the frequency change due to the surfactant desorption was monitored for 30 min.

2.3. Results and Discussions

2.3.1. Determination of Component Parameters for Nonpolar Samples

In principle, solving equation 2.4 analytically with three independent experimental interfacial tensions $\gamma_{L_1L_2}$ would yield the three unknown vOCG parameters $\gamma_{L_1}^{LW}$, $\gamma_{L_1}^+$, and $\gamma_{L_1}^-$ for the nonpolar sample liquid. This requires a very judicious selection of the triplet of reference liquids to avoid “ill-conditioning” in the equation set, *i.e.* the unfavorable propagation of uncertainties or errors in the experimental input.^{26,30-32} Della Volpe and co-workers³² have studied in detail the problem of ill-conditioning in the (linear) equation set from which the vOCG parameters of a *solid surface* can be determined from experimental contact angles. They showed that only “well-balanced triplets” of reference liquids, *i. e.* those containing dispersive, predominantly basic, and predominantly acidic liquids, produced an acceptably low *condition number* (*i.e.* the factor by which the relative error in the experimental input data has to be multiplied in the worst case to obtain the resulting relative error in the extracted vOCG parameters).³² Besides finding a reference triplet with low condition number, another well-known strategy to avoid unfavorable error propagation consists of producing a larger, “over-determined” equation set with experimental data from more than three reference liquids, and of determining an approximate best fit solution for the three unknown vOCG parameters.^{19,32-34}

In the case of equation 2.4 with experimentally determined interfacial tensions between a nonpolar surfactant solution and a set of polar reference liquids, the mathematical analysis of the condition number is severely complicated by (a) the non-

linearity of the equation and (b) the need to restrict the analysis to sample solutions and reference liquids which form an interface and thus have a measureable, positive interfacial tension. We instead adopt the strategy of the over-determined equation set and work with *four* instead of *three* reference liquids: water (W), ethylene glycol (E), dimethyl sulfoxide (D), and glycerol (G), using a least squares fit to their measured interfacial tensions with the nonpolar sample liquid. The choice of the set {W, E, D, G} is conceptually justified by the fact that the tabulated basicity/acidity ratios ($\gamma_{L_2}^-/\gamma_{L_2}^+$) of these liquids differ widely (Table 2.1), which helps ensure that the respective interfacial tension measurements yield complementary information.^{19,35} We also impose an additional constraint for the total surface energy of the oil-based system, $\gamma_{L_1}^{total} = \gamma_{L_1}^{LW} + 2(\gamma_{L_1}^+)^{1/2}(\gamma_{L_1}^-)^{1/2}$, to be below 40 mJ/m², which is justified by the observed complete spreading of all our nonpolar samples on a PMMA surface with surface energy 38.8 mJ/m² (we found that without this constraint, the least squares fit sometimes yielded a physically meaningless, large LW parameter).

In the following sections, we will first verify that the proposed method produces reasonable results when applied to a pure, nonpolar solvent for which literature values of the vOCG parameters are available; next we apply it to nonpolar solutions of surfactants with small structural variations, and show that the result is consistent with expectations based on the surfactant chemistry, and that it can help rationalize qualitative differences in one surfactant's affinity for different solid surfaces. Lastly, we use the proposed method to determine the vOCG parameters for a commercial surfactant in hexane-based solution, derive a prediction for the interfacial tension of that solution with a polar

solvent (formamide), and test the prediction experimentally. Potential limitations of the current approach are discussed throughout.

2.3.2. Component Parameters of Pure Hexane

First, we examine whether the constrained best fit to the over-determined equation set (Eq. 2.4) produces a meaningful solution set for the case of the pure nonpolar solvent hexane, as a model sample whose component parameters are known.^{21,28} Table 2.2 shows the measured interfacial tensions and their standard deviation over four independent measurements. Using these four measured interfacial tensions in Equation 2.4 and solving for the vOCG parameters of hexane by the constrained least squares fit, yields the result reported in Table 2.3. The result is in reasonably good agreement with the literature values^{21,28} also shown in the Table 2.3.

Table 2.2. Measured interfacial tensions of pure hexane with four polar reference liquids (in mJ/m^2). Here the reported error margin is the experimental standard deviation over four measurements.

Oil	Measured Interfacial Tension γ_{LL} (mJ/m^2)			
	Water (W)	Ethylene Glycol (E)	Dimethyl Sulfoxide (D)	Glycerol (G)
Pure Hexane	49.3 ± 0.2	16.0 ± 0.1	8.8 ± 0.07	27.5 ± 0.04

Table 2.3. Inferred surface energy component parameters for hexane based on the best fit solution to the over-determined equation set (Eq. 2.4) with interfacial tension data from the four reference liquids (in mJ/m²). The literature values are also shown.^{21,28}

Condensed Phase	Component Parameters		
	$\gamma_{L_1}^{LW}$	$\gamma_{L_1}^+$	$\gamma_{L_1}^-$
Pure Hexane (<i>inferred from above tension data</i>)	17.6	0.08	0
Pure Hexane (<i>literature</i>) ^{21, 28}	18.4	0	0

Encouraged by this result for pure hexane, we proceed to explore applying the same strategy to hexane-based surfactant solutions in contact with a polar phase.

2.3.3. Lewis Acid/Base Behavior of Surfactant Solutions in Contact with a Polar Phase

We now use the proposed approach to characterize the acid/base properties of a series of PIBS surfactants in hexane and discuss the plausibility and usefulness of the results. As an example demonstrating the practical merit of the obtained parameters, we show how they can be used to explain the outcome of an adsorption study that would otherwise be difficult to rationalize. We also show that the parameters $\gamma_{L_1}^{LW}$, $\gamma_{L_1}^+$, and $\gamma_{L_1}^-$ obtained for a hexane solution of commercial surfactant can be used predict the interfacial tension of that solution with a polar liquid (formamide) that is *not* part of the employed reference set (but “well represented” by it).

The measured interfacial tensions of three surfactants solutions, PIBS-C, PIBS-O, and PIBS-N in pure hexane, with four reference liquids {W, E, D, G} are shown in Figure 2.4 to 2.7 as a function of the surfactant concentration.

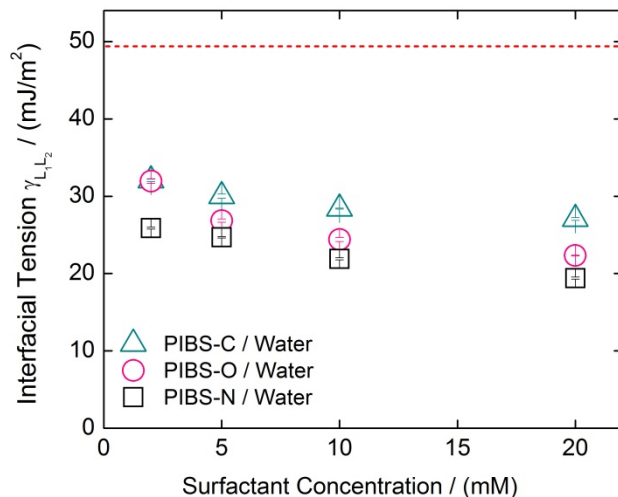


Figure 2.4. Measured interfacial tensions of PIBS/hexane solutions with water, shown as a function of surfactant concentration (in mJ/m²). Interfacial tensions of pure hexane are indicated with the red-dotted lines for comparison.

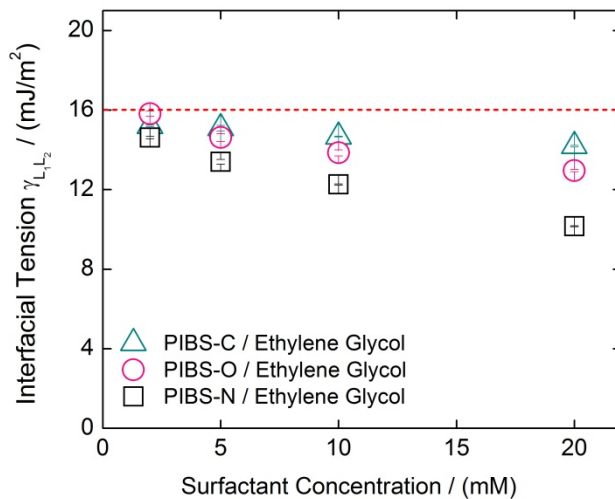


Figure 2.5. Measured interfacial tensions of PIBS/hexane solutions with ethylene glycol, shown as a function of surfactant concentration (in mJ/m²). Interfacial tensions of pure hexane are indicated with the red-dotted lines for comparison.

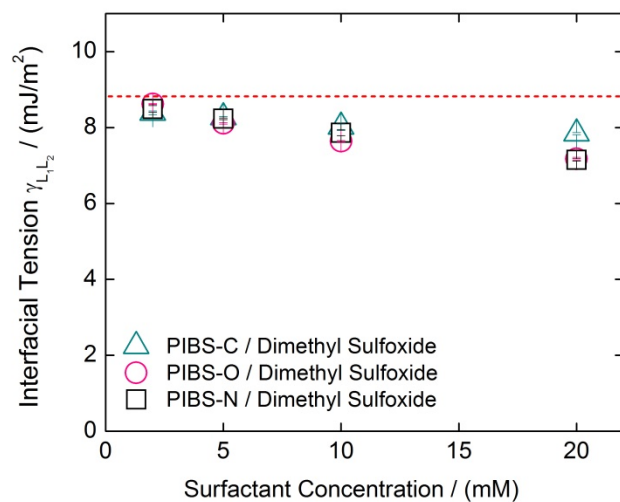


Figure 2.6. Measured interfacial tensions of PIBS/hexane solutions with dimethyl sulfoxide, shown as a function of surfactant concentration (in mJ/m²). Interfacial tensions of pure hexane are indicated with the red-dotted lines for comparison.

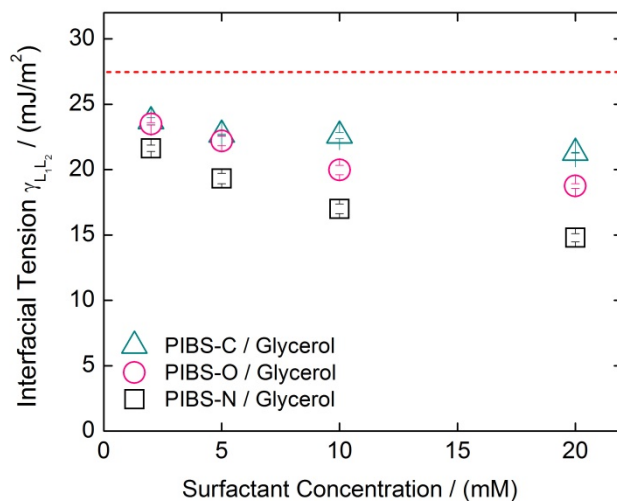


Figure 2.7. Measured interfacial tensions of PIBS/hexane solutions with glycerol, shown as a function of surfactant concentration (in mJ/m²). Interfacial tensions of pure hexane are indicated with the red-dotted lines for comparison.

Several clear trends can be observed. As would be expected, the oil-borne surfactants systematically lower the interfacial tension with polar reference liquids by interfacial adsorption (the corresponding interfacial tensions of pure hexane are indicated by the red-dotted lines in Figures). By contrast, *no* decrease in the surface tension at the air/oil interface is found (data not shown), confirming that the apolar gas phase does not promote surfactant adsorption at the oil surface, and that conversely the surfactant adsorption at polar interfaces suggested by Figures only occurs *in response* to the presence of the polar phase and is thus an adaptive behavior, not the reflection of an intrinsic property of the solution. It is further observed that the interfacial tension decreases as the bulk surfactant concentration increases, consistent with an increase in the effective polarity of the oil phase caused by the increased number of surfactant polar moieties in the interfacial region. There are also systematic differences in the interfacial tension between the three types of surfactant solutions, which likely reflect different acid/base properties of the surfactants' polar moieties. The tendency of decreasing the interfacial tension of hexane-based solutions with polar reference liquids follows the order PIBS-N > PIBS-O > PIBS-C.

The resulting vOCG component parameters for the three surfactant solutions based on the constrained fit to the overdetermined equation set (2.4) are shown in Figure 2.8 to Figure 2.10. It is found that the presence of surfactants imparts an effective nonzero basicity ($\gamma_{L_1}^- > 0$) or acidity ($\gamma_{L_1}^+ > 0$) to the nonpolar solution, whereas both parameters for the pure solvent were essentially zero ($\gamma_{L_1}^+ \approx 0 \approx \gamma_{L_1}^-$). As one would expect, these parameters are found to increase with increasing surfactant concentration.

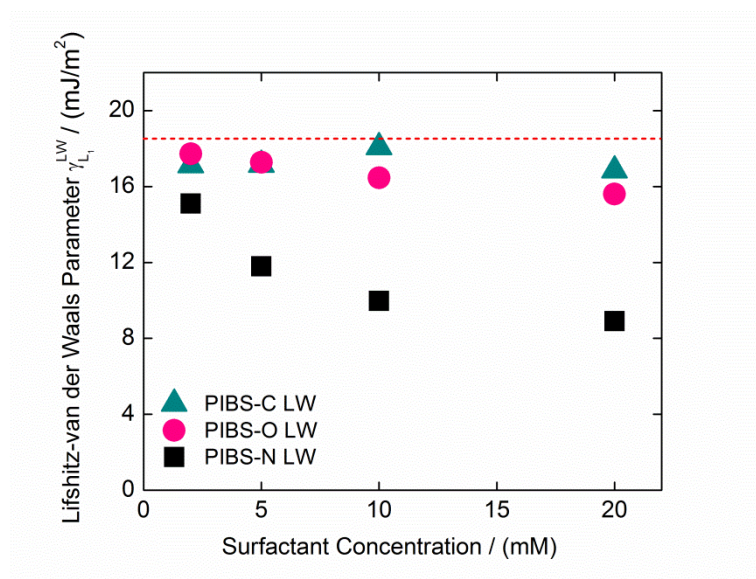


Figure 2.8. Inferred Lifshitz-van der Waals parameters γ_L^{LW} of PIBS/hexane solutions, shown as a function of surfactant concentration (in mJ/m²). Literature parameters for pure hexane are indicated with the red-dotted lines for comparison.

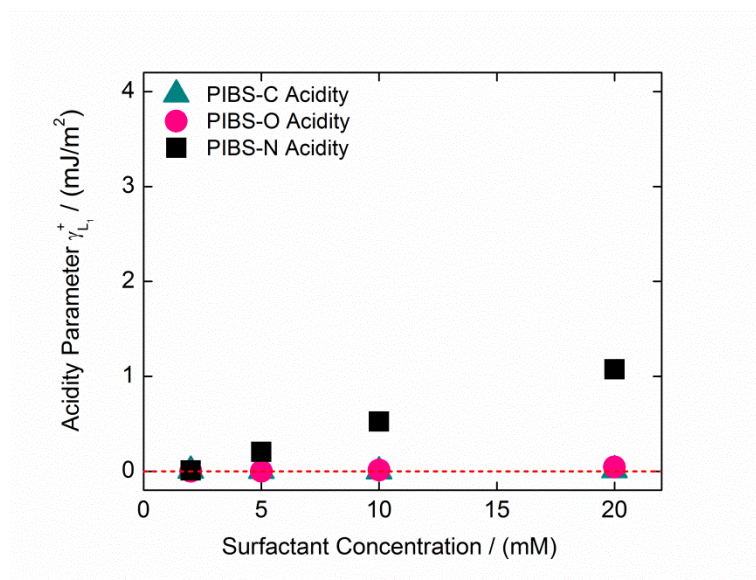


Figure 2.9. Inferred acidity parameters γ_L^+ of PIBS/hexane solutions, shown as a function of surfactant concentration (in mJ/m²). Literature parameters for pure hexane are indicated with the red-dotted lines for comparison.

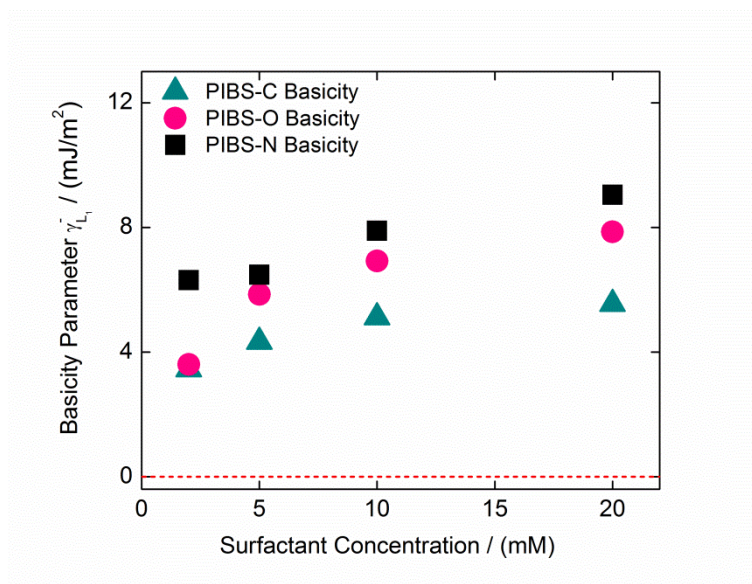


Figure 2.10. Inferred basicity parameters $\gamma_{L_1}^-$ of PIBS/hexane solutions, shown as a function of surfactant concentration (in mJ/m²). Literature parameters for pure hexane are indicated with the red-dotted lines for comparison.

Especially the inferred base parameters (Figure 2.10) for these succinimide-based molecules with a tertiary amine group are large, which is consistent with qualitative descriptions of the commercial surfactant mixture of PIBS analogs.^{7,11,17} Here, the systematic differences in the basicity parameter for the three surfactant solutions allow for a facile comparison of the surfactants' Lewis basicity. The order of basicity is PIBS-N > PIBS-O > PIBS-C, following the general trend of interfacial tension decrease for the three systems. The larger basicity of PIBS-O and PIBS-N compared to PIBS-C can be readily understood considering the larger number of lone electron pairs of the oxygen and the nitrogen in their hydrophilic head-group. The systematically larger basicity of PIBS-N compared to PIBS-O can be rationalized by considering the difference in

electronegativity between the oxygen and the nitrogen atom; the oxygen exerts a stronger pull on the electrons and thus limits the electron donicity.

We further observe only a small acid parameter for all surfactants (Figure 2.9). This does not warrant the conclusion that all surfactants in this study are inherently more basic than acidic. It has been pointed out that the somewhat arbitrary stipulation $\gamma_{Water}^+ = \gamma_{Water}^-$ of the vOCG model defines a reference scale by which values of γ^- for other materials tend to exceed the corresponding values of γ^+ , and alternative reference scales that do not result in the apparent predominance of basicity over acidity can be chosen.²⁶ Since the scale is arbitrary, the acidity and basicity parameter of the same material cannot be compared meaningfully; comparisons should only be made between the acidity parameters (or between the basicity parameters) of different materials.²⁶ In our system, the acidity parameter of PIBS-N is observed to be larger than that of PIBS-O and PIBS-C. This can be appreciated by considering the presence of an unsubstituted nitrogen (N-H) in the hydrophilic head-group which can act as a proton donor

Advantages of Working with “Component” Parameters

The possibility of separately comparing the acid and the base properties of different surfactants can be a significant advantage of the present method over characterizations based on potentiometric titration, such as the traditional “base number” commonly used to characterize commercial PIBS surfactants.²⁵ This traditional metric does not indicate any Lewis acidity of the surfactant, but merely reflects a “net balance” between acidity and basicity (in the *Brønsted* sense and with respect to one particular medium). A surfactant like our PIBS-N would only be identified as “strongly basic” by

this metric. By contrast, our analysis identified this surfactant as having non-negligible Lewis acidity, too (Figure 2.9), which could manifest itself for instance in attractive acid-base interaction with surfaces of significant Lewis basicity but negligible acidity.

Some support for such interactions was found in a study of PIBS-N adsorption from hexane solution onto different polymer surfaces with negligible Lewis acidity and different degrees of Lewis basicity. Here, we conducted a direct surfactant mass deposition experiment using a quartz crystal microbalance (QCM). We passed the PIBS-N/hexane solution over the quartz crystals coated with either polymethyl methacrylate (PMMA, $\gamma_{PMMA}^{LW} = 38.8 \text{ mJ/m}^2$, $\gamma_{PMMA}^+ \approx 0$, and $\gamma_{PMMA}^- = 15.4 \text{ mJ/m}^2$)^{10,19} or polystyrene (PS, $\gamma_{PS}^{LW} = 39.1 \text{ mJ/m}^2$, $\gamma_{PS}^+ \approx 0$, and $\gamma_{PS}^- = 1.5 \text{ mJ/m}^2$).^{10,19} Upon exposure of the polymer surface to the surfactant solution, we observed a remarkably larger decrease in the resonance frequency (Δf) for the PMMA surface than for the PS surface (Figure 2.11). Since the decrease in the resonance frequency (Δf) is directly proportional to the increase in the mass coupled to the surface,²⁹ this result indicates that a significantly larger amount of surfactant adsorbed onto the PMMA. Moreover, after flushing the surface with pure hexane, a much larger amount of surfactant remained adsorbed on the PMMA surface than on the PS surface, indicating a much stronger surfactant adhesion to the PMMA. Given the similar LW components and negligibly small acidity components of both polymeric surfaces, the observed difference in surfactant adsorption and adhesion can be understood qualitatively by noting the surfactant's non-negligible Lewis acidity, which causes a stronger donor-acceptor interaction with the surface of higher Lewis basicity (PMMA). This kind of analysis has not been possible with the traditional acid/base analysis for oil-soluble surfactants.

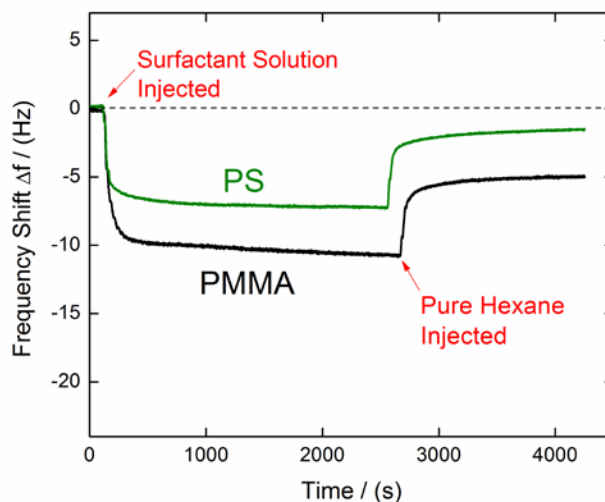


Figure 2.11. The resonance frequency shift of polymer-coated quartz crystal microbalances in response to the change in surfactant mass coupled to the surfaces; data for a PS surface is shown in green, data for a PMMA surface in black.

As exemplified above, our method of characterizing the effective Lewis acid/base properties of surfactants may provide useful insights into donor-acceptor interactions of nonionic surfactants in nonpolar solutions, and from our results of Figure 2.4 – 2.10 it appears that the parameters used to quantify these interactions are sensitive enough to resolve differences caused by subtle variations in surfactant chemistry. It should however be remembered these parameters reflect a complex interfacial phenomenon rather than an intrinsic surfactant property; as *effective* quantities for surfactant solutions in contact with a polar phase, they still depend on the surfactant concentration. Therefore, the surfactant concentration in the sample solutions needs to be consistent for a meaningful comparison of the acid/base properties of different surfactants of interest. It must also be expected that surface-active impurities in surfactant solutions can alter the resulting acid/base

parameters or even mask the surfactant properties. Careful purification thus appears critical to studying the surfactant properties. Measurements without prior purification, on the other hand, may still be useful if the goal is to compare the net acid/base properties of different (possibly impure) nonpolar solutions; and if the surfactant properties in pure solutions were known independently, the suggested method may in fact be used as a tool for examining the purity of solution samples.

Due Caution Required for Practical Calculations Using the Inferred Parameters

Since the nonpolar solutions' effective acid/base properties result from an *adaptive response* to the presence of the contacting phase and are determined from measurements of interfacial tensions with a series of the polar reference liquids ({W, E, D, G} in our study), it should be understood that the inferred "solution parameters" $\gamma_{L_1}^{LW}$, $\gamma_{L_1}^+$, and $\gamma_{L_1}^-$ can only be expected to accurately reflect the behavior at interfaces with polar phases "well-represented" by the reference liquids in the sense that their component parameters fall within the parameter region covered by the reference liquids. For interfaces with media of weaker or stronger polarity, the inferred parameters will give a poorer approximation of the solutions' actual acid/base characteristics, and the behavior at interfaces with nonpolar media will not be described by them at all. Therefore, we note once again, that the information provided by the inferred parameters should be considered at best *semi-quantitative*.

To demonstrate an application with a well-represented polar phase, we prepared a solution of a commercial PIBS mixture (OLOA11000, Chevron Oronite) at a randomly chosen concentration (1 mg/mL); the exact chemical identity/proportion of the main

PIBS constituents and possible impurities of this proprietary material are poorly defined.¹⁷ The measured interfacial tensions of this solution with reference liquids {W, E, D, G} are shown in Table 2.4. We observe somewhat larger standard deviations than for our custom-synthesized surfactant systems, which may be related to various factors including sample aging, the content of impurities, or absorbed moisture. Using the means of the measured interfacial tensions (Table 2.4) in Equation 2.4 and applying our constrained least squares fit to the resulting overdetermined equation set, we obtain the acid/base parameters for this sample shown in Table 2.5. Next, we use these “solution parameters” to estimate (“predict”) the interfacial tension of this sample with formamide, another polar solvent besides our reference liquids whose vOCG parameters are available in the literature¹⁹ and listed in Table 2.5. Formamide falls squarely into the parameter range described by the reference liquids: the location of formamide in the triangular diagram of $\gamma^{LW}/\gamma^{total}$, γ^+/γ^{total} , and γ^-/γ^{total} lies in fact inside the polygon generated by linking the locations of our reference liquids.²⁶ From Equation 2.4 with the parameters of formamide and of our surfactant solution, we calculate an estimated value for the interfacial tension of those two liquids of 11.3 mJ/m² (Table 2.5). This quantity is in excellent agreement with the independently measured interfacial tension of 10.9 ± 0.5 mJ/m², suggesting that the inferred vOCG parameters can indeed afford some predictive power if used with due caution and within the narrow confines of contacting phases well-represented by the set of reference liquids used to measure the parameters.

Table 2.4. Measured interfacial tensions of OLOA11000/hexane solution using four polar reference liquids.

Oil	Measured Interfacial Tension $\gamma_{L_1L_2}$ (mJ/m ²)			
	Water (W)	Ethylene Glycol (E)	Dimethyl Sulfoxide (D)	Glycerol (G)
OLOA11000 / Hexane	20.1 ± 0.9	7.3 ± 0.3	4.7 ± 0.1	13.1 ± 0.4

Table 2.5. Inferred parameters of OLOA11000/hexane solution and comparison of the calculated and measured interfacial tension between OLOA11000/hexane solution and formamide.

Condensed Phase	Component Parameters (mJ/m ²)			Interfacial Tension (mJ/m ²)	
	$\gamma_{L_1}^{L_1W}$	$\gamma_{L_1}^+$	$\gamma_{L_1}^-$	Calculated	Measured.
OLOA11000 / Hexane	10.6	1.4	7.4	11.2	10.9 ± 0.5
Formamide ¹⁹	39	2.28	39.6		

To avoid confusion, we would like to stress in closing, that the parameters we propose to analyze, although formally evaluated like the familiar energy component parameters of the vOCG theory, are used here simply and pragmatically as a phenomenological indicator of the solution's net and adaptive behavior when contacting a specific type of condensed phase. As such they have no precise *thermodynamic* meaning and certainly do not quantify any “intrinsic property of the solution”; in this sense they differ very much from the energy component parameters assigned to pure phases in the vOCG theory. We have adopted the parameter notation and an experimental

approach inspired by the vOCG energy component theory, because it provides a formal framework that is easily applicable to both solid and liquid interaction partners. We imply no endorsement of the vOCG method over competing approaches in the thermodynamic analysis of pure phases for which it was originally developed.

2.4. Conclusion

We propose a simple and economic method of characterizing the effective Lewis acid/base properties of oil-soluble nonionic surfactants at the interface of nonpolar oils with a more polar phase. It involves measuring the interfacial tension of surfactant solutions in a purely dispersive solvent (like alkanes) with at least four polar reference liquids of known energy component parameters and substantially different ratios of the acidity and basicity parameter, such as the quadruplet {water, ethylene glycol, dimethyl sulfoxide, glycerol}. The over-determined set of model equations (Eq. 2.4 for all reference liquids) is solved for the three “surfactant solution parameters” $\gamma_{L_1}^{LW}$, $\gamma_{L_1}^+$, and $\gamma_{L_1}^-$ using a constrained least squares fit to the measured interfacial tensions. The parameters obtained in this way are useful indicators of the solution’s effective acid/base behavior when in contact with a second phase that is *sufficiently polar* to be well represented by the employed set of reference liquids. When applied to pure hexane (solution in the infinite dilute limit), the method yielded parameters values consistent with the literature. For hexane-based solutions of several custom-synthesized PIBS surfactants with systematic chemical variations, we obtained parameter values consistent with the surfactants’ chemical composition and helpful in interpreting an independent

experiment probing the adsorption of one surfactant type to different polymer substrates. Parameters determined for a commercial surfactant in hexane allowed us to accurately predict the interfacial tension of that solution with a polar liquid outside the set of reference liquids used in the analysis. These results suggest that the proposed method, when used with due caution, allows for a useful heuristic characterization of nonionic surfactants in nonpolar solutions interacting with a polar condensed phase. It follows a simple protocol requiring only standard equipment for interfacial tensiometry and small amounts of sample. We believe that the extracted attributes, which refer to an adaptive behavior rather than an intrinsic material property, are highly relevant for a number of industrial applications and expect that the suggested method will be particularly useful for applications/studies involving hydrophilic solid surfaces in contact with nonpolar surfactant solutions, where the direct measurement of the interfacial energy via contact angle measurements is practically impossible.

2.5. References

1. Manisha Mishra; Muthuprasanna, P.; Surya Prabha, K.; Sobhita Rani, P; Satish Babu, I. A.; Sarath Chandiran, I.; Arunachalam, G.; Shalini, S. Basics and Potential Applications of Surfactants – A Review. *Int. J. PharmTech Res.* **2009**, *1*, 1354-1365.
2. Tomlinson, A.; Scherer, B.; Karakosta, E.; Oakey, M.; Danks, T. N.; Heyes, D. M.; Taylor S.E. Adsorption Properties of Succinimide Dispersants on Carbonaceous Substrates. *Carbon* **2000**, *38*, 13-28.
3. Texter, J. *Reactions and Synthesis in Surfactant Systems*; CRC Press: New York, 2001.
4. Shen, Y; Duhamel, J. Micellization and Adsorption of a Series of Succinimide Dispersants. *Langmuir* **2008**, *24*, 10665-10673.

5. Tomlinson, A.; Danks, T. N.; Heyes, D. M. Interfacial Characterization of Succinimide Surfactants. *Langmuir* **1997**, *13*, 5881-5893.
6. Atta, A. M.; Elsaed, A. M. Use of Rosin-Based Nonionic Surfactants as Petroleum Crude Oil Sludge Dispersants. *J. Appl. Polym. Sci.* **2011**, *122*, 183-192.
7. Parent, M. E.; Yang, J.; Jeon, Y.; Toney, M. F.; Zhou, Z-L.; Henze, D. Influence of Surfactant Structure on Reverse Micelle Size and Charge for Nonpolar Electrophoretic Inks. *Langmuir* **2011**, *27*, 11845-11851.
8. Guo, Q.; Singh, V.; Behrens, S. H. Electric Charging in Nonpolar Liquids Because of Nonionizable Surfactants. *Langmuir* **2010**, *26*, 3203-3207.
9. Espinosa, C.E.; Guo, Q.; Singh, V.; Behrens, S. H. Particle Charging and Charge Screening in Nonpolar Dispersions with Nonionic Surfactants. *Langmuir* **2010**, *26*, 16941-16948.
10. Guo, Q.; Lee, J.; Singh, V.; Behrens, S. H. Surfactant Mediated Charging of Polymer Particles in a Nonpolar Liquid. *J. Colloid Interface Sci.* **2013**, *392*, 83-89.
11. Poovadorom, S.; Berg, J. C. Effect of Particle and Surfactant Acid-Base Properties on Charging of Colloids in Apolar Media. *J. Colloid Interface Sci.* **2010**, *346*, 370-377.
12. Gacek, M.; Brooks, G.; Berg, J. C. Characterization of Mineral Oxide Charging in Apolar Media. *Langmuir* **2012**, *28*, 3032-3036.
13. Gacek, M.; Berg, J. C. Investigation of Surfactant Mediated Acid-Base Charging of Mineral Oxide Particles Dispersed in Apolar Systems. *Langmuir* **2012**, *28*, 17841-17845.
14. Kanicky, J. R.; Shah, D. O. Effect of Degree, Type, and Position of Unsaturation on the pK_a of Long-Chain Fatty Acids. *J. Colloid Interface Sci.* **2002**, *256*, 201-207.
15. Schramm, L. L. *Surfactants: Fundamentals and Applications in the Petroleum Industry*; Cambridge University Press: Cambridge, 2000.
16. Asadov, Z. H.; Tantawy, A. H.; Zarbaliyeva, I. A.; Rahimov, R. A.; Ahmadova, G. A. Surfactants Based on Palmitic Acid and Nitrogenous Bases for Removing Thin Oil Slicks from Water Surface. *Chem. J.* **2012**, *2*, 136-145.
17. Morrison, I. D. Electrical Charges in Nonaqueous Media. *Colloids Surf., A* **1993**, *71*, 1-37.
18. Smith, G. N.; Eastoe, J. Controlling Colloid Charge in Nonpolar Liquids with Surfactants. *Phys. Chem. Chem. Phys.* **2013**, *15*, 424-439.
19. Pizzi, A.; Mittal, K. L. *Handbook of Adhesive Technology*; CRC Press: New York, 2003.

20. Solomons, T. W. G.; Fryhle, C. B. *Organic Chemistry*; Wiley: New York, 2009.
21. van Oss, C. J.; Chaudhury, M. K.; Good, R. J. Interfacial Lifshitz-van der Waals and Polar Interactions in Macroscopic Systems. *Chem. Rev.* **1988**, *88*, 927-941.
22. van Oss, C. J.; Good, R. J.; Chaudhury, M. K. Additive and Nonadditive Surface Tension Components and the Interpretation of Contact Angles. *Langmuir* **1988**, *4*, 884-891.
23. van Oss, C. J.; Giese, R. F.; Wu, W. On the Predominant Electron-Donicity of Polar Solid Surfaces. *J. Adhesion* **1997**, *63*, 71-88.
24. Standard Test Method for Acid Number of Petroleum Products by Potentiometric Titration (ASTM D664-11a). DOI: 10.1520/D0664-11A (accessed Oct 20, 2014).
25. Standard Test Method for Base Number of Petroleum Products by Potentiometric Perchloric Acid Titration (ASTM D2896-11). DOI: 10.1520/D2896-11 (accessed Oct 20, 2014).
26. Della Volpe, C.; Siboni, S. Acid-Base Surface Free Energies of Solids and the Definition of Scales in the Good-van Oss-Chaudhury Theory. *J. Adhes. Sci. Technol.* **2000**, *14*, 235-272.
27. Hwang, G.; Yang, J.; Lee, C.-H.; Ahn, I.-S.; Mhin, B. J. New Selection Criterion for a Base Polar Liquid in the Lifshitz-van der Waals/Lewis Acid-Base Approach. *J. Phys. Chem. C* **2011**, *115*, 12458-12463.
28. Giese, R. F.; van Oss, C. J. *Colloid and Surface Properties of Clays and Related Minerals*; CRC Press: New York, 2002.
29. Dixon, M. C. Quartz Crystal Microbalance with Dissipation Monitoring: Enabling Real-Time Characterization of Biological Materials and Their Interactions. *J. Biomol. Tech.* **2008**, *19*, 151-158.
30. Mittal, K. L. *Contact Angle, Wettability and Adhesion*; CRC Press: New York, 2009.
31. Della Volpe, C.; Maniglio, D.; Siboni, S.; Morra, M. Recent Theoretical and Experimental Advancements in the Application of van Oss-Chaudhury-Good Acid-Base Theory to the Analysis of Polymer Surfaces I. General Aspects. *J. Adhes. Sci. Technol.* **2003**, *17*, 1477-1505.
32. Della Volpe, C.; Maniglio, D.; Brugnara, M.; Siboni, S.; Morra, M. The Solid Surface Free Energy Calculation I. In Defense of the Multicomponent Approach. *J. Colloid Interface Sci.* **2004**, *271*, 434-453.
33. Good, R. J.; Hawa, A. K. Acid/Base Components in the Molecular Theory of Adhesion. *J. Adhesion* **1997**, *63*, 5-13.

34. Azioune, M.; Chehimi M. M.; Miksa, B.; Basinska, T.; Slomkowski, S. Hydrophobic Protein-Polypyrrole Interactions: The Role of van der Waals and Lewis Acid-Base Forces as Determined by Contact Angle Measurements. *Langmuir* **2002**, *18*, 1150-1156.
35. Hollander, A. On the Selection of Test Liquids for the Evaluation of Acid-Base Properties of Solid Surfaces by Contact Angle Goniometry. *J. Colloid Interface Sci.* **1995**, *169*, 493-496.

CHAPTER 3

INVESTIGATION OF PARTICLE CHARGING WITH SYSTEMATIC VARIATION OF SURFACTANT CHEMISTRY

3.1. Introduction

The underlying mechanisms of the particle charging, as introduced earlier, are not yet understood, although different hypotheses exist.¹⁻¹⁶ Some of these assume that surface charges are “created at the particle surface” via charge transfer between neutral surface moieties and neutral surfactants,³⁻⁸ whereas others favor the notion that surface charges are “acquired from the liquid bulk” via adsorption of the charged species.⁹⁻¹⁶

The first pathway of surface charging, sometimes referred to as “acid-base mechanism” of particle charging, was initially proposed by Fowkes and co-workers³⁻⁴ decades ago, and strongly promoted in some recent studies.⁵⁻⁸ This hypothetical charging mechanism implies a three-step process, in which electrically neutral surfactants first adsorb to the particle surfaces, donate or accept protons or electrons according to the relative acid/base (donor/acceptor) strength between the surfactant and particle, and finally desorb from the particle surface in a charged state, leaving the particle oppositely charged.

According to the second hypothetical mechanism, surfactant-stabilized charges of different sign generated in the liquid bulk adsorb asymmetrically to the particle surface, thus generating a net surface charge. The preference for a particular sign of charge has

been attributed tentatively to differences in the strength of the adsorbing ions' charge – dipole interaction with surface dipoles.¹⁰ For systems containing *ionic* surfactants such as the popular Aerosol-OT (AOT, sodium bis(2-ethyl-1-hexyl)-sulfosuccinate), it has been proposed that the net surface charge is achieved by the preferential adsorption of either the ionized surfactant or its counter-ion, depending on the *hydrophilicity* of the particle surface.¹³

Results from our own recent study on polymer particles with different surface functionalities in nonpolar solutions of either ionic or nonionic surfactants¹⁷ could not be fully explained by any one of the previously proposed mechanisms alone.

A better understanding of electric charging in nonpolar dispersions, important in both industrial applications and academic research, calls for a more general theory that reconciles previously competing models and recovers their individual merits. We believe that progress towards that goal will depend on experimental data in which relevant physicochemical parameters are precisely controlled and systematically varied.

An important aspect in this regard is the “surfactant chemistry”.^{2,18} It has been pointed out that studies of surface charging in nonpolar dispersions have focused on only few surfactants with vastly different chemical structures.¹⁻² The direct comparison of such widely dissimilar systems provides little help in identifying the influence of individual material properties on the observed charging phenomena.

In this Chapter, we investigate particle charging mediated by a series of surfactants with “minimal” variations in their chemical structure, PIBS-C, PIBS-N, and PIBS-O (Figure 2.3) – featuring similar nonpolar tails and differing in their polar section

only by a single electronegative atom at a fixed position. The micellar aggregates of these surfactants will be referred to, in the following, as “inverse micelles” and sometimes, for brevity, simply as “micelles”, with the understanding that in the nonpolar systems of our study, *all* micelles are characterized by the polar surfactant heads pointing inward and nonpolar tails facing outward – the inverse of the micelle structure familiar from aqueous solutions.

3.2. Materials and Methods

3.2.1. Surfactant Synthesis and Purification

Procedures for synthesis and purification of three custom surfactants, PIBS-C, PIBS-N, and PIBS-O, were described in the previous Chapter (section 2.2.2). In brief, polyisobutylene succinic anhydride (PIBSA) and different polyamines, N,N-diethylpentane-1,5-diamine, N,N-diethyldiethylenetriamine, and [2-(2-aminoethoxy)ethyl]diethylamine, were coupled to synthesize the three types of PIBS analogs. Here, the only difference in the chemical structure between three species is the type of electronegative atom located at the central position within the surfactant’s polar head portion. The tertiary amine end groups with diethyl substitutes were chosen to eliminate a possibility for generating a byproduct with di-PIB tails.¹⁸ The reaction products were purified by flash chromatography using silica gel as the stationary phase and a mixture of 20:1 chloroform / ethanol anhydrous as the mobile phase.

3.2.2. Preparation of Particle Dispersions (“Solvent Swap”)

The colloidal particles used in this Chapter were poly(methyl methacrylate) (PMMA) microsphere with a mean diameter 1.1 μm purchased from Bangs Laboratories (catalog #PP04N, lot #10710). Particles originally received as a stabilizer-free aqueous dispersion were transferred into isopropanol (>99.5%, Sigma-Aldrich) as the intermediate solvent and finally into the nonpolar surfactant solutions at a minimal surfactant concentration (0.5 mM), following the “solvent swap” procedure described previously.^{17,19} Centrifugation, disposal of the supernatant, and redispersion of particles in the target solvent via sonication were repeated three times in each transfer step. The washed particles were diluted to a particle concentration of ~0.003% wt. in nonpolar solutions in a range of surfactant concentrations (2 mM – 20 mM) for electrophoretic particle mobility measurements.

3.2.3. Electrophoresis

The electrophoretic mobility in nonpolar dispersions was measured by phase analysis light scattering (PALS)²⁰ using a Zetasizer Nano ZS90 (Malvern Instruments). A dip cell with two planar palladium electrodes spaced 2 mm apart was submerged in a sample dispersion held in a glass cuvette. An electric field of systematically varied strength (2.5 – 50 kV/m) was applied across the electrodes to obtain the field dependent mobility²¹⁻²⁴ based on time domain phase information of the light scattered by the particles. The field dependent mobility was then extrapolated to zero field strength to infer the equilibrium charging state of the particles in the absence of the applied electric field.^{7-8,17,19,25} Prior to the measurements, the dip cell and glass cuvette were sonicated in

tetrahydrofuran (THF, a good solvent for PIBS), carefully rubbed with a soft wipe in hot aqueous detergent solution, rinsed copiously, first with hot water and then with methanol, and dried with air.

3.2.4. Dynamic Light Scattering

The solvodynamic diameters of the inverse micelles formed by surfactants in nonpolar solutions were measured by dynamic light scattering (DLS) using the Zetasizer Nano ZS90. Measurements were taken at the forward scattering angle of 13° to maximize the scattering volume and signal intensity. A roughly constant solvodynamic diameter for the inverse micelles was observed above a surfactant concentration ~ 2 mM for all surfactant solutions; below this concentration, measurements were often aborted by the instrument because of the very low count rate – all the other experiments were conducted above this surfactant concentration where the formation of the inverse micelles could be confirmed (note that pinpointing the CMC in nonpolar surfactant solutions is known to be difficult^{1-2,5,26}). Glass cuvettes used for these measurements were cleaned as described above for the electrophoresis experiments.

3.2.5. Karl Fischer Titration

The residual water content of the nonpolar surfactant solutions and particle dispersions was determined by volumetric Karl Fischer titration using TitroLine KF titrator (SCHOTT). HYDRANAL®-Composite 5 was used as a Karl Fischer titration reagent. A mixture of chloroform and methanol (50:50) was used as a titration medium, rather than pure methanol, to avoid the accumulation of surfactants on the electrodes which prevents the diffusion of titration reagents. We confirmed a water content

~0.003 % wt. for pure hexane, consistent with the literature^{9,26}. For the particle dispersions used for electrophoresis, we found no measurable difference in water content from the surfactant solutions, within the instrumental measurement sensitivity.

3.2.6. Conductivity

The electric conductivity of the nonpolar surfactant solutions was measured using the nonaqueous conductivity probe DT-700 (Dispersion Technology, Inc.). During the measurement, a low frequency (1 Hz) AC field is applied between coaxial cylindrical electrodes. The measured current is displayed in the form of the specific conductivity based on the cell constant for the given electrode geometry. Conductivity in the order of 0.1 pS/m was confirmed for pure hexane, consistent with the literature.²⁶ Prior to the measurements, the probe was rinsed with THF, wiped in hot aqueous detergent solution, rinsed with acetone and methanol, air-dried, stabilized in a fume hood overnight, and finally rinsed with pure hexane.

3.3. Results and Discussions

3.3.1. Electrophoretic Particle Mobility

Surfactant-mediated electric charging of the PMMA particles was investigated by measuring the particles' electrophoretic mobility in nonpolar dispersions at various surfactant concentrations.

The mobility shows a non-monotonic field dependence in a range of the applied field strength from 2.5 kV/m to 50 kV/m (Figure 3.1, 3.3, and 3.5). Such a field

dependence is not usually encountered in aqueous dispersions where the Debye screening length tends to be small, and the electric field inside a particle's ion atmosphere so large, that the externally applied field in electrophoresis can be considered a small perturbation. By contrast, in nonpolar dispersions where the screening length can be very large (in the micron range) and the impact of external fields is more pronounced, field dependent mobilities are often observed^{7-8,17,19,21-25} and have been attributed hypothetically to the disintegration of the diffuse layer of ions surrounding the particle surface.^{21,23-24} Special caution is required in characterizing the field dependent mobility with PALS since strong external fields distort the measured signal (amplitude-weighted phase difference) to be fitted in calculating the particle mobility.²²

To avoid misinterpretations and to infer the particles' equilibrium surface charging state in the absence of external electric fields, we adopt the widely used strategy of extrapolating the field dependent mobility to zero field strength,^{7-8,17,19,25} the extrapolated "zero-field mobility" is shown in Figure 3.2, 3.4, 3.6, and 3.7.

Remarkably, the subtle structural difference in the surfactant chemistry led to a very different electrophoretic particle mobility, indicating clear differences in the magnitude and even the sign of particle charge; the PMMA particles acquired a positive surface charge in dispersions with PIBS-C and PIBS-O (with PIBS-O producing a larger charge magnitude), and a negative surface charge in the dispersion with PIBS-N. An attempt to rationalize this behavior will be presented in the following sections.

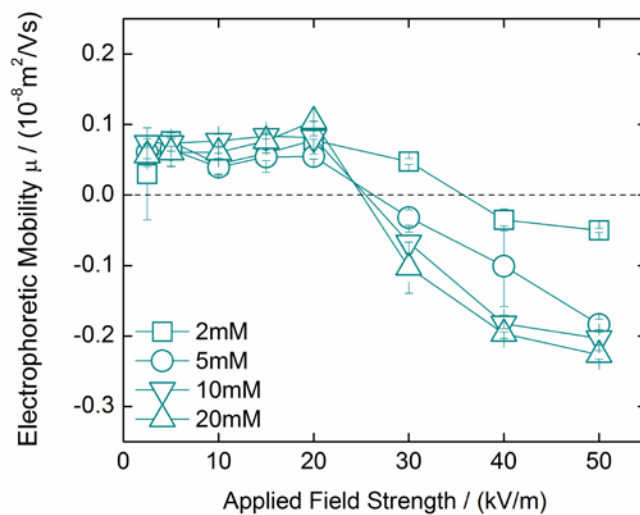


Figure 3.1. The field dependent electrophoretic mobility of the charged PMMA particle in hexane-based dispersions of the surfactant PIBS-C in the range of applied field strength between 2.5 kV/m to 50 kV/m.

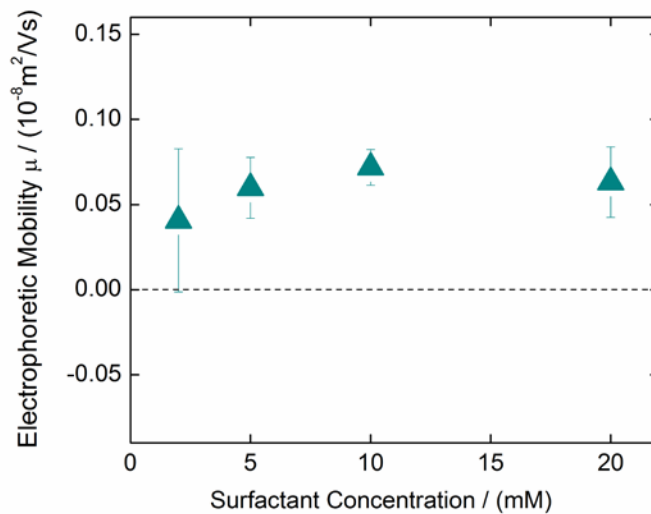


Figure 3.2. The zero-field electrophoretic mobility of the charged PMMA particle in hexane-based dispersions of the surfactant PIBS-C, represented as a function of surfactant concentration.

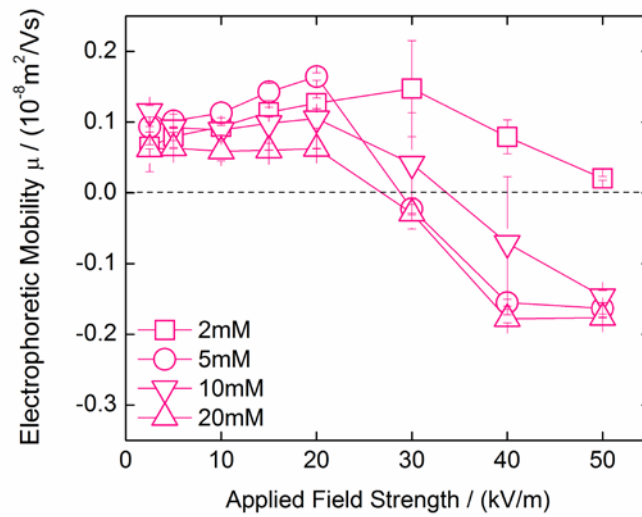


Figure 3.3. The field dependent electrophoretic mobility of the charged PMMA particle in hexane-based dispersions of the surfactant PIBS-O in the range of applied field strength between 2.5 kV/m to 50 kV/m.

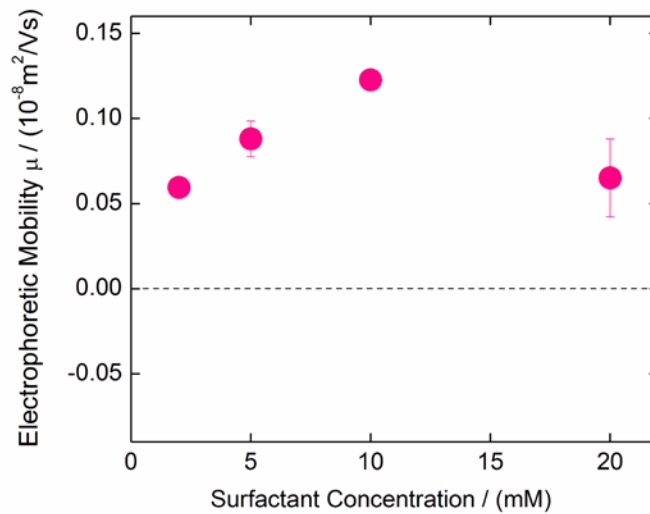


Figure 3.4. The zero-field electrophoretic mobility of the charged PMMA particle in hexane-based dispersions of the surfactant PIBS-O, represented as a function of surfactant concentration.

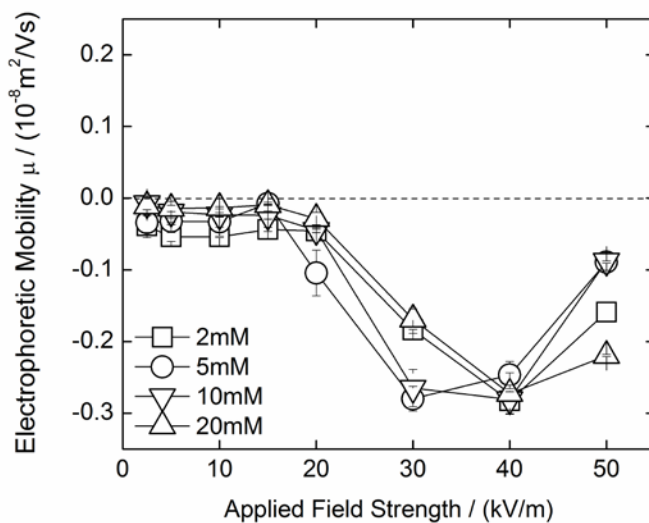


Figure 3.5. The field dependent electrophoretic mobility of the charged PMMA particle in hexane-based dispersions of the surfactant PIBS-N in the range of applied field strength between 2.5 kV/m to 50 kV/m.

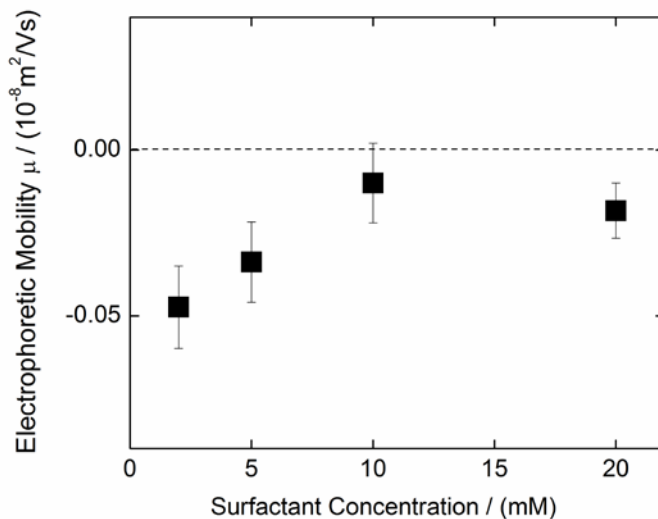


Figure 3.6. The zero-field electrophoretic mobility of the charged PMMA particle in hexane-based dispersions of the surfactant PIBS-N, represented as a function of surfactant concentration.

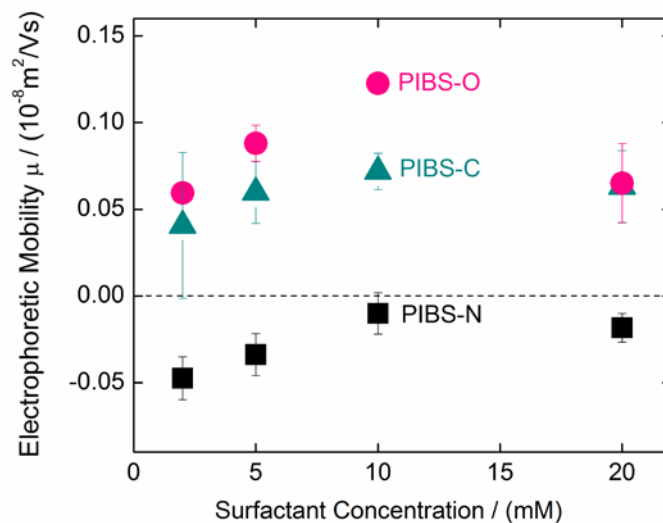


Figure 3.7. The zero-field electrophoretic mobility of the charged PMMA particle in hexane-based dispersions of the three PIBS surfactants, represented as a function of surfactant concentration.

3.3.2. Interpretation in Terms of Acid-Base Interaction between Particles and Surfactants

We first interpret the observed charging behavior in terms of acid-base interactions. The acid/base properties of the interaction partners, PMMA^{17,27-31} and the PIBS surfactant solutions,³² can be characterized separately, using the acidity (γ_i^+) and basicity (γ_i^-) parameters of the van Oss-Chaudhury-Good (vOCG) surface energy component model.²⁷⁻³¹

Acid/Base Parameters of the Solid Particle Surface

Although often referred to as “hydrophobic”,² the solid PMMA surface has non-negligible “polar” character;²⁸ it has long been considered predominantly basic^{3,17,27-31} due to the abundance of lone electron pairs from the carbonyl groups. In the framework

of the vOCG model, this is reflected by a large basicity parameters ($\gamma_s^- \gg 1$) and a negligibly small acidity parameters ($\gamma_s^+ \approx 0$), obtained by solving the equation²⁸

$$(1 + \cos \theta)\gamma_L = 2 \left[(\gamma_L^{LW} \gamma_s^{LW})^{\frac{1}{2}} + (\gamma_L^+ \gamma_s^-)^{\frac{1}{2}} + (\gamma_L^- \gamma_s^+)^{\frac{1}{2}} \right] \quad (3.1)$$

for the work of adhesion between the solid (PMMA) surface and a series of reference liquids with the measured contact angles θ as experimental coefficients. Here, the subscript “L” and “S” indicate the “(reference) liquid” and “solid”, the superscript “LW” indicates the “Lifshitz-van der Waals” parameter, a “nonpolar” surface energy component associated with the London dispersion interaction of fluctuating and induced dipoles (as opposed to the “polar” acidity and basicity components), and the parameter γ_L indicates the total surface tension of the reference liquid, which can be expressed in this framework as a combination of the surface energy components ($\gamma_L = \gamma_L^{LW} + 2(\gamma_L^+ \gamma_L^-)^{1/2}$). We have previously used contact angle measurements to characterize the acidity (γ_s^+) / basicity (γ_s^-) parameters of macroscopic surfaces fabricated from the type of PMMA particles used in the present study via dissolution and spin coating.¹⁷ The reported parameters are shown in Table 3.1 with other literature values^{27,29} for PMMA surfaces; they all identify the PMMA surfaces are *monopolar basic* ($\gamma_s^- = 15.4 \text{ mJ/m}^2$ and $\gamma_s^+ \approx 0$), confirming a significant ability to act as electron donor or proton acceptor in acid-base interactions with a contacting phase, but no or little propensity to act as proton donor or electron acceptor. We note that, differently from the PMMA particles used in some other studies,^{9-10,14-15} our particles do not have any steric stabilizer such as polyhydroxystearic acid (PHSA) grafted to their surface.

Table 3.1. Acid (γ_s^+) and base (γ_s^-) parameters of the solid PMMA, measured for films cast from our PMMA particles¹⁷ and adopted from the literature.^{27,29}

Solid	Component Parameters (mJ/m ²)	
	Acidity (γ_s^+)	Basicity (γ_s^-)
PMMA ^{*17}	≈ 0	15.4
PMMA ²⁷	≈ 0	14.6
PMMA ²⁹	≈ 0	9.5-22.4

* The parameters for surface coatings cast from our PMMA particles¹⁷ were used in the following analysis

Acid/Base Parameters of the Surfactant Solutions

The energy component model referenced above strictly addresses material properties of pure phases. We have proposed a heuristic extension of the acid/base parameter concept applicable to nonpolar solutions of nonionic surfactants in contact with a polar condensed phase, in the previous Chapter.³² In brief, we inferred the effective acidity ($\gamma_{L_1}^+$) and basicity ($\gamma_{L_1}^-$) of the PIBS/hexane solutions, caused by the interfacially adsorbed surfactants at polar contacting phases, by numerically solving a set of equations of the form^{28,32}

$$\gamma_{L_1 L_2} = [(\gamma_{L_1}^{LW})^{1/2} - \gamma_{L_2}^{LW}]^2 + 2[(\gamma_{L_1}^+)^{1/2} - (\gamma_{L_2}^+)^{1/2}][(\gamma_{L_1}^-)^{1/2} - (\gamma_{L_2}^-)^{1/2}] \quad (3.2)$$

where $\gamma_{L_1L_2}$ are measured interfacial tensions of the PIBS/hexane solution (L_1) with a series of polar reference liquids (L_2). It should be noted that the “solution parameters” $\gamma_{L_1}^{LW}$, $\gamma_{L_1}^+$, $\gamma_{L_1}^-$ obtained by this method do not reflect a material property, but the adaptive behavior of the surfactant in response to solution contact with a polar phase. Details of this behavior depend both on the surfactant concentration, which makes the solution parameters concentration dependent, and on the polar partner phase, which implies that predictions based on the solution parameter are necessarily approximative in nature. Nonetheless the solution parameters can be quite useful for comparisons of the relative acid or base strength of different surfactants or for estimates of the polar interaction energy of the surfactants with a polar second phase (a polar solid or liquid).³³ The measured acidity ($\gamma_{L_1}^+$) and basicity ($\gamma_{L_1}^-$) parameters of the three PIBS/hexane solutions can be found in Figure 2.8 and 2.9.

Analysis of the Particle Charging with the Predicted Acid-Base Interactions between the Particle Surface and Surfactant Solutions.

Now, we can predict the propensity of charge donor-acceptor (acid-base) interactions between the solid particle surface and the liquid surfactant solutions using their respective acidity and basicity parameters. This can be achieved by calculating the acid-base (polar) contribution $W_{SL_1}^{AB}$ to the work of adhesion $W_{SL_1} = W_{SL_1}^{LW} + W_{SL_1}^{AB}$, which further contains a Lifshitz-van der Waals (“nonpolar”) contribution $W_{SL_1}^{LW}$. The polar work of adhesion

$$W_{SL_1}^{AB} = -2(\gamma_s^+ \gamma_{L_1}^+)^{1/2} - 2(\gamma_s^- \gamma_{L_1}^-)^{1/2} \quad (3.3)$$

describes the energy of adduct formation between donor sites and acceptor sites of two condensed phases.

The basic sites of the solid surface can form adducts with acidic moieties of the liquid solution, *i.e.* with the acidic site of the interfacially adsorbed surfactant, to a free energy benefit around $-2(\gamma_s^- \gamma_L^+)^{1/2}$, according to Equation 3.3, and favor the formation of a *positive* charge on the solid surface upon separation of the Lewis pair. Similarly, acidic sites of the solid surface would form adducts with the basic moieties of the interfacially adsorbed surfactant, with an interaction energy of about $-2(\gamma_s^+ \gamma_L^-)^{1/2}$, favoring the formation of a *negative* surface charge, but this latter contribution is negligible in our case according to the negligible low surface acidity (Table 3.1). Figure 3.8 shows the non-negligible energy of adduct formation between the solid's (electron) donor sites with the liquid's acceptor sites (favoring *positive* surface charging), which roughly equals the total polar work of adhesion between the solid PMMA surface and the liquid surfactant solutions. According to these considerations, the PMMA surface should only acquire a positive charge through the acid-base interactions with the liquid-borne surfactants. While such interactions may contribute to the positive particle charging observed in the dispersions with PIBS-C and PIBS-O (Figure 3.7), the negative particle charging found in the PIBS-N dispersions *cannot* be explained by this mechanism; given that PIBS-N has relatively larger acidity than the other two surfactants, one should instead expect the most strongly *positive* particle charge in the presence of PIBS-N if donor-acceptor interactions between the particles and these surfactants were indeed responsible for the particle charge.

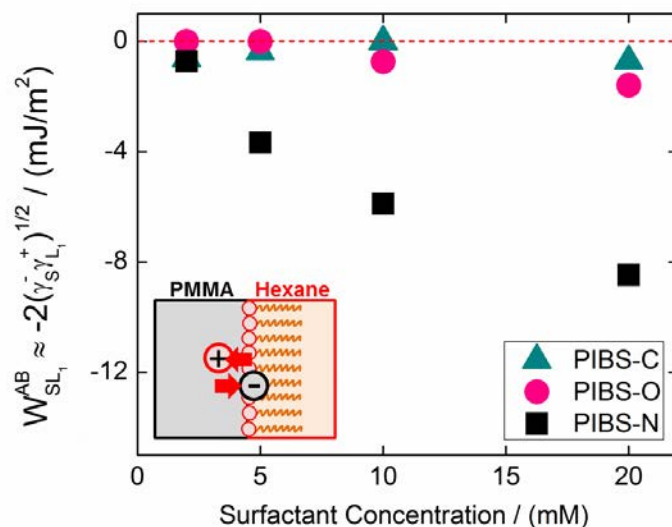


Figure 3.8. The polar (acid-base) work of adhesion between the solid PMMA surface (S) and the liquid surfactant solutions (L_1), which roughly equals the interaction energy (per unit area) of the solid's basic and the liquid's acidic moieties (favoring positive surface charging). The contribution of solid acid – liquid base interaction (which favors negative surface charging) is negligible according to the negligibly low surface acid parameter (Table 3.1).

3.3.3. Interpretation in Terms of Inverse Micellar Ion Adsorption

As an alternative source of the net particle charge, we will consider the preferential adsorption, at the particle surface, of charged entities with a particular sign of charge. In this case we face the challenge of rationalizing the selectivity of the adsorption process. For systems containing ionic, dissociable surfactants this task is facilitated by the fact that the dissociation products typically differ in size, hydrophobicity, etc.^{1,13} and might therefore be expected to interact differently with the particle surfaces. In our system of PIBS surfactants, which lack a clearly dissociable moiety, the situation is less clear. As mentioned before, charge fluctuation theory can account for the presence of

charged inverse micelles in the nonpolar surfactant solutions.^{1-2,5,9-10,26,33-38} Their generation is often pictured as arising from a disproportionation of neutral micelles,^{5,9-10,26,33-34} $2M \rightleftharpoons M^+ + M^-$, the details of which may involve dissociable impurities, such as water, in the polar micelle cores.^{1-2,8-9,14,26} Only the formation of “monovalent micellar ions” is typically considered, because more highly charged entities in the typical micelle size range would come at an excessive energy cost (Born energy).²⁶ It has been proposed that the micellar ions, rather than individual ionized molecules, adsorb to the particle surface⁹⁻¹⁰, where the surface preference of a certain sign of charge is determined by some unknown parameters.^{10,12} Assuming that both the positive and negative micellar ions are identical except for their charge sign,³⁴ the positive surface charging in the PIBS-C and PIBS-O solutions might be explained by the preferential adsorption of the positive micellar ions to the surface in terms of ion-dipole interaction,¹⁰ with the nucleophilic character of our PMMA particle reflected in its significantly nonzero basicity parameter γ_s^- . Again this simple framework does not explain the negative particle charging observed specifically in the dispersions with the surfactant PIBS-N, since the negative ions are not chemically preferred by the nucleophilic surface.

Instead of a *chemical* surface preference for the negatively charged PIBS-N micelles over their positively charged counterparts, we found evidence for a significant size asymmetry between the oppositely charged micelles that could explain a *physical* preference for the micellar anions. We recall that the polymer (micelle) adsorption can be achieved not only by specific *chemical anchoring*, but also by *physical binding* to the solid surface; and in the latter case, the “size” (degree of association) of adsorbates can influence the equilibrium adsorption state significantly.³⁹⁻⁴¹ In competitive physisorption

of larger and smaller aggregates, in particular, adsorption of the larger ones is favored by the minimization of the overall translational entropy loss associated with the adsorbate's confinement to the surface.⁴⁰ In a similar vein, the adsorption of anionic PIBS-N micelles should be favored entropically, if these were systematically larger than the corresponding cationic micelles.

This kind of size asymmetry is precisely what electrophoretic light scattering experiments in the micellar, particle-free solutions suggest. Figure 3.9 to 3.11 show the measured field-dependent electrophoretic mobility, where a net *negative* electrophoretic mobility is observed for micellar solutions of all three surfactant types. Given that electroneutrality dictates an equal number of positive and negative charges (and neglecting the energetically disfavored formation of multi-valent ions) one should expect a zero net electrophoretic mobility, if oppositely charged micelles were differed only in their sign of charge. The observed deviation from zero mobility, which is especially pronounced for the PIBS-N solutions, suggests that negatively charged micelles in these solutions scatter the incident laser light more strongly during the electrophoretic measurements than their positively charged counterparts, a strong indication that the micellar anions are systematically larger. Next, we discuss a possible origin of such a size asymmetry.

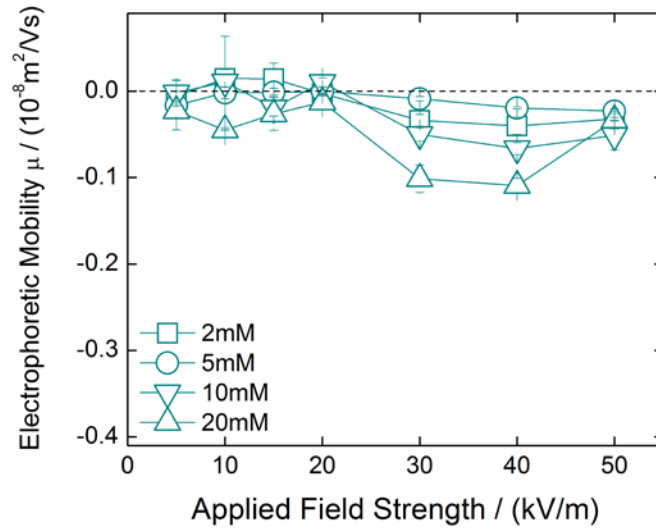


Figure 3.9. The field dependent electrophoretic mobility in the particle-free, hexane-based solutions of the surfactant PIBS-C.

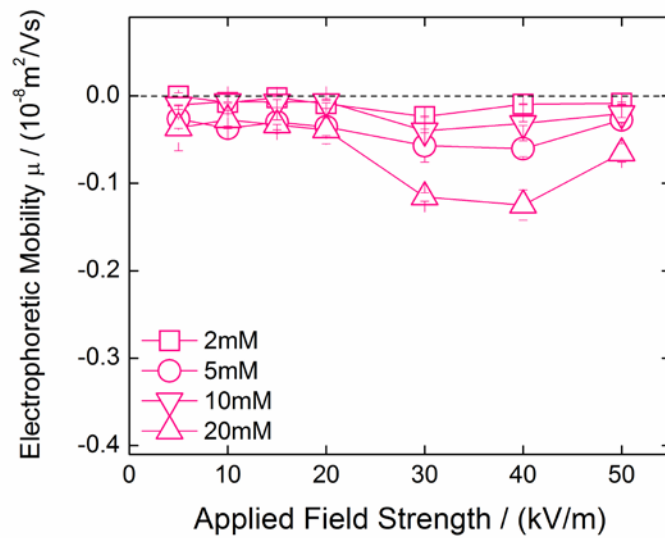


Figure 3.10. The field dependent electrophoretic mobility in the particle-free, hexane-based solutions of the surfactant PIBS-O.

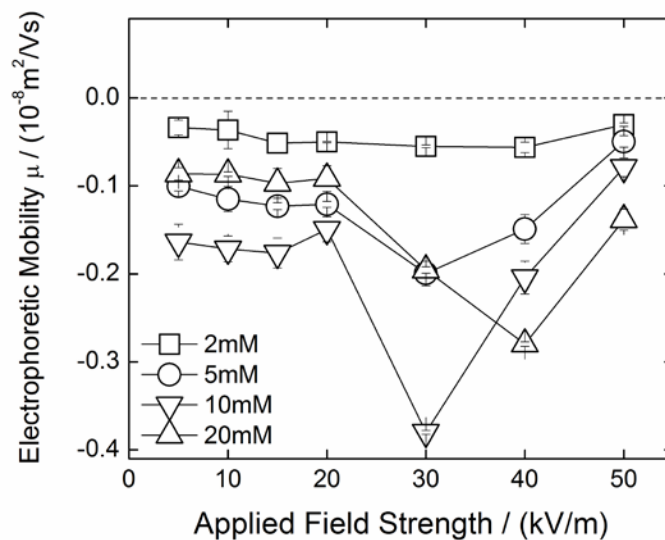


Figure 3.11. The field dependent electrophoretic mobility in the particle-free, hexane-based solutions of the surfactant PIBS-N.

Mechanisms of Micellar Ion Formation

(a) Size distribution of micellar structures in the presence of water as the third species.

First we recall that the micelle size, although commonly reported as a single (mean) value, is not usually uniform, but more realistically described by a distribution of finite width.⁴²⁻⁴³ Along with the variation in micelle size, one should expect a variation in the number of water molecules incorporated in hydrophilic micelle cores.^{1-2,5,8-10,26} We note that it is experimentally unrealistic² to avoid the presence of water in a nonpolar system completely: even nominally “pure” nonpolar solvents contain water molecules,^{9,26}

solutions of hygroscopic surfactants can absorb the ambient moisture during the course of experiments,⁹ and “drying” the surfactant can be impossible without partly decomposing it.¹⁴ Without any “added” water the inverse micelles can therefore exist in a “water-swollen” form,¹⁰ where the micelle size increases with the amount of water incorporated in the micelle core.^{14,26,44-46} Since the statistical probability of micelle charging is expected to increase dramatically with the core size^{26,37} and experiments typically suggest that only a small fraction of micelles becomes charged,^{26,43} it makes sense that this charged fraction would be dominated by exceptionally large micelles (those with a large aqueous core), a notion strongly supported by recent experiments using electrochemical impedance spectroscopy.⁴³ Our electrophoresis data of Figure 4 then further suggests that within this population of large, charged micelles, the very largest ones are more likely to carry a negative charge than a positive one, with an especially large bias for micelles of PIBS-N. Before speculating on the possible origin of this bias, we recall that micelles exist in a *dynamic* equilibrium^{1,4,42,45,47-49} that allows for spontaneous micelle fusion and fission, as well as for the dynamic exchange of individual surfactant molecules between two micelles or between a micelle and the solution bulk.^{1, 42, 45, 47-49}

(b) Intra-micellar donor-acceptor interaction and heterolysis.

A possible pathway toward charged micelles with the described size asymmetry involves i) intra-micellar donor-acceptor (acid-base) interaction and charge transfer between water and a surfactant molecule within a large swollen micelle and ii) transfer of the charged surfactant to a different micelle by molecular surfactant exchange as depicted in Figure 3.12.

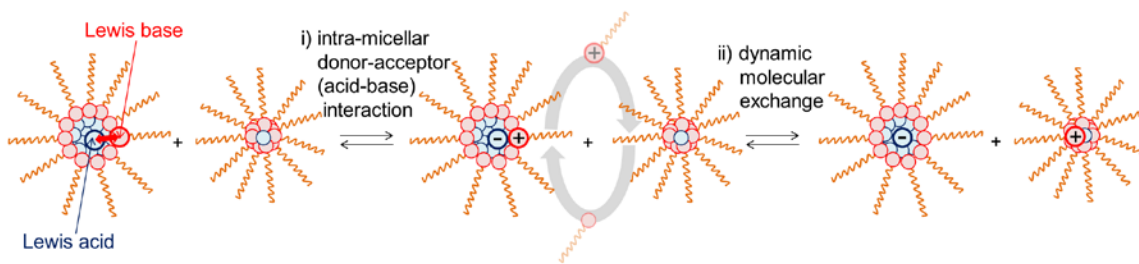


Figure 3.12. Hypothetical mechanisms for the creation of micellar ions with a significant size asymmetry, consisting of the (i) intra-micellar acid-base interaction between the surfactant (Lewis base) and water (Lewis acid) and (ii) inter-micellar exchange of surfactant molecules.

Recalling that a major driving force for the incorporation of water molecules in the micelle cores is the acid-base (polar) interaction between water and the surfactants' polar head-group moieties,^{1,50} we can calculate the polar work of adhesion ($W_{L_1L_2}^{AB}$) at the interface between the water in micelle core (L_2) and the surrounding surfactant solution (L_1), using the acid/base parameters of water ($\gamma_{L_2}^+ = 25.5 \text{ mJ/m}^2 = \gamma_{L_2}^-$)²⁸ and the solution parameters of Figure 2.8 and 2.9; the result is shown in Figure 3.13. To predict the most likely direction of charge transfer via donor-acceptor interaction between water and the surfactant, we proceed, as before in the discussion of surfactant-particle interaction, by comparing the energy contribution of water-surfactant adduct formation in which the surfactant acts as the acid (Figure 3.14) with the corresponding adduct formation energy between the surfactant as the base (proton acceptor or electron donor) and water as the acid (Figure 3.15). We see that the latter type of adduct formation appears energetically

avored. In this case a donor-acceptor complex⁵¹ of the negatively charged conjugate base of water and the positively charged conjugate acid of surfactant polar head is created in a water-swollen micelle (step i in Scheme 3.12). Now, the heterolysis of the donor-acceptor complex⁵¹ and the formation of a micellar ion pair can be achieved by micelle fission or when the positively charged surfactant is transferred to another micelle by molecular exchange (step ii of Scheme 3.12). In such an exchange, the micelle from which charged surfactant originates, is likely to contain an exceptionally large pool of water in its core to facilitate the initial intra-micellar charge separation, whereas the micelle accepting the charged surfactant molecule is likely to be a more “typical” or “average” micelle in sufficiently close proximity for the exchange. Overall, it is therefore plausible that the process produces pairs of micellar ions in which the micellar anions are larger, on average, than the micellar cations. We further expect that the larger, more water-swollen micellar ions scatter light more strongly and therefore produce a larger signal in the electrophoretic mobility measurements, and that these larger micelles on average comprise a larger number of surfactant molecules, which explains the entropic bias toward the adsorption of anionic micelles over that of cationic micelles.

We note that the intra-micellar donor-acceptor interactions of surfactant head moieties and the incorporated water (or other solvent molecules) have been studied extensively with molecular dynamic (MD) simulations⁵²⁻⁵⁵ or molecular probes,⁵⁶⁻⁵⁷ although only a limited number of surfactants have been considered, and the connection with micelle charging by molecular surfactant exchange has not yet been explored to our knowledge.

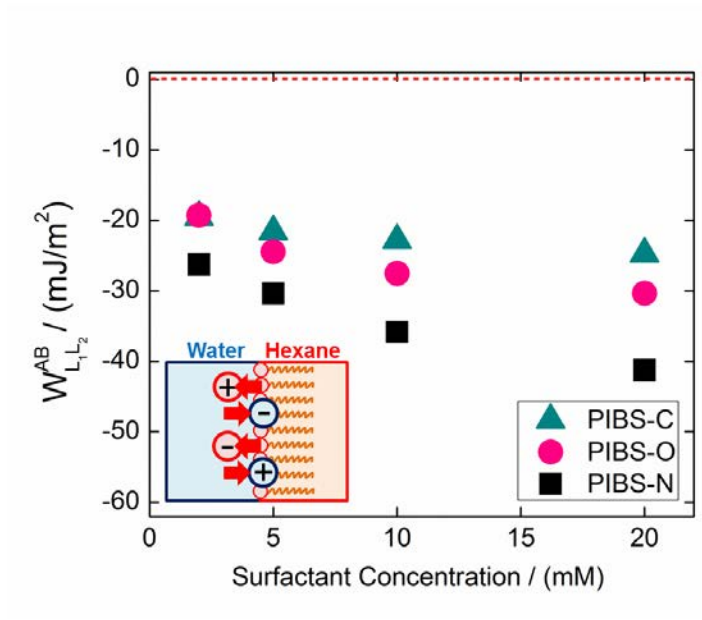


Figure 3.13. The total acid-base work of adhesion between the water surface (L_2) and surfactant solutions (L_1).

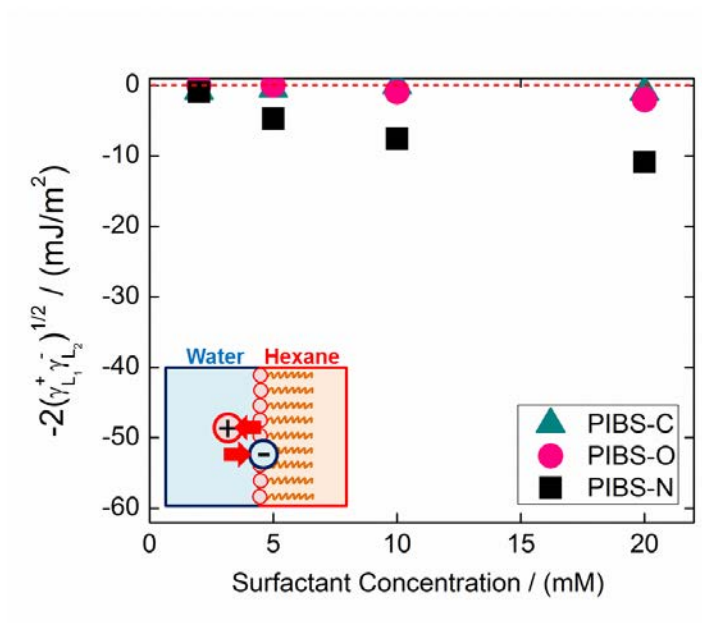


Figure 3.14. The adduct formation energy of the water surface's basic (electron donor or proton acceptor) sites with the surfactant solutions' acidic (electron acceptor or proton donor) sites.

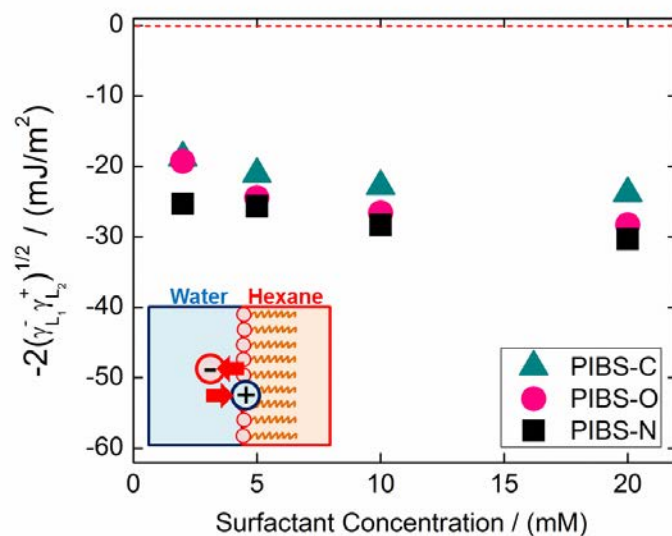


Figure 3.15. The adduct formation energy of the water surface's acidic (electron acceptor or proton donor) sites with the surfactant solutions' basic (electron donor or proton acceptor) sites.

(c) *The degree of size asymmetry.*

The fact that in our study solutions of PIBS-N appear to have the strongest size asymmetry between positively and negatively charged micelles can be explained by a particularly large amount of water incorporated in these systems. We measured the water content in solutions of the three PIBS surfactant types with Karl Fisher titration (Figure 3.16). The solutions were generally found to contain a somewhat larger amount of water than pure hexane, as would be expected for nonpolar solutions of typical hygroscopic surfactants^{9,14,26} (although the measured values indicate only a low water content compared to the systems of commercial surfactants).^{17,26} The highest water content in our study was found in the PIBS-N solutions, which also suggests the largest fluctuations in

the size of the water-swollen micelle cores and ultimately results in the most pronounced size asymmetry between oppositely charged micellar ions. The particularly large water inclusion is related to the solutions' large polar interaction energy $W_{L_1L_2}^{AB}$ with water (Figure 3.13).

We confirmed by dynamic light scattering that the average size of micellar structures in the PIBS-N solution was larger than that in the other two solutions. The (intensity-weighted mean) solvodynamic diameter d_s was 4.5 nm for the micellar structures in the PIBS-N solutions, significantly larger than micelles of the other two surfactant types (3 nm for PIBS-C and 3.1 nm for PIBS-O).

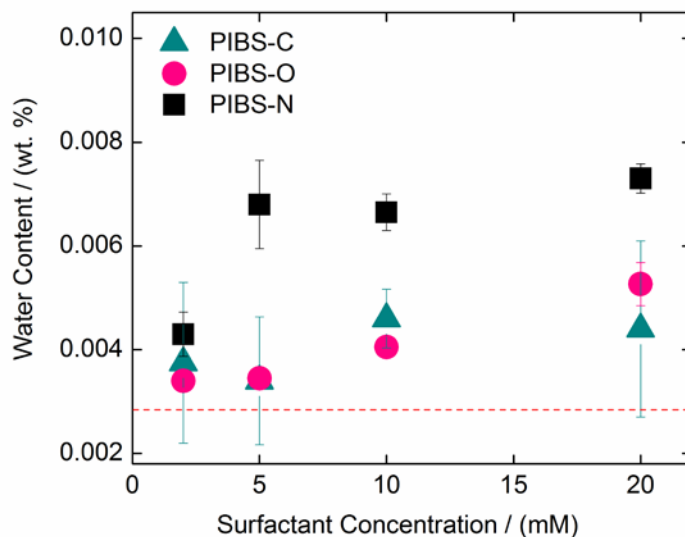


Figure 3.16. Water content in the three PIBS surfactant solutions as a function of surfactant concentration. The dashed red line indicates the water content of pure hexane.

(d) Electric conductivity caused by the micellar ions and relation to the existing theories.

We measured the electric conductivity σ in solutions of our three surfactant types and found, not surprisingly, that the PIBS-N solutions exhibit by far the largest conductivity (Figure 3.17).

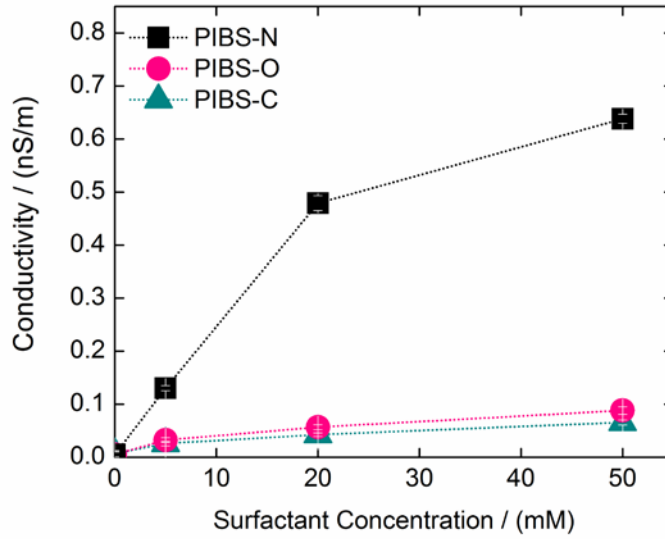


Figure 3.17. Electric conductivity in the three types of PIBS surfactant solutions.

For the largest, most water-swollen type of surfactant micelles to also produce the largest conductivity is consistent with *charge fluctuation theory*,^{1-2,9-10,26,33-38} according to which the statistical probability χ with which a micelle acquires a charge is proportional to the Boltzmann factor^{26,37}

$$\chi \propto \exp\left(-\frac{\lambda_B}{2a}\right), \quad (3.4)$$

containing the Bjerrum length λ_b of the nonpolar medium, and the micellar ion's Born diameter $2a$ (the size of the polar micelle core hosting the charge). A popular hypothesis for the charging pathway involves the concept of micellar “charge disproportionation” according to the reaction $M + M \rightleftharpoons M^+ + M^-$.^{5,9-10,26,34-35} The charging scheme proposed here (Figure 3.12) is somewhat similar in that it also describes the conversion of two neutral micelles into two oppositely charged ones; but it releases the simplifying assumption of symmetry implied in the disproportionation concept and provides a rationale for asymmetric charging according to the overall reaction $M + m \rightleftharpoons M^\pm + m^\mp$, where the upper and lower case symbol denotes micellar species of difference size and water content, and where the resulting sign of charge depends on the relative acid/base properties of the polar micelle core and of the surfactant ($M + m \rightleftharpoons M^- + m^+$ for the case of our PIBS-N micelles). We also note that since the micelle charges are understood to represent fluctuations around a zero mean, and the micelle charge is closely connected to the micelle size (as suggested by Equation 3.4), *size fluctuations* are obviously important, too, and all attempts to describe micelle charging by considering only “typical” micelles of a mean size are based on a false premise. As for the sub-linear conductivity increase with increasing surfactant concentration (Figure 3.17), we refrain from attempting a quantitative interpretation, but point out a likely connection with the highly nonlinear relation between water content and surfactant concentration (Figure 3.16).

Duhkin and co-workers^{11,58-59} proposed another mechanistic model for nonpolar solutions of “dried” surfactants, which has some similarity to our model. They proposed that the surfactants would *sterically stabilize* ionic impurities in a fashion reminiscent of ion *solvation* in polar solvents. Oppositely charged ion-surfactant complexes would

typically have unequal size (in analogy to the unequal solvation radii of salt ions in water) and tend to combine into *ion pairs* given their strong electrostatic attraction in the nonpolar medium, although some fraction of these ion pairs would be *dissociated* in equilibrium. The formation of ion pairs, overall neutral complexes of locally separated charges, somewhat resembles the intra-micellar charging proposed in step (i) of Figure 3.12, whereas the postulated ion pair dissociation resembles our proposed inter-micellar charge exchange (step ii of Figure 3.12) in that it produces micellar ions of unequal size. Our proposed pathway of micelle charging, however, has the distinct advantage of explaining qualitatively the correlation between the size of the micellar ions and their sign of charge, and of addressing the role of water in micellar charging.

3.3.4. Surface Charging of the PMMA Particles

With our tentative picture of micelle charging in our nonpolar surfactant solution, we now return to the surface charging of dispersed PMMA particles. Considering the *nucleophilicity* of the particle surface, reflected in its basicity parameter γ_s^- , the preferential adsorption of positively charged molecules or micelles seems plausible and may be thought of as driven by favorable ion-dipole interaction. We note that this interaction can also be regarded as a type of donor-acceptor (acid-base) interaction,⁶⁰ although one distinguished from the previously discussed surface interaction with electrically neutral surfactants.³⁻⁸ The classical concept of particle charging via acid-base interaction with surfactants considered the direct charge exchange between neutral surface sites and neutral surfactant molecules, and assumed that the extent of ion formation in the liquid bulk would be small.^{1,4} Especially for the charging of

“hydrophobic” polymer particles, this should probably be reconsidered. As suggested by Figure 3.8 and Figure 3.13 – 3.15, the magnitude of the donor-acceptor interaction energy of the surfactants with water is significantly larger than that with the hydrophobic solid surface; and the amount of residual water typically present in nonpolar liquids (30 – 80 ppm in our study, 5 – 45 ppm in the literature⁸), when distributed over micelle cores in the nanometer size range, has an interfacial area that can easily surpass the total surface area of the colloid particles at the low particle concentrations typically used in electrophoresis measurements^{8,10,16-18,25} (only 30 ppm in our study). Indeed, it is found that the charge concentration in the liquid bulk of surfactant solutions^{10,26,34,43} would easily suffice to achieve, via adsorption, the typical magnitude of particle surface charge reported in the literature.^{10,19} Although this does *not* rule out the possibility of direct charge exchange between the solid surface and neutral surfactants, we consider the preferential adsorption of the *chemically favored* “ion” (cations for basic and anions for acidic surfaces) from the liquid bulk a very plausible contribution to net surface charging.

The positive surface charging of PMMA particles in the dispersions containing the surfactant PIBS-C or PIBS-O, could thus result from the bias in the competitive adsorption of positively and negatively charged micelles introduced by the nucleophilic character of the surface (Figure 3.18). A slightly larger degree of positive surface charging in the PIBS-O system (suggested by Figure 3.7) may be caused by the larger overall ion concentration (suggested by the conductivity, Figure 3.17). The same surface chemical bias for cation adsorption might also explain the previously reported positive charging of the same particles in solutions of the commercial sorbitan oleate surfactant Span 85.^{17,19} The *negative* particle charging witnessed in solutions of PIBS-N (Figures

3.7), however, calls for a different explanation. We propose that in these systems the chemically disfavored micellar anions may nonetheless adsorb preferentially because the adsorption of the largest micelles is favored entropically as mentioned before, and because the negatively charged micelles in PIBS-N solutions are significantly larger than their positively charged counterparts, as suggested by electrophoretic light scattering (Figure 3.11) and rationalized in section 3.3.3. We note again that the asymmetry between “large” anions and “small” cations implies a difference in their “average degree of association” in dynamic equilibrium, which related to the loss of translational entropy upon ion adsorption to the particle surfaces.

Moreover, we note the qualitative resemblance between the electrophoretic particle mobility in dispersions containing micelles of PIBS-N (Figure 3.5) and the electrophoretic mobility measured in the corresponding particle-free PIBS-N solutions (Figure 3.11): in both cases we observe a negative mobility with little dependence on the applied electric field up to a field strength around 15-20 kV/m, followed by a pronounced mobility variation at higher field strength, with a maximum magnitude around 30-40 kV/m. We cannot currently explain the features of these mobility curves, but the apparent electrophoretic similarity of particles and micelles in the PIBS-N systems lends further credence to the notion that the particle mobility may be determined primarily by adsorption of those negatively charged PIBS-N micelles that dominate the electrophoresis signal in the absence of particles (Figure 3.19).

The “dryer” micelles of PIBS-C and PIBS-O (Figure 3.16), on the other hand, appear to form ions with smaller size asymmetry (as inferred from Figure 3.9 – 3.11), which may explain why their competition for adsorption sites on the particles would be

determined less by size differences than by differences in their chemical affinity for the nucleophilic PMMA surface.

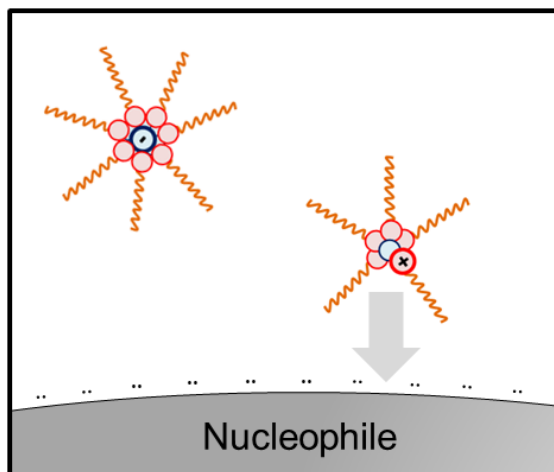


Figure 3.18. Surface charging of a hydrophobic particle via preferential adsorption of size-asymmetric micellar ions in case of a small size asymmetry. Dots on the surface represent lone electron pairs.

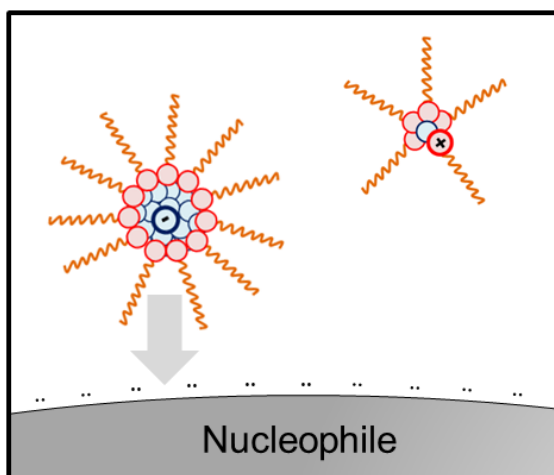


Figure 3.19. Surface charging of a hydrophobic particle via preferential adsorption of size-asymmetric micellar ions in case of a large size asymmetry. Dots on the surface represent lone electron pairs.

3.4. Conclusion

Inverse micelles of purified polyisobutylene succinimide polyamine surfactants with minimal structural variations in the polar headgroup exhibit distinctly different charging behavior in nonpolar solutions and can lead to qualitatively different surface charging of dispersed polymer particles. Positive charging of PMMA particles by the less hygroscopic surfactant in our study (PIBS-C and PIBS-O) may be facilitated either by acid-base interaction of the surfactant with the particle surface or by the preferential adsorption of cationic micelles from solution bulk to the nucleophilic PMMA surface. The negative surface charging in the presence of the more water-swollen micelles of the surfactant PIBS-N points to the preferential adsorption of anionic PIBS-N micelles, which appear to be significantly larger than their cationic counterparts and are therefore favored *entropically*. We propose that the size asymmetry between oppositely charged micelles may arise from an asymmetric charging pathway, in which intra-micellar charge separation between surfactant molecules and the aqueous core in the most highly swollen micelles is followed by an inter-micellar exchange of a charged surfactant molecule. In order to estimate the strength and quality of the surfactant's acid-base interaction with the particles and the aqueous cores of swollen micelles, we have adopted the framework of acid/base parameters proposed by van Oss, Chaudhury and Good²⁷⁻³¹ with a recent adaptation to nonpolar surfactant solutions.³² Our main findings, however, do not depend on this particular choice for the analysis. It seems difficult, for instance, to imagine that *any* model for particle charging via donor-acceptor interactions would be able to explain the observed unintuitive variation in particle mobility (Figure 3.7) in the order PIBS-N < PIBS-C < PIBS-O through direct surfactant-particle interactions only. Similarly, the

presented data suggest that fluctuations in the micelles' water content can play a key role for particle charging. The proposed charging pathway represents one plausible suggestion of what this role might be. For industrially relevant nonpolar dispersions, we expect that particle charging is further complicated by the usual presence of surfactant mixtures and additional co-solutes besides water.

3.5. References

1. Morrison, I. D. Electric Charges in Nonaqueous Media. *Colloids Surf., A* **1993**, *71*, 1-37.
2. Smith, G. N.; Eastoe, J. Controlling Colloid Charge in Nonpolar Liquids with Surfactants. *Phys. Chem. Chem. Phys.* **2013**, *15*, 424-439.
3. Fowkes, F. M.; Jinnai, H.; Mostafa, M. A.; Anderson, F. W.; Moore, R. J. Mechanism of Electric Charging of Particles in Nonaqueous Liquids. *ACS Symposium Series* **1982**, *200*, 307-324.
4. Fowkes, F. M.; Pugh, R. J. Steric and Electrostatic Contributions to the Colloidal Properties of Nonaqueous Dispersions. *ACS Symposium Series* **1984**, *240*, 331-354.
5. Poovadorom, S.; Berg, J. C. Effect of Particle and Surfactant Acid-Base Properties on Charging of Colloids in Apolar Media. *J. Colloid Interface Sci.* **2010**, *346*, 370-377.
6. Gacek, M.; Brooks, G.; Berg, J. C. Characterization of Mineral Oxide Charging in Apolar Media. *Langmuir* **2012**, *28*, 3032-3036.
7. Gacek, M. M.; Berg, J. C. Investigation of Surfactant Mediated Acid-Base Charging of Mineral Oxide Particles Dispersed in Apolar Systems. *Langmuir* **2012**, *28*, 17841-17845.
8. Gacek, M. M.; Berg, J. C. Effect of Surfactant Hydrophile-Lipophile Balance (HLB) Value on Mineral Oxide Charge in Apolar Media. *J. Colloid Interface Sci.* **2015**, *449*, 192-197.
9. Hsu, M. F.; Dufresne, E. R.; Weitz, D. Z. Charge Stabilization in Nonpolar Solvents. *Langmuir* **2005**, *21*, 4881-4887.
10. Roberts, G. S.; Sanchez, R.; Kemp, R.; Wood, T.; Barlett, P. Electrostatic Charging of Nonpolar Colloids by Reverse Micelles. *Langmuir* **2008**, *24*, 6530-6541.

11. Dukhin, A. S.; Dukhin, S. S. How Non-Ionic “Electrically Neutral” Surfactants Enhance Electrical Conductivity and Ion Stability in Non-Polar Liquids. *Electrophoresis* **2005**, *26*, 2149-2153.
12. Kitahara, A.; Satoh, T.; Kawasaki, S.; Kon-No, K. Specific Adsorption of Surfactants Containing Mn or Co on Polymer Particles Revealed by Zeta-Potential in Cyclohexane. *J. Colloid Interface Sci.* **1982**, *86*, 105-110.
13. Smith, P. G.; Patel, M. N.; Kim, J.; Milner, T. E.; Johnston, K. P. Effect of Surface Hydrophilicity on Charging Mechanism of Colloids in Low-Permittivity Solvents. *J. Phys. Chem. C* **2007**, *111*, 840-848.
14. Kemp, R.; Sanchez, R.; Mutch, K. J.; Bartlett, P. Nanoparticle Charge Control in Nonpolar Liquids: Insights from Small-Angle Neutron Scattering and Microelectrophoresis. *Langmuir* **2010**, *26*, 6967-6976.
15. Smith, G. N.; Alexander, S.; Brown, P.; Gillespie, D. A. J.; Grillo, I.; Heenan, R. K.; James, C.; Kemp, R.; Rogers, S. E.; Eastoe, J. Interaction between Surfactants and Colloidal Latexes in Nonpolar Solvents Studied Using Contrast-Variation Small-Angle Neutron Scattering. *Langmuir* **2014**, *30*, 3422-3431.
16. Smith, G. N.; Grillo, I.; Rogers, S. E.; Eastoe, J. Surfactants with Colloids: Adsorption or Absorption? *J. Colloid Interface Sci.* **2015**, *449*, 205-214.
17. Guo, Q.; Lee, J.; Singh, V.; Behrens, S. H. Surfactant Mediated Charging of Polymer Particles in a Nonpolar Liquid. *J. Colloid Interface Sci.* **2013**, *392*, 83-89.
18. Parent, M. E.; Yang, J.; Jeon, Y.; Toney, M. F.; Zhou, Z.-L.; Henze, D. Influence of Surfactant Structure on Reverse Micelle Size and Charge for Nonpolar Electrophoretic Inks. *Langmuir* **2011**, *27*, 11845-11851.
19. Espinosa, C.E.; Guo, Q.; Singh, V.; Behrens, S. H. Particle Charging and Charge Screening in Nonpolar Dispersions with Nonionic Surfactants. *Langmuir* **2010**, *26*, 16941-16948.
20. Miller, J. F.; Schatzel, K.; Vincent, B. The Determination of Very Small Electrophoretic Mobilities in Polar and Nonpolar Colloidal Dispersions Using Phase Analysis Light Scattering. *J. Colloid Interface Sci.* **1991**, *143*, 532-554.
21. Stotz, S. Field Dependence of the Electrophoretic Mobility of Particles Suspended in Low-Conductivity Liquids. *J. Colloid Interface Sci.* **1977**, *65*, 118-130.
22. Thomas, J. C.; Crosby, B. J.; Keir, R. I.; Hanton, K. L. Observation of Field-Dependent Electrophoretic Mobility with Phase Analysis Light Scattering (PALS). *Langmuir* **2002**, *18*, 4243-4247.
23. Dukhin, A. S.; Dukhin, S. S. Aperiodic Capillary Electrophoresis Method Using an Alternating Current Electric Field for Separation of Macromolecules. *Electrophoresis* **2005**, *26*, 2149-2153.

24. Hashimi, S. M.; Firoozabadi, A. Field- and Concentration-Dependence of Electrostatics in Non-Polar Colloidal Asphaltene Suspensions. *Soft Matter* **2012**, *8*, 1878-1883.
25. Gacek, M. M.; Berg J. C. Effect of Synergists on Organic Pigment Particle Charging in Apolar Media. *Electrophoresis* **2014**, *0*, 1-7.
26. Guo, Q.; Singh, V.; Behrens, S. H. Electric Charging in Nonpolar Liquids Because of Nonionizable Surfactants. *Langmuir* **2010**, *26*, 3203-3207.
27. van Oss, C. J.; Chaudhury, M. K.; Good, R. J.; Monopolar Surfaces. *Adv. Colloid Interface Sci.* **1987**, *28*, 35-64.
28. van Oss, C. J.; Chaudhury, M. K.; Good, R. J.; Interfacial Lifshitz-van der Waals and Polar Interactions in Macroscopic Systems. *Chem. Rev.* **1988**, *88*, 927-941.
29. Lee, L.-H. *Fundamentals of Adhesion*; Plenum Press; New York, 1991.
30. van Oss, C. J.; Giese, R. F.; Wu, W. On the Predominant Electron-Donicity of Polar Solid Surfaces. *J. Adhesion* **1997**, *63*, 71-88.
31. Pizzi, A.; Mittal, K. L. *Handbook of Adhesive Technology*; CRC Press; New York, 2003.
32. Lee, J.; Zhou, Z.-L.; Behrens, S. H. Characterizing the Acid/Base Behavior of Oil-Soluble Surfactants at the Interface of Nonpolar Solvents with a Polar Phase. *J. Phys. Chem. B* **2015**, *119*, 6628-6637.
33. Kim, J.; Anderson, J. L.; Garoff, S.; Schlangen, L. J. M. Ionic Conduction and Electrode Polarization in a Doped Nonpolar Liquid. *Langmuir* **2005**, *21*, 8620-8629.
34. Strubbe, F.; Verschueren, A. R. M.; Schlangen, L. J. M.; Beunis, F.; Neyts, K. J. Generation Current of Charged Micelles in Nonaqueous Liquids: Measurements and Simulations. *J. Colloid Interface Sci.* **2006**, *300*, 396-403.
35. Eicke, H. F.; Borkovec, M.; Das-Gupta, B. J. Conductivity of Water-In-Oil Microemulsions: A Quantitative Charge Fluctuation Model. *J. Phys. Chem.* **1989**, *93*, 314-317.
36. Hall, D. G. Conductivity of Microemulsions: An Improved Charge Fluctuation Model. *J. Phys. Chem.* **1990**, *94*, 429-430.
37. Kallay, N.; Chittofrati, A. Conductivity of Microemulsions: Refinement of Charge Fluctuation Model. *J. Phys. Chem.* **1990**, *94*, 4755-4756.
38. Kallay, N.; Tomic, M.; Chittofrati, Conductivity of Water-In-Oil Microemulsions: Comparison of the Boltzmann Statistics and the Charge Fluctuation Model. *A. Colloid Polym. Sci.* **1992**, *270*, 194-196.
39. Israelachvili, J. N. *Intermolecular and Surface Forces*, 3rd ed.; Academic Press; Oxford, 2011.

40. Netz, R. R.; Andelman, D. Neutral and Charge Polymers at Interfaces. *Phys. Rep.* **2003**, *380*, 1-95.
41. Cox, A. R.; Mogford, R.; Vincent, B.; Harley, S. The Effect of Polymer Chain Architecture on the Adsorption Properties of Derivatized Polyisobutylenes at the Carbon/n-Heptane Interface. *Colloids Surf., A* **2001**, *181*, 205-213.
42. Bru, R.; Sanchez-Ferrer, A.; Garcia-Carmona, F. Kinetic Models in Reverse Micelles. *Biochem. J.* **1995**, *310*, 721-739.
43. Yezer, B.; Khair, A. S.; Sides, P. J.; Prieve, D. C. Use of Electrochemical Impedance Spectroscopy to Determine Double-Layer Capacitance in Doped Nonpolar Liquids. *J. Colloid Interface Sci.* **2014**, *449*, 2-12.
44. Mathews, M. B.; Hirschhorn, E. Solubilization and Micelle Formation in a Hydrocarbon Medium. *J. Colloid Sci.* **1953**, *8*, 86-96.
45. Robinson, B. H.; Toprakcioglu, C.; Dore, J. C. Small-Angle Neutron-Scattering Study of Microemulsions Stabilised by Aerosol-OT. *J. Chem. Soc., Faraday Trans.* **1984**, *80*, 13-27.
46. De. T. K.; Maitra, A. Solution Behaviour of Aerosol OT in Non-Polar Solvents. *Adv. Colloid Interface Sci.* **1995**, *59*, 95-193.
47. Halperin, A.; Alexander, S. Polymeric Micelles: Their Relaxation Kinetics. *Macromolecules* **1989**, *22*, 2403-2412.
48. Lund, R.; Willner, L.; Stellbrink, J.; Lindner, P.; Richter, D. Logarithmic Chain-Exchange Kinetics of Diblock Copolymer Micelles. *Phys. Rev. Lett.* **2006**, *96*, 068302.
49. Choi, S.-H.; Lodge, T. P.; Bates, F. S. Mechanism of Molecular Exchange in Diblock Copolymer Micelles: Hypersensitivity to Core Chain Length. *Phys. Rev. Lett.* **2010**, *104*, 047802.
50. Shinoda, K. *Solvent Properties of Surfactant Solutions*; Dekker; New York, 1967.
51. Labib, M. The Origin of the Surface Charge on Particles Suspended in Organic Liquids. *Colloids. Surf.* **1988**, *29*, 293-304.
52. Faeder, J.; Ladanyi, B. M. Molecular Dynamics Simulations of the Interior of Aqueous Reverse Micelles. *J. Phys. Chem. B* **2000**, *104*, 1033-1046.
53. Pal, S.; Vishal, G.; Gandhi, K. S.; Ayappa, K. G. Ion Exchange in Reverse Micelles. *Langmuir* **2005**, *21*, 767-778.
54. Rodriguez, J.; Marti, J.; Guardia, E; Laria, D. Protons in Non-Ionic Aqueous Reverse Micelles. *J. Phys. Chm. B* **2007**, *111*, 4432-4439.
55. Blach, D.; Correa, M.; Silber, J. J.; Falcone, R. D. Interfacial Water with Special Electron Donor Properties: Effect of Water-Surfactant Interaction in Confined

- Reversed Micellar Environments and Its Influence on the Coordination Chemistry of a Copper Complex. *J. Colloid Interface Sci.* **2011**, *355*, 124-130.
56. Baruah, B.; Roden, J. M.; Sedgwick, M.; Correa, N. M.; Crans, D. C.; Levinger, N. E. When is Water Not Water? Exploring Water Confined in Large Reverse Micelles Using a Highly Charged Inorganic Molecular Probe. *J. Am. Chem. Soc.* **2006**, *129*, 12758-12765.
57. Correa, N. M.; Silber, J. J.; Riter, R. E.; Levinger, N. E. Nonaqueous Polar Solvents in Reverse Micelle Systems. *Chem. Rev.* **2012**, *112*, 4569-4602.
58. Dukhin, A.; Parlia, S. Ions, Ion Pairs and Inverse Micelles in Non-Polar Media. *Curr. Opin. Colloid Interface Sci.* **2013**, *18*, 93-115.
59. Dukhin, A. Critical Concentration of Ion-Pairs Formation in Nonpolar Media. *Electrophoresis* **2014**, *0*, 1-9.
60. Della Volpe, C.; Siboni, S. Acid-Base Surface Free Energies of Solids and the Definition of Scales in the Good-van Oss-Chaudhury Theory. *J. Adhesion Sci. Technol.* **2000**, *14*, 235-272.

CHAPTER 4

INVESTIGATION OF PARTICLE CHARGING WITH SYSTEMATIC VARIATION OF SURFACE PROPERTIES

4.1. Introduction

In the previous Chapter, we demonstrated the importance of “micellar-ion adsorption” in surface charging, by investigating a model colloid’s charging behavior mediated by a series of surfactants under subtle chemical structure variations.

However, this does *not* indicate that surface charging must be determined solely by this charging pathway as a single regulation theory. In our own recent study¹ conducted with a couple of commercial surfactant products, the apparent surface charging phenomena could only be explained by interplays between “multiple charging mechanisms”, not by any single one of existing hypotheses.

In nonpolar solutions of a commercial surfactant Span85, for example, a series of polystyrene (PS) particles with different surface functional groups were charged, where the relative charging behavior reflected the acid/base chemistry of functionality especially at low surfactant concentrations, as the traditional acid-base charging mechanism would predict.²⁻⁸ However, at high surfactant concentrations, all the PS particles were charged similar with no evidence for the ionization of surface functionality, which is against the traditional theory. In the same solutions, surface charging of an acid-functionalized polymethyl methacrylate (PMMA) particle was regardless of the

chemistry of such functionality in the entire range of surfactant concentrations; the particle acquired a significant amount of positive charge, which seemed to reflect the basicity (nucleophilicity) of particle bulk,⁹⁻¹² rather than the character of specific functionality. In solutions of the other commercial surfactant Aerosol-OT (AOT), on the other hand, the ionization of functional groups for the same particles appeared significant in the entire range of surfactant concentrations.

Some correlations between the “polarity” of different surfaces and surface charging may still suggest a possible contribution of the surfaces’ acid-base interaction in net surface charging process (in competition with other charging pathways, *e. g.* entropy-driven asymmetric partitioning of large micellar anions). With respect to this *chemical* contribution, the complication may come from the ambiguity associated with defining the “polarity” of surfaces which are the most relevant to charging process in nonpolar media – is it the acid/base character of “functional groups” (as the traditional theory suggested), or “particle bulk”? Which one is important/unimportant and when? Why is the surface polarity system dependent?

In this Chapter, we will represent in-depth discussions on multiple pathways of surface charging in nonpolar dispersions. We characterize charging behavior of a series of “well-defined” polymer particles under systematic variations of their surface properties: we vary the type of particle bulk and specific functional groups, both of which are tentatively thought to be relevant to surface charging in a system dependent manner.

4.2. Materials and Methods

4.2.1. Custom and Commercial Surfactants

We employed one of our well-defined custom surfactants, “PIBS-N” (Figure 2.3), as a charging agent in this Chapter. Synthesis and purification of this surfactant were carried out by following the procedures described in the previous Chapters. In brief, we conducted the condensation reaction where a polyisobutylene succinic anhydride (PIBSA) and polyamine N,N-diehtyldiehtylenetriamine were coupled. We purified the reaction products with flash chromatography using silica gel as the stationary phase and a mixture of 20:1 chloroform / ethanol anhydrous as the mobile phase.

We also employed a commercial charging agent product, OLOA11000. As mentioned, the exact chemical composition of this proprietary material is poorly defined, although it is known that the product is a mixture of several PIBS derivatives and mineral oils.¹³⁻¹⁴ The material was received from Chevron Oronite and used without further purification. A molecular weight $M_w \sim 1200$ g/mol was assumed¹⁵ as the exact molecular weight of this material is unknown.

4.2.2. Nonpolar Dispersions

We employed a series of polymer particles under systematic variations of surface properties. Polymethyl methacrylate particles with sulfate functional groups were purchased from Bangs Laboratories (PMMA-sulfate, 1.1 μm , PP04N), and polystyrene particles with sulfate groups (PS-sulfate, 1.0 μm , C37498), carboxyl groups (PS-carboxyl, 1.0 μm , C37274) and amidine groups (PS-amidine, 1.0 μm , A37322) were purchased

from Life Technologies. Particles were originally received as surfactant-free aqueous suspensions, transferred into isopropanol (> 99.5%, Sigma Aldrich) as an intermediate solvent, and finally into hexane based surfactant solutions at a minimal surfactant concentration (0.5 mM). In each transfer step, particles were washed three times via centrifugation, disposal of the supernatant, and redispersion of particles in the target solvent.

4.2.3. Electrophoresis

We implemented phase analysis light scattering (PALS)¹⁶ with Zetasizer Nano ZS90 (Malvern Instruments) to measure the particles' electrophoretic mobility in nonpolar dispersions, as an indicator of particle surface charging. A dispersion sample at particle concentration ~30 ppm (in wt.; diluted to avoid multiple scattering) was loaded in a glass cuvette, and a dip cell with two planar palladium electrodes spaced by 2 mm was submerged in the sample. An AC electric field was applied across the electrodes under systematic variations of field strength (2.5 to 50 kV/m) and the field dependent electrophoretic mobility¹⁷⁻²⁰ of particles was measured based on phase information of light scattered by the particles. To infer the particles' equilibrium charging state in the absence of external electric fields, we extrapolated the field dependent mobility to zero field strength ("zero-field" mobility), following a widely adopted strategy in past studies.^{6-9,20-22} Prior to the measurements, the glass cuvette and dip cell were sonicated in tetrahydrofuran, wiped in a hot aqueous detergent solution, rinsed copiously, first with hot water and then with methanol and dried with air.

4.2.4. Quartz Crystal Microbalance (QCM)

We compare the relative surfactant adsorption to different polymer surfaces using quartz crystal microbalance (QCM) techniques.²³ The commercial Q-Sense E4 system (Biolin Scientific) was employed to implement QCM. Prior to preparing polymer surfaces, bare gold crystals (purchased from Biolin Scientific) were thoroughly cleaned by being treated in an UV/ozone system for 10 min, soaked in a 5:1:1 mixture of DI water, ammonia (25%, Merck) and hydrogen peroxide (30%, Merck) at an elevated temperature (75 °C) for 10 min, rinsed with DI water, dried with nitrogen gas, and cleaned in the UV/ozone system for 10 min. The polymer surfaces were prepared by spin-coating the cleaned bare gold crystals with 1 wt. % chloroform solutions of dissolved polymer particles. The spin-coated crystal was dried in the oven at 80 °C for 30 min and cooled at room temperature. In performing QCM, the resonance frequency of polymer-coated crystal was initially obtained under alternating electric fields without mass coupled to the surface. The surface was then flushed with pure hexane (background solvent), at least for 30 min, to obtain a stable baseline, and once the baseline was achieved, was exposed to a parallel flow of the surfactant solution with a rate of 200 $\mu\text{L}/\text{min}$. The frequency shift (Δf), which is directly proportional to the change in mass coupled to the surface,²³ was monitored for 45 min to infer the relative surfactant adsorption to polymer surfaces. The surface was finally flushed again with pure hexane and Δf due to the surfactant desorption was monitored for 30 min.

4.2.5. Karl Fischer Titration

We measured the residual water content of nonpolar surfactant solutions and particle dispersions using volumetric Karl Fischer titration. The commercial TitroLine KF titrator (SCHOTT) was employed to implement the titration. We used HYDRANAL®-Composite 5 as a titration reagent and a 1:1 mixture of chloroform and methanol as a titration medium. A water content around 30 ppm (in wt.) was found for pure hexane, consistent to the literature.²⁴⁻²⁵ We found no remarkable difference in water content between surfactant solutions and particle dispersion samples used for electrophoresis within the instrumental sensitivity.

4.3. Results and Discussions

4.3.1. Surface Charging Correlated to the Type of “Particle Bulk”

We characterized surface charging behavior of the polymer particles in nonpolar dispersions with the surfactant PIBS-N, by measuring the particles’ electrophoretic mobility. Similar to charging behavior shown in the previous Chapter, a non-monotonic field dependent mobility was observed in a range of the applied field strength from 2.5 kV/m to 50 kV/m (Figure 4.1, 4.3, 4.5, and 4.7). To avoid misinterpretations and to infer the particles’ equilibrium surface charging state in the absence of external electric fields, we adopted the widely used strategy of extrapolating the field dependent mobility to zero field strength.^{6-9,20-22} Figure 4.2, 4.4, 4.6, 4.8 and 4.9 show the extrapolated “zero-field mobility”. Even though aqueous charging of the same particles followed the acid/base

character of their surface functional groups (Figure 4.10),¹ we found no evidence that such functionality played a similar role in charging in nonpolar media. For example, the PS-amidine particles, which were positively charged in water with a wide range of pH (isoelectric point above 9) due to the basic character of amidine functional groups, were negatively charged in nonpolar media as similar as PS-carboxyl and PS-sulfate particles, which were negatively charged in water (isoelectric point below 3) due to the acidic character of functional groups. This is in stark contrast to the traditionally proposed acid-base particle charging mechanism²⁻⁸ where particle charging was attributed to direct interaction of acidic/basic moieties of surfactants and particles' acidic/basic functional groups, and therefore, the relative charging in nonpolar media must in principle have some qualitative similarity as the same particles' aqueous charging behavior.

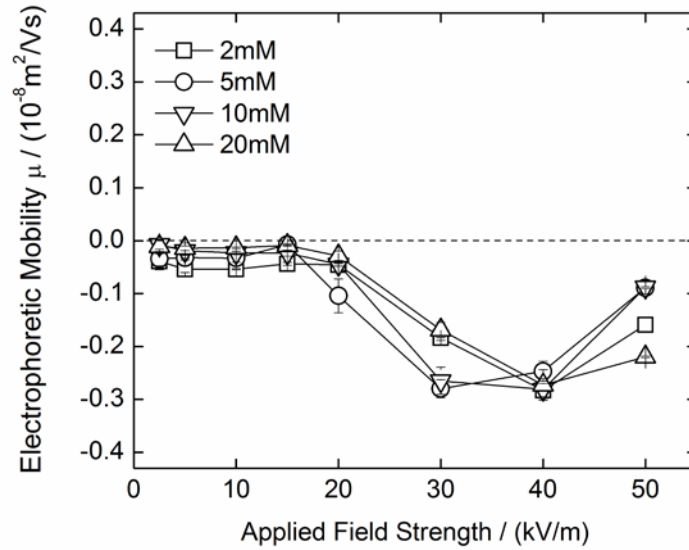


Figure 4.1. The field dependent electrophoretic mobility of the charged PMMA-sulfate particle in hexane-based dispersions of the surfactant PIBS-N in the range of applied field strength between 2.5 kV/m to 50 kV/m.

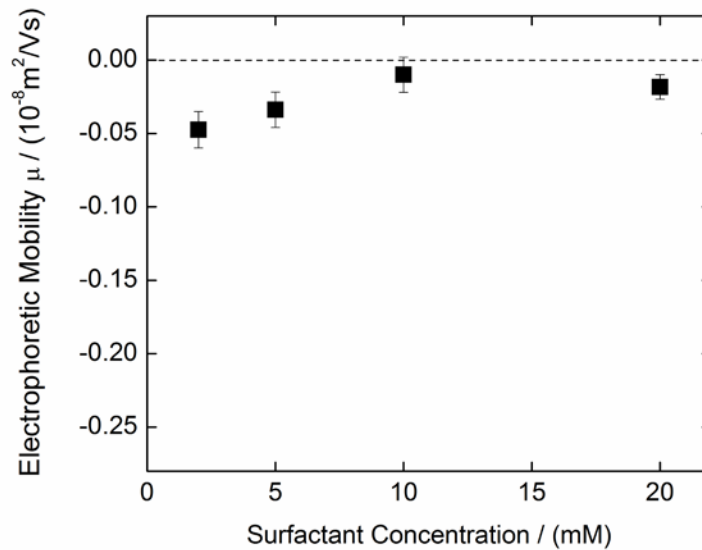


Figure 4.2. The zero-field electrophoretic mobility of the charged PMMA-sulfate particle in hexane-based dispersions of the surfactant PIBS-N, represented as a function of surfactant concentration.

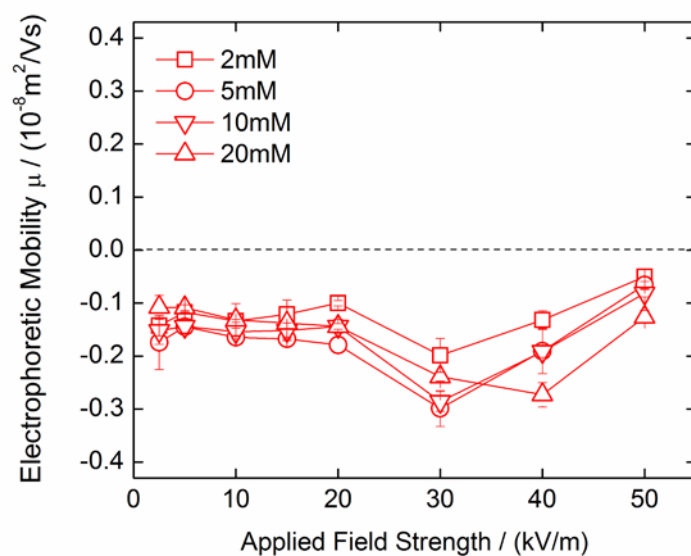


Figure 4.3. The field dependent electrophoretic mobility of the charged PS-sulfate particle in hexane-based dispersions of the surfactant PIBS-N in the range of applied field strength between 2.5 kV/m to 50 kV/m.

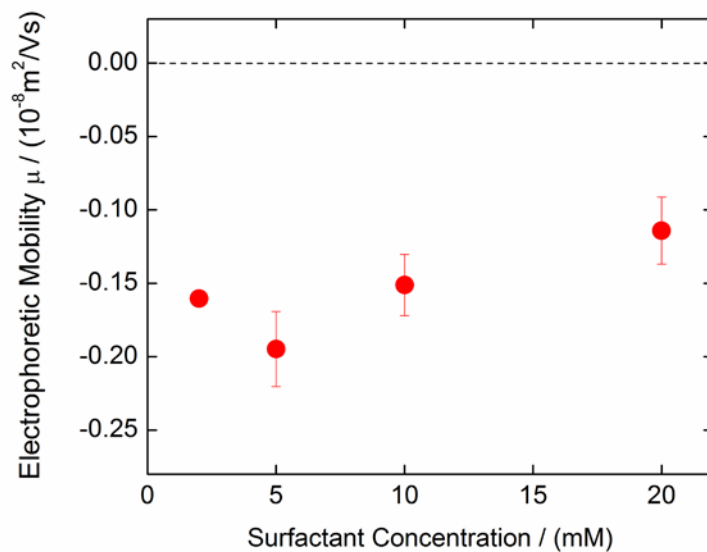


Figure 4.4. The zero-field electrophoretic mobility of the charged PS-sulfate particle in hexane-based dispersions of the surfactant PIBS-N, represented as a function of surfactant concentration.

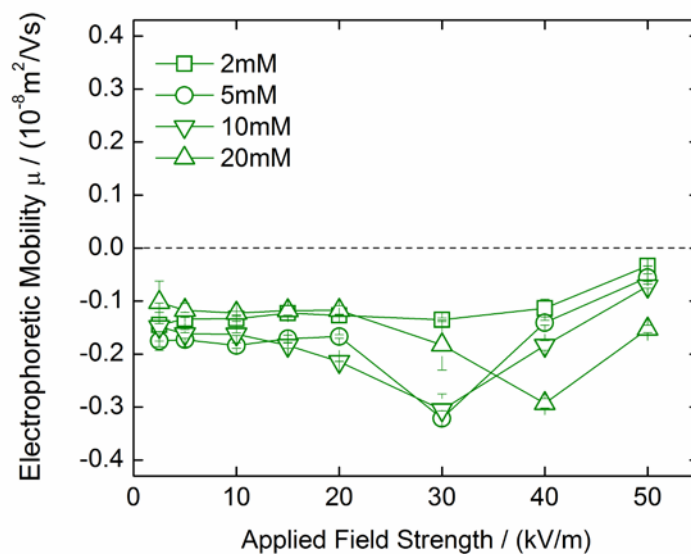


Figure 4.5. The field dependent electrophoretic mobility of the charged PS-carboxyl particle in hexane-based dispersions of the surfactant PIBS-N in the range of applied field strength between 2.5 kV/m to 50 kV/m.

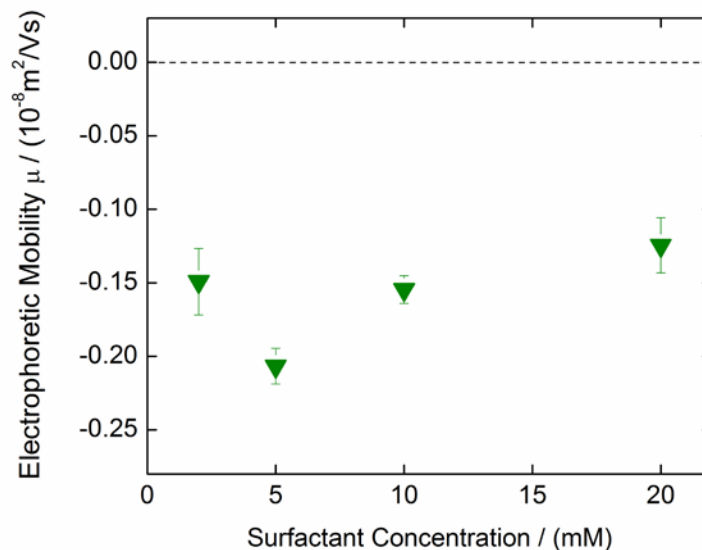


Figure 4.6. The zero-field electrophoretic mobility of the charged PS-carboxyl particle in hexane-based dispersions of the surfactant PIBS-N, represented as a function of surfactant concentration.

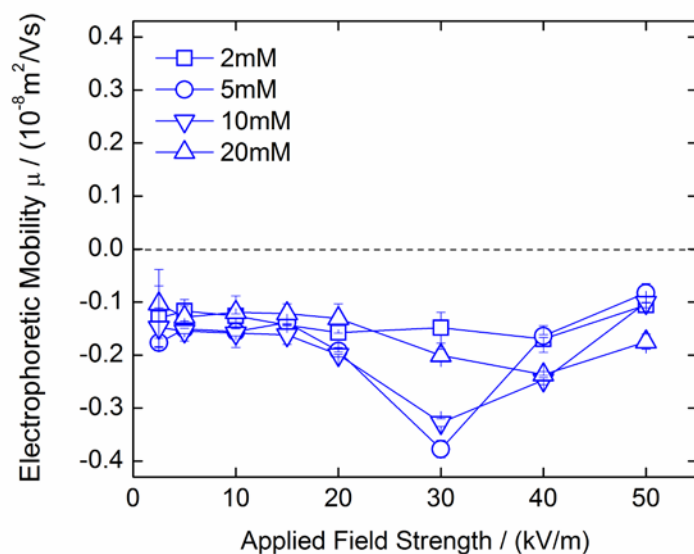


Figure 4.7. The field dependent electrophoretic mobility of the charged PS-amidine particle in hexane-based dispersions of the surfactant PIBS-N in the range of applied field strength between 2.5 kV/m to 50 kV/m.

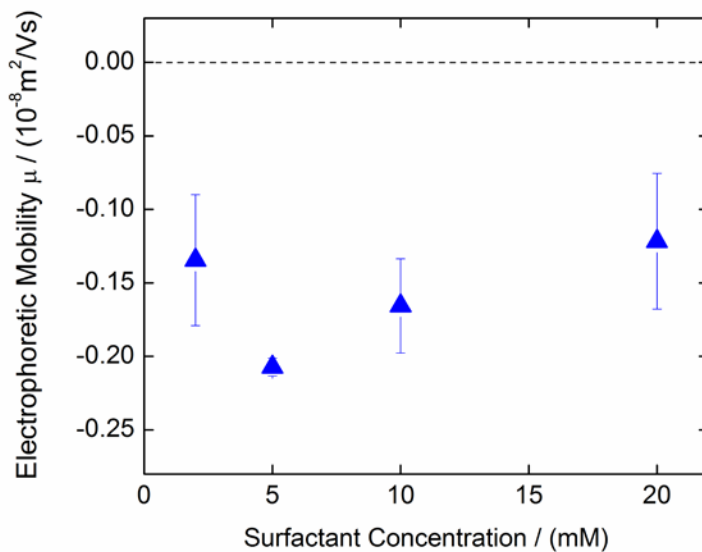


Figure 4.8. The zero-field electrophoretic mobility of the charged PS-amidine particle in hexane-based dispersions of the surfactant PIBS-N, represented as a function of surfactant concentration.

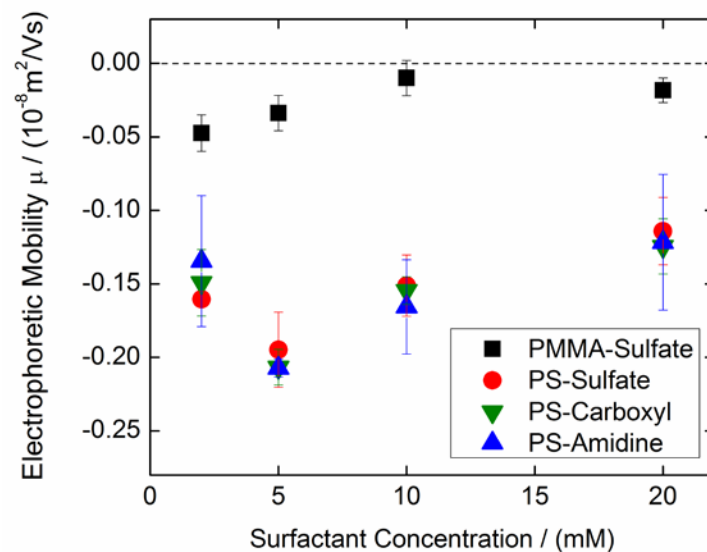


Figure 4.9. The zero-field electrophoretic mobility of the charged polymer particles in hexane-based dispersions of the surfactant PIBS-N, represented as a function of surfactant concentration.

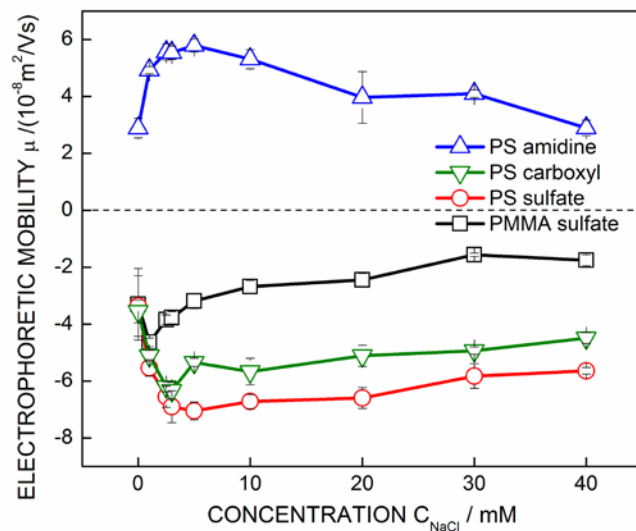


Figure 4.10. The electrophoretic mobility of the charged polymer particles in aqueous NaCl solutions, represented as a function of NaCl concentration.

We point out that the relative charging behavior appears correlated with the type of “particle bulk”,¹ *i. e.* the chemical identity of primary polymer phase, PMMA and PS, rather than the specific functional groups; all PS particles, regardless of their functionality, were more negatively charged than PMMA. Then, the next question can be whether this surface charging would be a consequence of direct acid-base (donor-acceptor) interactions of surfactants with particle bulk, polymer species with some donor-acceptor character. A recent review⁸ proposed a hypothesis, for similar observation of surface charging correlated better with the type of particle bulk than specific functionality in solutions of the commercial surfactant Span85,¹ that surfactants, as “soft” acids or bases, would undergo donor-acceptor interaction selectively with “soft” bases or acids polymers, not with “hard” surface functional groups. From such a perspective, one would infer that PS surfaces were stronger (soft) acids than PMMA, forming stronger donor-acceptor adducts with surfactants as (soft) bases. This “inference” based on “results”, however, seems against some common knowledge of these materials. PS is often considered hydrophobic or largely nonpolar in many scientific studies,²⁶⁻²⁷ and when it comes to its polarity, it is considered base rather than acid because of the electron donor capability of π electrons of oligomeric aromatic rings in terms of molecular orbital theory²⁸⁻²⁹ or Lewis acid/base theory.¹⁰⁻¹²

The improbability of such inference (“strong acid polystyrene”) is revealed by comparing the relative adsorption affinity of oil-borne surfactants to polymer surfaces, which is, in nonpolar continuous phases, related to the relative strength of polar (=acid-base or donor-acceptor) interaction of surfactants with surfaces.^{8,13,30} We employed quartz crystal microbalance (QCM) to measure directly the mass deposition of surfactants to

surfaces while surfactant solutions passed over the macroscopic polymer surfaces spin-coated on the quartz crystal. As the surfaces were exposed to the parallel flow of surfactants solutions, a significantly larger decrease in the resonance frequency (Δf) was found for PMMA than PS (Figure 4.11). Since the decrease in Δf is directly proportional to the increase in mass coupled to the surface,²³ the result indicates that more surfactants adsorbed on PMMA than PS. Moreover, a significantly larger amount of surfactants remained on PMMA, as the surfaces were flushed subsequently with pure hexane, indicating that surfactants formed stronger adducts with PMMA than PS. In the framework of acid-base mechanism, therefore, the propensity of charge transfer (or charge heterolysis)³¹ from donor-acceptor adducts should also be, in principle, more significant for PMMA than PS. Clearly, this is inconsistent with relative surface charging behavior of these particles, as shown in Figure 4.9, where the apparent surface charging of PS was significantly larger than PMMA. Therefore, the PS particles' acquisition of more ("net") negative charge cannot be simply attributed to the stronger adduct formation, as a single charging pathway, of stronger (soft)³² "acids" PS with surfactants. This is likely a wrong speculation based solely on "results".

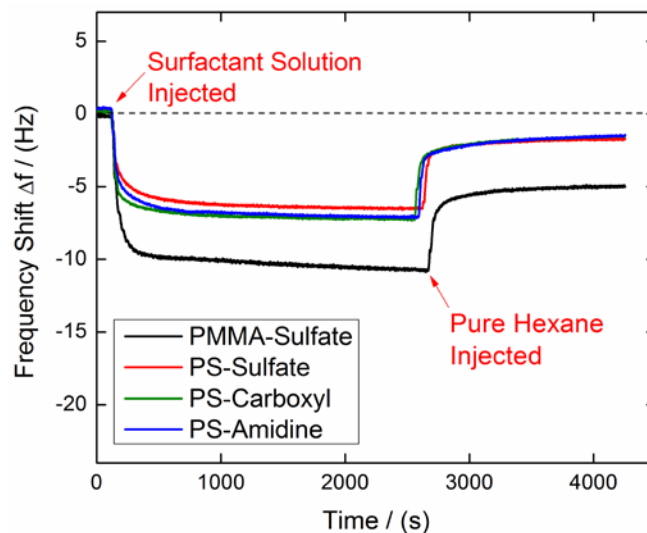


Figure 4.11. The shift in resonance frequency (Δf) of quartz crystal microbalances coated with polymer surfaces, in response to the surfactant adsorption (mass increase) to the surfaces.

We claim that above seen physical phenomena in nonpolar media, both the relative surfactant adsorption to polymer surfaces (Figure 4.11) and relative surface charging (Figure 4.9), are explained by “Lewis basicity”^{10-12,28-29} of particle bulk, analogous terms of which may include electron donicity, proton acceptability, or nucleophilicity.^{9,33} The surfaces of PMMA are known to have significant electron donicity, originated from lone electron pairs of carbonyl oxygen, and the strength of donicity is often characterized to be stronger than that of PS from π electrons of phenyl ring.^{1,10,12,28,30} From this perspective, it would be PMMA surfaces rather than PS that form stronger donor-acceptor adducts with surfactants (as consistent with Figure 4.11) if surfactants had an amphoteric (acidic and basic) character, specifically as the basic

(electron donor) sites of solid surfaces interact with acidic (electron acceptor) sites of surfactants. As a consequence, the propensity of “positive” surface charging, by heterolysis of donor-acceptor adducts, could be higher for PMMA. In the premise that another contribution to surface charging¹ may exist to cause the “net” sign of charge for all surfaces to be “negative”, this adduct formation of surfaces’ basic sites with surfactants’ acidic sites (and their subsequent heterolysis) may explain why PMMA was “less negatively” (=more positively) charged than PS.

An example of representing the relative Lewis basicity of polymeric surfaces in a quantitative way can be found in a surface thermodynamic theory of van Oss, Chaduhury, and Good (vOCG),^{1,9-12,30} which we adopted for interpretation of surface charging mediated by three PIBS analogs, in the previous Chapter. The theory defines a surface tension of condensed phase i (γ_i [=] mJ/m²) as a sum of apolar and polar (acid/base) contributions, *i. e.* $\gamma_i = \gamma_i^{LW} + 2(\gamma_i^+)^{1/2}(\gamma_i^-)^{1/2}$, where γ_i^{LW} is an apolar Lifshitz van der Waals component, γ_i^+ is an acid component, and γ_i^- is a base component. According to the theory, one can characterize the surface energy components of a solid surface (S), γ_S^{LW} , γ_S^+ , and γ_S^- , by measuring the contact angle (θ) of a series of reference liquids (L) with known surface energy components, γ_L^{LW} , γ_L^+ , and γ_L^- , on the solid surface, and solving the equation

$$(1 + \cos \theta)\gamma_L = 2 \left[(\gamma_L^{LW} \gamma_S^{LW})^{\frac{1}{2}} + (\gamma_L^+ \gamma_S^-)^{\frac{1}{2}} + (\gamma_L^- \gamma_S^+)^{\frac{1}{2}} \right] \quad (4.1)$$

with the measured θ as an experimentally determined coefficient. In our previous study, we have characterized γ_s^{LW} , γ_s^+ , and γ_s^- of the polymer materials used in the current study, by measuring θ of reference liquids on macroscopic surfaces spin-casted from solutions of dissolved polymer particles (Table 4.1).¹

Table 4.1. Surface energy components, γ_s^{LW} , γ_s^+ , and γ_s^- , of solid polymer surfaces (in mJ/m^2).¹

Solids	Surface Energy Component Parameters / (mJ/m^2)		
	γ_s^{LW}	γ_s^+	γ_s^-
PS-amidine	37	≈ 0	0.55
PS-carboxyl	39.1	≈ 0	1.5
PS-sulfate	37.1	≈ 0	2.05
PMMA-sulfate	38.8	≈ 0	15.4

This parameterization indicates that apolar (γ_s^{LW}) and acid (γ_s^+) contribution to the total surface tension are similar for all particles, and the acidity strength (electron acceptor or proton donor character) is negligibly small. It also indicates that basicity strength (γ_s^- , electron donor or proton acceptor character) of PMMA is significantly larger than PS, as we anticipated. It is interesting that “commonsensical” acid/base character of particle surface “functionality”, shown in the “wet” environment (Figure 4.10), are not reflected in the vOCG parameters obtained for the “dry” surfaces. We again note that the physical phenomena we actually observed in “nonpolar” media (Figure 4.9 and Figure 4.11) are described better with the properties of “dry” surfaces than those known from “wet” acid-base chemistry.

In the same theoretical framework, we can compare the relative donor-acceptor interaction of polymer surfaces with surfactants in a quantitative fashion, which should be directly related to the relative propensity of charge transfer as the donor-acceptor adducts heterolyze. This can be achieved by approximating the polar work of adhesion ($W_{SL_1}^{AB}$) of polymer surfaces (S) with surfactant solutions (L_1), which is defined as¹¹

$$W_{SL_1}^{AB} = -2(\gamma_S^+ \gamma_{L_1}^-)^{\frac{1}{2}} - 2(\gamma_S^- \gamma_{L_1}^+)^{\frac{1}{2}}, \quad (4.2)$$

using the acid/base parameters of polymer surfaces, γ_S^{LW} , γ_S^+ , and γ_S^- , and surfactant solution parameters $\gamma_{L_1}^{LW}$, $\gamma_{L_1}^+$, and $\gamma_{L_1}^-$. The solution parameters $\gamma_{L_1}^+$ and $\gamma_{L_1}^-$ reflect the nonpolar solutions' "adaptive" polarity exhibited by surfactants adsorbing at the interface with polar phases.³⁰ As suggested in previous Chapters, these can be estimated by measuring the interfacial tension ($\gamma_{L_1 L_2}$) with a series of polar reference liquids (L_2), and solving the equation

$$\gamma_{L_1 L_2} = [(\gamma_{L_1}^{LW})^{1/2} - \gamma_{L_2}^{LW}]^2 + 2[(\gamma_{L_1}^+)^{1/2} - (\gamma_{L_2}^+)^{1/2}][(\gamma_{L_1}^-)^{1/2} - (\gamma_{L_2}^-)^{1/2}] \quad (4.3)$$

with the measured $\gamma_{L_1 L_2}$ as an experimentally determined coefficient. The parameters for hexane solutions of the surfactant PIBS-N were measured in previous Chapters and can be found in Figure 2.8 and 2.9.

Using the acid/base parameters of solid surfaces and surfactant solutions, each term of Eq. 4.2 was calculated and shown in Figure 4.12 and 4.13. The first term of the right-hand side of Eq.4.2, $-2(\gamma_S^+ \gamma_{L_1}^-)^{1/2}$, represents the free energy gain by formation of

adducts between surfaces' acidic sites (with strength γ_s^+) and solutions' basic sites (with strength $\gamma_{L_1}^-$), heterolysis of which is likely to cause “negative” surface charging (Figure 4.12). The second term, $-2(\gamma_s^- \gamma_{L_1}^+)^{1/2}$, represents the free energy gain by adduct formation between surfaces' basic sites (with strength γ_s^-) and solutions' acidic sites ($\gamma_{L_1}^+$), which is related to the propensity of “positive” surface charging (Figure 4.13). The result shows in a quantitative fashion that the adduct formation is dominated by the interaction between the surfaces' basic sites and solutions' acidic sites, indicating that the acid-base or donor-acceptor interaction of surfaces and surfactants in the current system is mostly relevant to charging the surfaces more positively (or “less” negatively, Figure 4.14). Moreover, the magnitude of such interaction is significantly larger for PMMA and there is essentially no huge qualitative difference between PS particles despite the significant difference in their specific functional groups – these are consistent to the phenomena represented in Figure 4.9 and Figure 4.11.

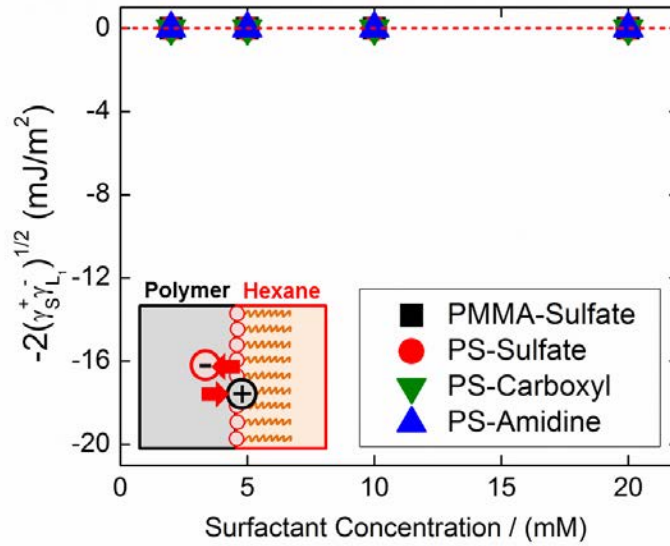


Figure 4.12. The adduct formation energy of the solid surfaces' acidic (electron acceptor or proton donor) sites with the surfactant solutions' basic (electron donor or proton acceptor) sites.

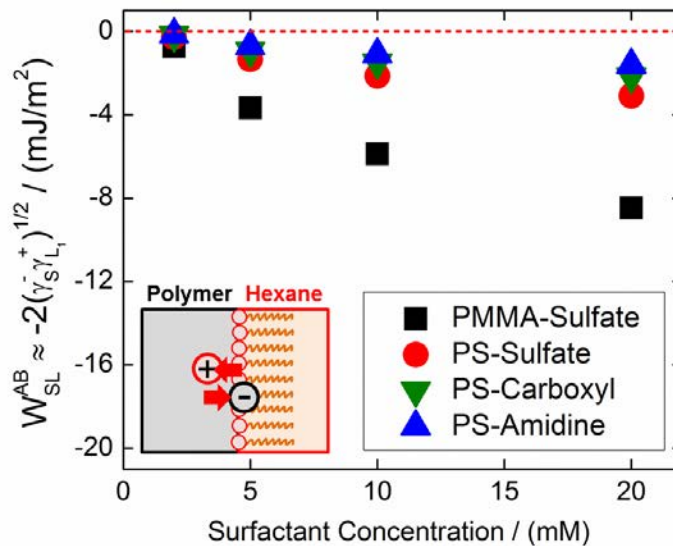


Figure 4.13. The adduct formation energy of the solid surfaces' basic (electron donor or proton acceptor) sites with the surfactant solutions' acidic (electron acceptor or proton donor) sites.

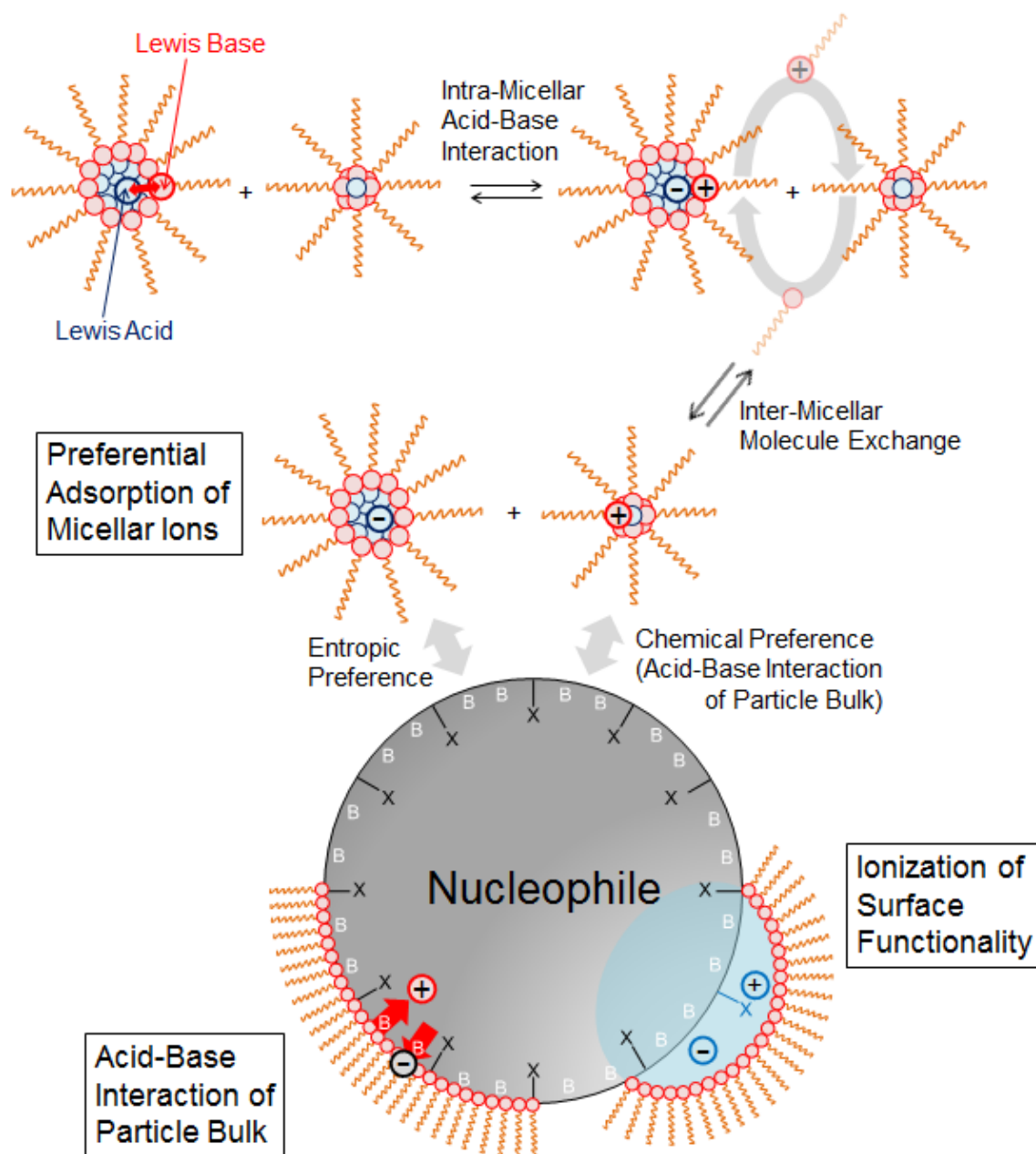


Figure 4.14. Schemes of multiple surface charging pathways which determine the *net* surface charge of colloidal particles in nonpolar dispersions: i) direct acid-base (donor-acceptor) interaction of particle bulk with surfactants, ii) preferential adsorption of inverse micellar ions (formed in the liquid bulk by intra-micellar acid-base interaction of moisture and surfactants), and iii) ionization of surface functionality promoted by excess moisture.

4.3.2. Preferential Adsorption of Inverse Micellar Ions

Even though the adopted surface thermodynamic theory may provide with some idea on the “relative” surface charging behavior of polymer particles, an important question has not been resolved. Why do the particles have “negative” sign of charge?

Indeed, the same question was raised in the previous Chapter, too. We demonstrated the origin of nucleophilic surfaces’ negative charging with the presence of the *third* polar component “moisture” and the entropy-driven adsorption of micellar anions created by the polar interaction of this third component with surfactants (Figure 4.14).⁹

We pointed out that even pure alkanes²⁴⁻²⁵ and nominally “dry” surfactants (unless partly decomposed)³⁴ contain trace water, with a concentration small but essentially larger than the number of charged inverse micelles in typical nonpolar surfactant solutions.^{4,7,24,35} Thus, the inverse micelles are often present as swollen with water,³⁶ the complete removal of which can be experimentally unreachable.³⁷ Although the presence of water, as a provider of (locally high dielectric) polar pools where ions can reside, has been considered important in charging processes in nonpolar media, its elusive role as the third polar component has not often been discussed deeply.⁹

As the water molecules are dispersed and incorporated in inverse micelle cores, they form nanoscale (intra-micellar) interfaces³⁸ with surfactant polar groups. The primary driving force for this self-assembly in a nonpolar continuous phase is essentially the polar interaction or acid-base (donor-acceptor) adduct formation of surfactant polar groups with water molecules.¹³ Therefore, we could in principle estimate the free energy

gain by donor-acceptor adduct formation of surfactant solutions with water molecules to compare the propensity of charge transfer between the two condensed phases, in a similar manner to estimate the solid surfaces' charging in contact with surfactant solutions. In the framework of vOCG surface thermodynamic theory, as an example, we calculated each term of Eq. 4.2 using the acid/base parameters of water ($\gamma_{L_2}^+ = 25.5 \text{ mJ/m}^2 = \gamma_{L_2}^-$)¹¹ and the solution parameters (Figure 2.8 and 2.9), and the results were shown in Figure 3.14 and 3.15. The calculation indicated quantitatively that the adduct formation of water's acidic sites with solutions' basic sites (Figure 3.15) dominated that of water's basic sites with solutions' acidic sites (Figure 3.14), *i. e.* the water phase was likely to be charged “negatively” via heterolysis of donor-acceptor adducts⁴⁷ with surfactants.

As the heterolysis of intra-micellar donor-acceptor complex happened (Figure 4.14), either by dynamic micelle fission or molecular exchange with another micelle,^{13,39-41} the precursor micelle from which the (positively) charged surfactant is expelled was likely to contain an “atypically” large amount of water to promote the initial charge separation, becoming a large swollen micelle ion (with negative sign). On the other hand, the micelle into which the (positively) charged surfactant was inserted could be a more “average” micelles only in close proximity to the precursor micelle for the molecular exchange, and therefore, was likely to become a relatively small micelle ion (with positive sign). As a result, a pair of inverse micelle ions could have significant size asymmetry where the anion, on average, tends to be larger than the cation.⁹ Here, the “size” would also imply the difference in aggregation number between the larger water-swollen anions and smaller dry cations, not simply indicating the physical size, since a larger amount of water molecules were likely to attract a more number of surfactant

molecules^{25,42} via donor-acceptor adduct formation. In a dynamic equilibrium state where spontaneous fusion of inverse micelles as well as the exchange of individual molecules between an inverse micelle and the solution bulk were allowed,^{13,39-41,43} some extremes in size asymmetry, e. g. *n*-fused water-swollen inverse micelles (carrying a negative charge) and dryer micelles with a smallest aggregation number (carrying a positive charge), might even be anticipated among the “distribution” of size. We noted that the size of micelles is, in a more realistic way, described by a distribution of finite width,^{35,44} although often represented by a single average value (e. g. the average solvodynamic diameter $d_s = 4.5$ nm for inverse micellar aggregates of the surfactant PIBS-N).⁹ The generation of micelle ions was confirmed by the increase in electric conductivity upon the addition of surfactants (Figure 3.16). The size asymmetry between micelle ion pairs was supported by implementing electrophoretic light scattering in particle-free micelle solutions (Figure 3.11). A *net* negative electrophoretic mobility was systematically observed in micelle solutions, indicating that micelle anions scattered the incident light more strongly than cations being selectively detected. This could be a strong indication that the size of micelle anions was significantly larger than cations⁹ providing that an equal number of positive and negative charges were present (dictated by *electroneutrality*) and formation of multivalent ions was energetically disfavored (dictated by *charge fluctuation theory*).⁴⁵⁻⁴⁸

In competitive adsorption of the oppositely charged inverse micelle ions (Figure 4.14), this size asymmetry can be an “entropic” factor⁴⁹ influencing their “preferential”^{36,50-51} adsorption state; adsorption of “larger” micelle anions can be favored because it minimizes the overall translational entropy loss associated with confining the

(continuous-phase soluble) adsorbates on the surfaces.^{9,49} This can explain how hydrophobic and (somewhat) chemically basic polymer surfaces acquire net negative surface charge. As opposed to the assumption by the traditional acid-base particle charging mechanism,¹⁵ we claimed that the extent of ionization in the liquid bulk could dominate the ionization at the particle surface (depending on the system components), and the contribution of inverse micelle “ion” adsorption to net surface charge could be non-negligible. The same argument can be suggested for charging phenomena shown in this Chapter. For examples, comparing the total polar work of adhesion (γ mJ/m²) of surfactant solutions with surfaces (Figure 4.12 and 4.13) and water (Figure 3.14 and 3.15), it seems clear that the formation of donor-acceptor adducts is energetically more favorable in the liquid bulk. Moreover, we note that the oil-borne moisture (~30 ppm in pure hexane, 40~80 ppm in solutions of the PIBS-N),⁹ as dispersed and confined in inverse micelle cores with a few nanometer size, would have significantly larger surface area (γ m²) than the total surface area of micron-size colloidal particles (~30 ppm in our study, comparable to the concentrations in other studies^{1,8-9,14,21,36,38} where electrophoresis measurements were carried out) dispersed in nonpolar dispersions. Overall, the (total) free energy gain by donor-acceptor adduct formation (and so the propensity of charge transfer and ionization) of surfactants can be significantly larger with the third species water than with the surfaces, and therefore, the net surface charge is likely to be influenced by the partitioning of inverse micelle ions which are primarily generated in the liquid bulk.⁹ We note that the surface charge corresponding to the small electrophoretic mobility in nonpolar dispersions is only in the order of a few tens of elementary charge.^{22,36}

In the similar vein, the positive influence to net surface charging, which was tentatively attributed to the charge transfer between surfaces and electrically “neutral” surfactants, might also involve the contribution of micelle “cation” adsorption, favored chemically by basic surfaces (Figure 4.14). Note that this type of “ion-dipole” interactions³⁶ can also be considered “acid-base” interaction, although the essential mechanism is different from the charge transfer between two electrically neutral species.⁵² From this perspective, the mere qualitative correlations⁵⁻⁸ between relative surface charging behavior and acidity/basicity strength for a series of particles, although the phenological observation may still have some implications in practical formulation, cannot be an “evidence” for charge creation by direct donor-acceptor interaction of neutral surfaces with surfactants. For example, some chemically “acidic” surface sites may acquire negative influence to net surface charging either by undergoing donor-acceptor interaction with basic sites of neutral surfactants or by attracting some charged micellar anions. Similarly, some chemically “basic” surface sites may acquire positive influence to net surface charging by undergoing donor-acceptor interaction with acidic sites of neutral surfactants or by attracting some charged micellar cations. To avoid confusion, we stress that the entropic partitioning of (chemically unfavorable) micellar ions, discussed in the previous section, is distinguished from this modified acid-base particle charging mechanism which is essentially a contribution to net surface charging driven by chemical affinity between interacting components.

4.3.3. Ionization of Specific “Surface Functionality”

Although we have not observed any clear evidence for the role of particles’ specific surface functionality in solutions of the customized surfactant PIBS-N, surface charging behavior of the same particles in solutions of the commercial surfactant product OLOA11000 (Figure 4.15 to 4.23) indicate in what condition the functional groups may possibly influence the net surface charging.

The zero-field electrophoretic mobility of PMMA-sulfate, PS-sulfate, and PS-carboxyl particles in these solutions (Figure 4.23) appears similar to that in the PIBS-N solution (Figure 4.9) However, the mobility of PS-amidine is remarkably less negative than that of PS-sulfate and PS-carboxyl.

Explaining this particular difference with only a combination of above suggested charging pathways is not possible. One possible explanation is that the functional groups’ ionizability might have been particularly activated in this solution for some reason, and the amidine functional groups rendered the net surface charge less negative by acquiring extra positive influence in surface charging.

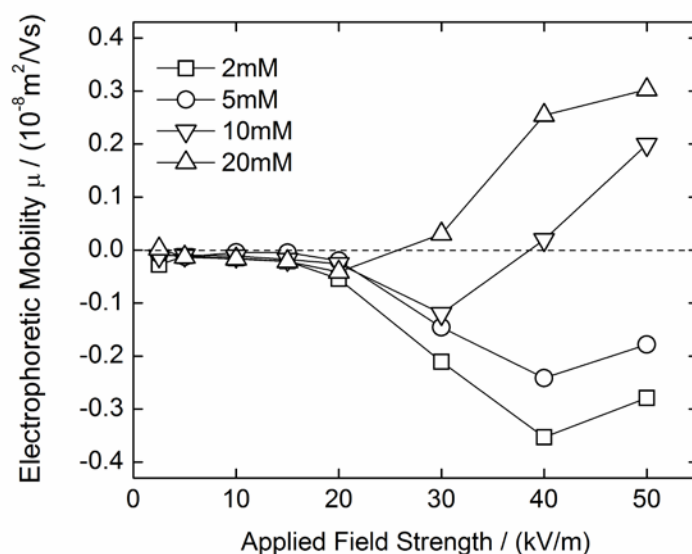


Figure 4.15. The field dependent electrophoretic mobility of the charged PMMA-sulfate particle in hexane-based dispersions of the surfactant OLOA11000 in the range of applied field strength between 2.5 kV/m to 50 kV/m.

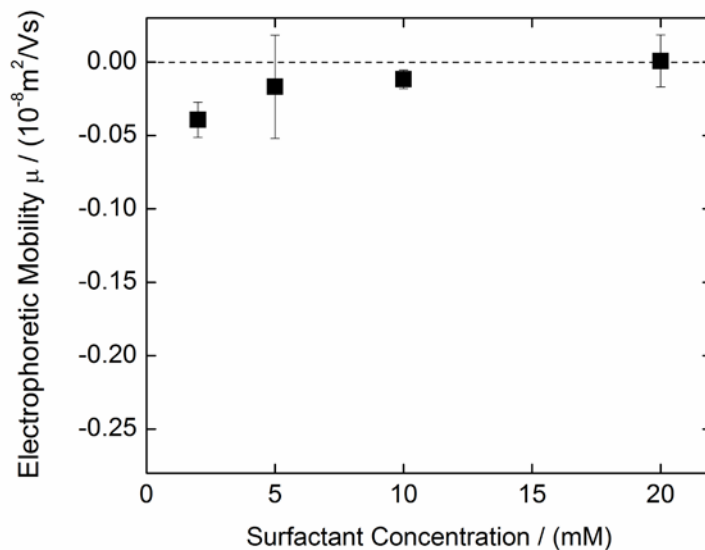


Figure 4.16. The zero-field electrophoretic mobility of the charged PMMA-sulfate particle in hexane-based dispersions of the surfactant OLOA11000, represented as a function of surfactant concentration.

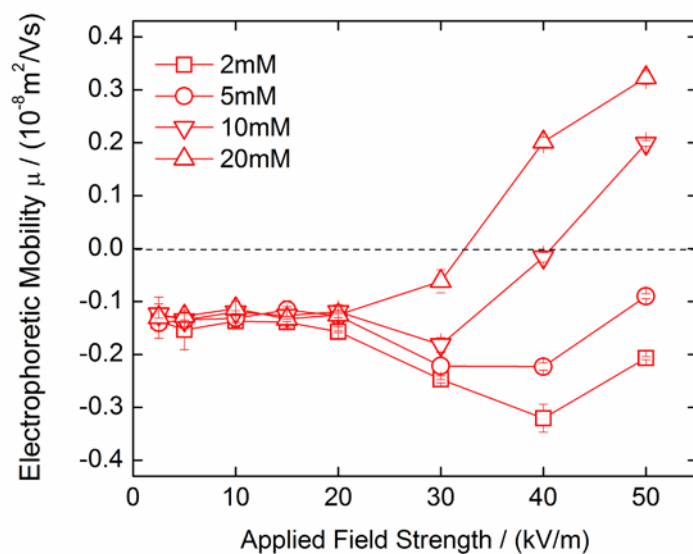


Figure 4.17. The field dependent electrophoretic mobility of the charged PS-sulfate particle in hexane-based dispersions of the surfactant OLOA11000 in the range of applied field strength between 2.5 kV/m to 50 kV/m.

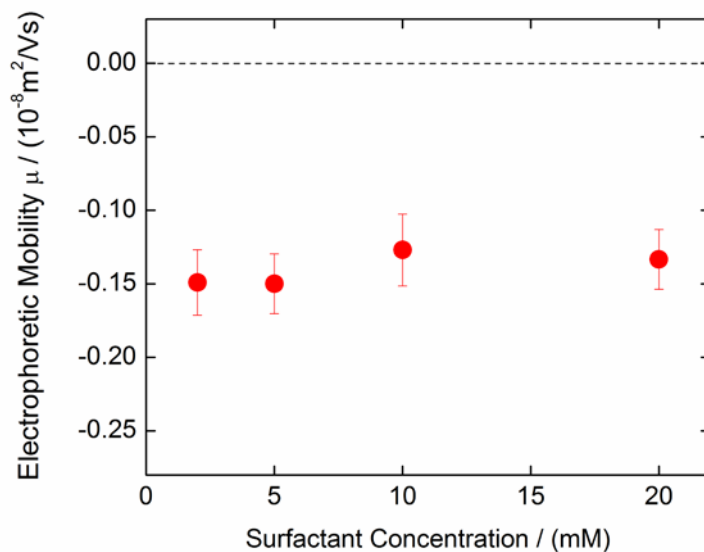


Figure 4.18. The zero-field electrophoretic mobility of the charged PS-sulfate particle in hexane-based dispersions of the surfactant OLOA11000, represented as a function of surfactant concentration.

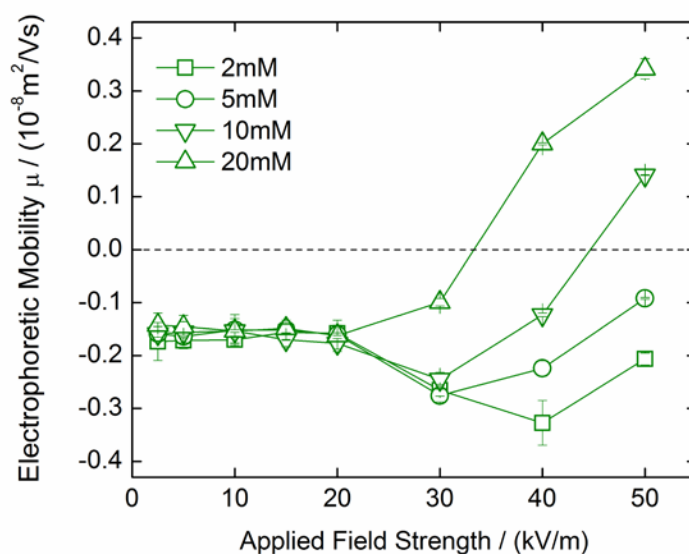


Figure 4.19. The field dependent electrophoretic mobility of the charged PS-carboxyl particle in hexane-based dispersions of the surfactant OLOA11000 in the range of applied field strength between 2.5 kV/m to 50 kV/m.

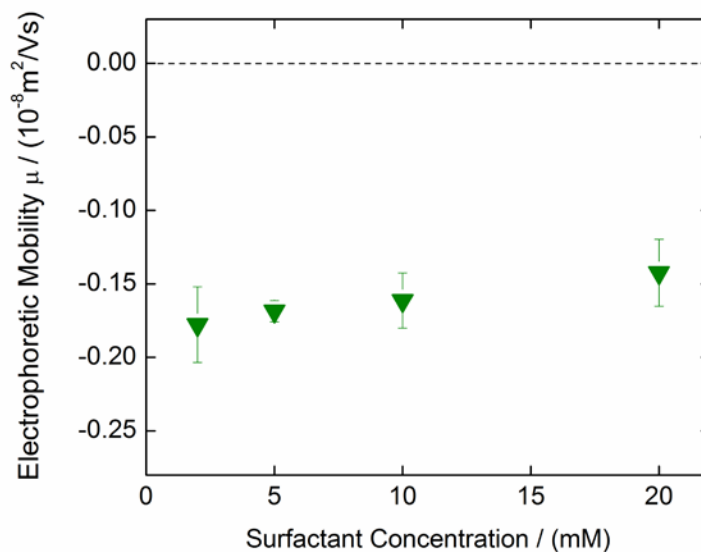


Figure 4.20. The zero-field electrophoretic mobility of the charged PS-carboxyl particle in hexane-based dispersions of the surfactant OLOA11000, represented as a function of surfactant concentration.

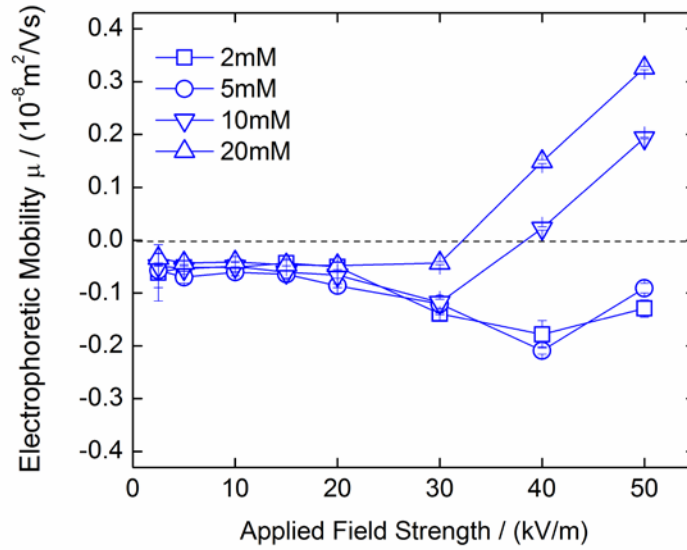


Figure 4.21. The field dependent electrophoretic mobility of the charged PS-amidine particle in hexane-based dispersions of the surfactant OLOA11000 in the range of applied field strength between 2.5 kV/m to 50 kV/m.

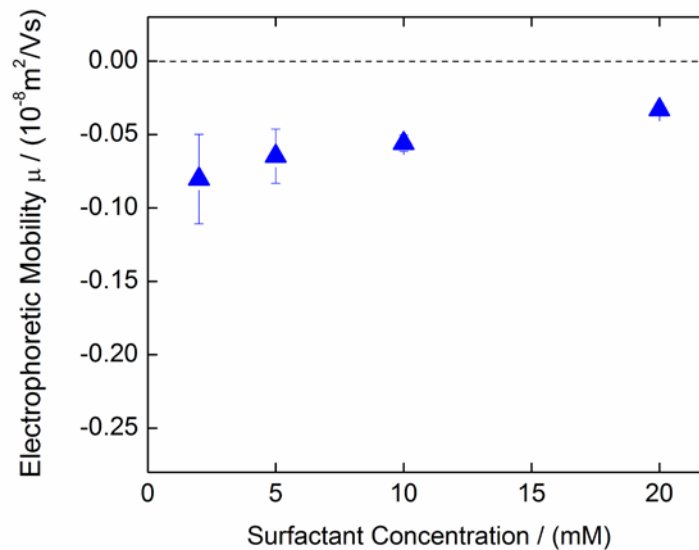


Figure 4.22. The zero-field electrophoretic mobility of the charged PS-amidine particle in hexane-based dispersions of the surfactant OLOA11000, represented as a function of surfactant concentration.

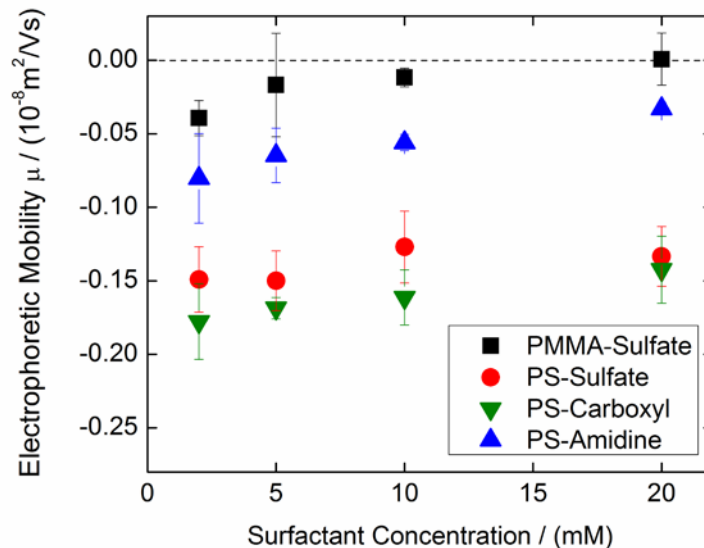


Figure 4.23. The zero-field electrophoretic mobility of the charged polymer particles in hexane-based dispersions of the surfactant OLOA, represented as a function of surfactant concentration.

A likely source promoting the ionization of surface functionality could be “excess moisture”,^{1,13} which might directly partition to the particle surface⁵³ or behave as an “aqueous bulk”⁵⁴⁻⁵⁵ rather than confined molecules adhered to the interfaces in inverse micelle cores.⁵⁶⁻⁵⁷ In such cases, the specific surface functional groups would be solvated more efficiently by water molecules and the locally high dielectric environments would promote their ionization by reducing the energy cost associated with this process – essentially the same principle as why the large water-swollen inverse micelles are more likely to contribute to the total charge distribution in nonpolar media.^{9,24,35,45-48} We measured the water content in nonpolar solutions of OLOA11000 using Karl Fischer

titration, and found that these solutions, prepared with the product as received without any purification or drying process, included significantly larger amount of water than in PIBS-N solutions (Figure 4.24). We note that the measured water content in OLOA11000 solutions is roughly in the same order of magnitude as the solutions of another hygroscopic surfactant AOT, where some evidences for the ionization of particles' functional groups were also observed.¹

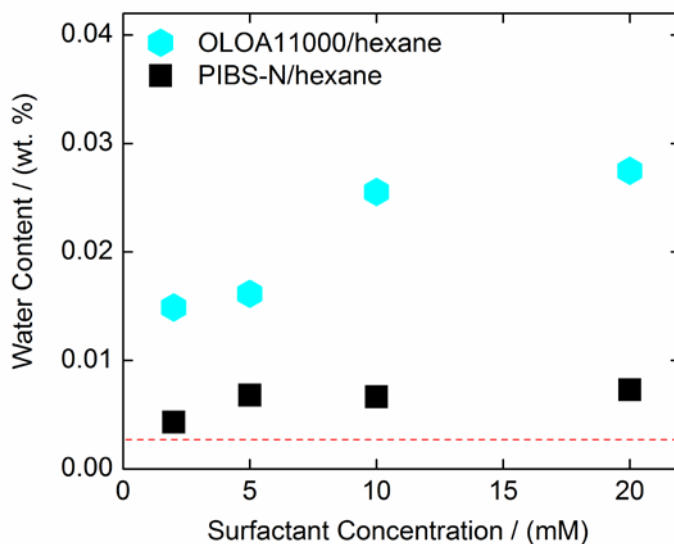


Figure 4.24. Water content in hexane solutions of the surfactant OLOA11000 and custom surfactant PIBS-N.

However, we stress that the ionization of surface functional groups, which is related to their acid/base characters, is just a “contribution” to “net” surface charging (Figure 4.14), not the “only” governing parameter – this is clearly distinguished from the traditional acid-base particle charging mechanism. For example, a speculation that only the direct acid-base interaction of OLOA11000 and particles’ functional groups might have caused the apparent surface charging shown in Figure 4.23, based on the shortsighted observation of a significant difference in surface charging between PS-amidine and PS-carboxyl/sulfate, can be simply objected by the fact that PS-amidine was more negatively charged than PMMA-sulfate (against the relative charging of two particles in aqueous media, shown in Figure 4.10). Moreover, the fact that only one type of particle’s surface charging was significantly differentiated in two different solutions, with otherwise particles maintaining similar charge, essentially reveals that surface charging may not be fully described by a single regulatory parameter such as acid/base strength but must be understood as a *net* consequence of multiple charging pathways (Figure 4.14).

We note that an excellent example that represents the interplays between multiple surface charging pathways has already been shown in our previous study.¹ In this study, surface charging behavior of the same polymer particles was characterized in solutions of the commercial surfactant Span85. At low surfactant concentrations (below the critical micelle concentration (CMC)), the relative charging of PS-amidine/carboxyl/sulfate was strongly correlated with the particles’ aqueous surface charging. This would possibly be because the oil-borne moisture, not being effectively solubilized by hydrophobic^{1,7,24} surfactant Span85 at low surfactant concentrations, might have partitioned significantly

to the particle surface, solvated functional groups, and promoted their ionization. At high surfactant concentrations (above the CMC), on the other hand, all PS particles acquired similarly positive charge. Moreover, PMMA-sulfate acquired significantly larger positive charge than any of PS-amidine/carboxyl/sulfate. The charging behavior at high surfactant concentrations are qualitatively correlated better with the polarity of particle bulk than with the particles' specific functional groups, similar as the current system containing the surfactant PIBS-N. This transition at high surfactant concentrations would possibly be because water might have been more effectively scavenged by inverse micelles at above the CMC so that the functional groups' ionization was effectively deactivated and the particles' acquisition of ions was more likely to depend on the polarity of dry (pristine) particle bulk.

4.4. Conclusion

In this Chapter, we observed charging behavior of a series of polymer particles, PMMA-sulfate, PS-sulfate, PS-carboxyl, and PS-amidine in nonpolar solutions of the surfactant PIBS-N.

We found *no* evidence that surface charging was correlated with the functional groups' acid/base chemistry, as opposed to the traditionally proposed acid-base particle charging mechanism. Instead, we found that charging was correlated with the Lewis basicity of "particle bulk", which can be understood by the particle bulk's chemical preference for positive sign of charges. We do not restrict this chemical preference only to direct donor-acceptor interaction of the surfaces with electrically neutral surfactants

but also consider the interaction with charged micellar ions in terms of ion-dipole interaction – we showed that the propensity of charge generation from donor-acceptor interactions of surfactants with moisture in the liquid bulk dominated that from direct interactions with surfaces (by approximating the polar work of adhesion for two cases), and therefore, the net surface charge was likely to be influenced by micellar ions primarily generated in the liquid bulk.

The overall negative charging of these hydrophobic and somewhat nucleophilic polymer surfaces was attributed to the “entropic” partitioning of deprotonated water molecules imbedded in large swollen micelles (micelle anions). We argued that concluding a surface to be more “acidic” than the other, by solely looking at the result where the surface was more negatively charged, could be an incorrect inference, as revealed by the QCM result where PS surfaces, more negatively charged than PMMA, formed weaker adducts with surfactants.

Finally, we showed that only in the system of commercial surfactant mixture with “excess moisture”, some evidence for ionization of acidic/basic surface functional groups appeared as a contribution to net surface charging. This is likely to be a consequence of having the excess polar pool which would solvate the specific functional groups more efficiently and reduce the energy cost for their ionization – related to the fact that inverse micelles containing larger polar pools are more likely to participate in spontaneous ionization process. This may eventually indicate that if surface charging in a nonpolar dispersion is similar as charging of the same particles in aqueous media, the system is likely to be more “contaminated” with water; conversely, if charging in a nonpolar dispersion deviates strongly from aqueous charging, the system is likely to be “drier”.

Thus, we claim that surfactant-mediated surface charging in nonpolar dispersions is likely a consequence of multiple charging pathways, rather than a simple product regulated by a single thermodynamic balance between the particle and surfactant. Because of this, a prediction based solely on the properties of particles and surfactants is likely to fail as already revealed by past studies.^{9-11,13,23,25-30}

We expect our finding can serve as a useful basic guideline to make a smart choice of formulation components to achieve a desired surface charging performance in practical applications.

4.5. References

1. Guo, Q.; Lee, J.; Singh, V.; Behrens, S. H. Surfactant Mediated Charging of Polymer Particles in a Nonpolar Liquid. *J. Colloid Interface Sci.* **2013**, *392*, 83-89.
2. Fowkes, F. M.; Jinnai, H.; Mostafa, M. A.; Anderson, F. W.; Moore, R. J. Mechanism of Electric Charging of Particles in Nonaqueous Liquids. *ACS Symposium Series* **1982**, *200*, 307-324.
3. Fowkes, F. M.; Pugh, R. J. Steric and Electrostatic Contributions to the Colloidal Properties of Nonaqueous Dispersions. *ACS Symposium Series* **1984**, *240*, 331-354.
4. Poovadorom, S.; Berg, J. C. Effect of Particle and Surfactant Acid-Base Properties on Charging of Colloids in Apolar Media. *J. Colloid Interface Sci.* **2010**, *346*, 370-377.
5. Gacek, M.; Brooks, G.; Berg, J. C. Characterization of Mineral Oxide Charging in Apolar Media. *Langmuir* **2012**, *28*, 3032-3036.
6. Gacek, M. M.; Berg, J. C. Investigation of Surfactant Mediated Acid-Base Charging of Mineral Oxide Particles Dispersed in Apolar Systems. *Langmuir* **2012**, *28*, 17841-17845.
7. Gacek, M. M.; Berg, J. C. Effect of Surfactant Hydrophile-Lipophile Balance (HLB) Value on Mineral Oxide Charge in Apolar Media. *J. Colloid Interface Sci.* **2015**, *449*, 192-197.
8. Gacek, M. M.; Berg, J. C. The Role of Acid-Base Effects on Particle Charging in Apolar Media *Adv. Colloid Interface Sci.* **2015**, *220*, 108-123.

9. Lee, J.; Zhou, Z.-L.; Behrens, S. H. Mechanisms of Particle Charging by Surfactants in Nonpolar Dispersions. *Langmuir*, accepted. DOI: 10.1021/acs.langmuir.5b02875
10. van Oss, C. J.; Chaudhury, M. K.; Good, R. J.; Monopolar Surfaces, *Adv. Colloid Interface Sci.* **1987**, 28, 35-64.
11. van Oss, C. J.; Chaudhury, M. K.; Good, R. J.; Interfacial Lifshitz-van der Waals and Polar Interactions in Macroscopic Systems, *Chem. Rev.* **1988**, 88, 927-941.
12. Pizzi, A.; Mittal, K. L. *Handbook of Adhesive Technology*; CRC Press; New York, 2003.
13. Morrison, I. D. Electric Charges in Nonaqueous Media. *Colloids Surf., A* **1993**, 71, 1-37.
14. Parent, M. E.; Yang, J.; Jeon, Y.; Toney, M. F.; Zhou, Z.-L.; Henze, D. Influence of Surfactant Structure on Reverse Micelle Size and Charge for Nonpolar Electrophoretic Inks. *Langmuir* **2011**, 27, 11845-11851.
15. Fowkes, F. M.; Pugh, R. J. Steric and Electrostatic Contributions to the Colloidal Properties of Nonaqueous Dispersions. *ACS Symposium Series* **1984**, 240, 331-354.
16. Miller, J. F.; Schatzel, K.; Vincent, B. The Determination of Very Small Electrophoretic Mobilities in Polar and Nonpolar Colloidal Dispersions Using Phase Analysis Light Scattering. *J. Colloid Interface Sci.* **1991**, 143, 532-554.
17. Stotz, S. Field Dependence of the Electrophoretic Mobility of Particles Suspended in Low-Conductivity Liquids. *J. Colloid Interface Sci.* **1977**, 65, 118-130.
18. Thomas, J. C.; Crosby, B. J.; Keir, R. I.; Hanton, K. L. Observation of Field-Dependent Electrophoretic Mobility with Phase Analysis Light Scattering (PALS). *Langmuir* **2002**, 18, 4243-4247.
19. Dukhin, A. S.; Dukhin, S. S. Aperiodic Capillary Electrophoresis Method Using an Alternating Current Electric Field for Separation of Macromolecules. *Electrophoresis* **2005**, 26, 2149-2153.
20. Hashimi, S. M.; Firoozabadi, A. Field- and Concentration-Dependence of Electrostatics in Non-Polar Colloidal Asphaltene Suspensions. *Soft Matter* **2012**, 8, 1878-1883.
21. Gacek, M. M.; Berg J. C. Effect of Synergists on Organic Pigment Particle Charging in Apolar Media. *Electrophoresis* **2014**, 0, 1-7.
22. Espinosa, C.E.; Guo, Q.; Singh, V.; Behrens, S. H. Particle Charging and Charge Screening in Nonpolar Dispersions with Nonionic Surfactants. *Langmuir* **2010**, 26, 16941-16948.

23. Dixon, M. C.; Quartz Crystal Microbalance with Dissipation Monitoring: Enabling Real-Time Characterization of Biological Materials and Their Interactions, *Journal of Biomolecular Techniques* **2008**, *19*, 151-158.
24. Guo, Q.; Singh, V.; Behrens, S. H. Electric Charging in Nonpolar Liquids Because of Nonionizable Surfactants. *Langmuir* **2010**, *26*, 3203-3207.
25. Hsu, M. F.; Dufresne, E. R.; Weitz, D. Z. Charge Stabilization in Nonpolar Solvents. *Langmuir* **2005**, *21*, 4881-4887.
26. Marinova, K. G.; Alargova, R. G.; Denkov, N. D.; Velev, O. D.; Petsev, D. N.; Ivanov, I. B.; Borwankar, R. P. Charging of Oil-Water Interfaces Due to Spontaneous Adsorption of Hydroxyl Ions, *Langmuir* 1996, *12*, 2045-2051.
27. Kim, J.-W.; Lee, D.; Shum, H. C.; Weitz, D. A. Colloid Surfactants for Emulsion Stabilization, *Adv. Mater.* 2008, *20*, 3239-3243.
28. Somasundaran, P. *Encyclopedia of Surface and Colloid Science*, 2nd ed.; CRC Press; New York, 2006
29. Solomons, T. W. G.; Fryhle, C. B. *Organic Chemistry*; Wiley: New York, 2009.
30. Lee, J.; Zhou, Z.-L.; Behrens, S. H. Characterizing the Acid/Base Behavior of Oil-Soluble Surfactants at the Interface of Nonpolar Solvents with a Polar Phase. *J. Phys. Chem. B* **2015**, *119*, 6628-6637.
31. Labib, M. The Origin of the Surface Charge on Particles Suspended in Organic Liquids. *Colloids. Surf.* **1988**, *29*, 293-304.
32. Mayr, H.; Breugst, M.; Ofial, A. R. Farewell to the HSAB Treatment of Ambident Reactivity, *Angew. Chem. Int. Ed.* **2011**, *50*, 6470-6505.
33. Izutsu, K. *Electrochemistry in Nonaqueous Solutions*, 2nd ed.; Wiley-VCH; Weinheim, 2009
34. Kemp, R.; Sanchez, R.; Mutch, K. J.; Bartlett, P. Nanoparticle Charge Control in Nonpolar Liquids: Insights from Small-Angle Neutron Scattering and Microelectrophoresis. *Langmuir* **2010**, *26*, 6967-6976.
35. Yezer, B.; Khair, A. S.; Sides, P. J.; Prieve, D. C. Use of Electrochemical Impedance Spectroscopy to Determine Double-Layer Capacitance in Doped Nonpolar Liquids. *J. Colloid Interface Sci.* **2014**, *449*, 2-12.
36. Roberts, G. S.; Sanchez, R.; Kemp, R.; Wood, T.; Barlett, P. Electrostatic Charging of Nonpolar Colloids by Reverse Micelles. *Langmuir* **2008**, *24*, 6530-6541.
37. Smith, G. N.; Eastoe, J. Controlling Colloid Charge in Nonpolar Liquids with Surfactants. *Phys. Chem. Chem. Phys.* **2013**, *15*, 424-439.
38. Smith, G. N.; Grillo, I.; Rogers, S. E.; Eastoe, J. Surfactants with Colloids: Adsorption or Absorption? *J. Colloid Interface Sci.* **2015**, *449*, 205-214.

39. Halperin, A.; Alexander, S. Polymeric Micelles: Their Relaxation Kinetics. *Macromolecules* **1989**, *22*, 2403-2412.
40. Lund, R.; Willner, L.; Stellbrink, J.; Lindner, P.; Richter, D. Logarithmic Chain-Exchange Kinetics of Diblock Copolymer Micelles. *Phys. Rev. Lett.* **2006**, *96*, 068302.
41. Choi, S.-H.; Lodge, T. P.; Bates, F. S. Mechanism of Molecular Exchange in Diblock Copolymer Micelles: Hypersensitivity to Core Chain Length. *Phys. Rev. Lett.* **2010**, *104*, 047802
42. Mathews, M. B.; Hirschhorn, E. Solubilization and Micelle Formation in a Hydrocarbon Medium. *J. Colloid Sci.* **1953**, *8*, 86-96.
43. Robinson, B. H.; Toprakcioglu, C.; Dore, J. C. Small-Angle Neutron-Scattering Study of Microemulsions Stabilised by Aerosol-OT. *J. Chem. Soc., Faraday Trans.* **1984**, *80*, 13-27.
44. Bru, R.; Sanchez-Ferrer, A.; Garcia-Carmona, F. Kinetic Models in Reverse Micelles. *Biochem. J.* **1995**, *310*, 721-739.
45. Eicke, H. F.; Borkovec, M.; Das-Gupta, B. J. Conductivity of Water-In-Oil Microemulsions: A Quantitative Charge Fluctuation Model. *J. Phys. Chem.* **1989**, *93*, 314-317.
46. Hall, D. G. Conductivity of Microemulsions: An Improved Charge Fluctuation Model. *J. Phys. Chem.* **1990**, *94*, 429-430.
47. Kallay, N.; Chittofrati, A. Conductivity of Microemulsions: Refinement of Charge Fluctuation Model. *J. Phys. Chem.* **1990**, *94*, 4755-4756.
48. Kallay, N.; Tomic, M.; Chittofrati, A. Conductivity of Water-In-Oil Microemulsions: Comparison of the Boltzmann Statistics and the Charge Fluctuation Model. *A. Colloid Polym. Sci.* **1992**, *270*, 194-196.
49. Netz, R. R.; Andelman, D. Neutral and Charge Polymers at Interfaces. *Phys. Rep.* **2003**, *380*, 1-95.
50. Smith, P. G.; Patel, M. N.; Kim, J.; Milner, T. E.; Johnston, K. P. Effect of Surface Hydrophilicity on Charging Mechanism of Colloids in Low-Permittivity Solvents. *J. Phys. Chem. C* **2007**, *111*, 840-848.
51. Kitahara, A.; Satoh, T.; Kawasaki, S.; Kon-No, K. Specific Adsorption of Surfactants Containing Mn or Co on Polymer Particles Revealed by Zeta-Potential in Cyclohexane. *J. Colloid Interface Sci.* **1982**, *86*, 105-110.
52. Della Volpe, C.; Siboni, S. Acid-Base Surface Free Energies of Solids and the Definition of Scales in the Good-van Oss-Chaudhury Theory. *J. Adhesion Sci. Technol.* **2000**, *14*, 235-272.

53. Gacek, M.; Bergsman, D.; Michor, E.; Berg, J. C. Effects of Trace Water on Charging of Silica Particles Dispersed in a Nonpolar Medium. *Langmuir* **2012**, *28*, 11633-11638.
54. De, T. K.; Maitra, A. Solution Behaviour of Aerosol OT in Non-Polar Solvents. *Adv. Colloid Interface Sci.* **1995**, *59*, 95-193.
55. Baruah, B.; Roden, J. M.; Sedgwick, M.; Correa, N. M.; Crans, D. C.; Levinger, N. E. When is Water Not Water? Exploring Water Confined in Large Reverse Micelles Using a Highly Charged Inorganic Molecular Probe. *J. Am. Chem. Soc.* **2006**, *129*, 12758-12765.
56. Blach, D.; Correa, M.; Silber, J. J.; Falcone, R. D. Interfacial Water with Special Electron Donor Properties: Effect of Water-Surfactant Interaction in Confined Reversed Micellar Environments and Its Influence on the Coordination Chemistry of a Copper Complex. *J. Colloid Interface Sci.* **2011**, *355*, 124-130.
57. Pal, S.; Vishal, G.; Gandhi, K. S.; Ayappa, K. G. Ion Exchange in Reverse Micelles. *Langmuir* **2005**, *21*, 767-778.
58. Dukhin, A. S.; Dukhin, S. S. Aperiodic Capillary Electrophoresis Method Using an Alternating Current Electric Field for Separation of Macromolecules. *Electrophoresis* **2005**, *26*, 2149-2153.
59. Cao, H.; Lu, N.; Ding, B.; Qi, M. Regulation of Charged Reverse Micelles on Particle Charging in Nonpolar Media, *Phys. Chem. Chem. Phys.* **2013**, *15*, 12227-12234.

CHAPTER 5

ATYPICAL IONIZATION PROCESSES OF OIL-BORNE AMPHIPHILES

5.1. Overview

In this Chapter, we review some important concepts discussed through the previous Chapters of the thesis, and represent in-depth discussions on elusive, atypical ionization processes of oil-borne surfactants with additional experimental supports. Also, an atypical oil-borne charging agent “amphiphile”, developed based on the knowledge gained from our investigation with small molecular surfactants, will be introduced.

5.2. “Ionization” of “Nonionic” Surfactants

Oil-soluble “nonionic” surfactants lack clear dissociable moieties and are often considered, as their literal term indicates, irrelevant to “ionization” processes.¹⁻⁴ However, a significant number of studies including our previous Chapters have reported that nonionic surfactants do participate in ionization processes in specific circumstances^{3,5-16} such as electric charging of nonpolar liquids⁵⁻¹² and surface charging of colloidal particles^{5-6,8-9,11,13-16} suspended in such media. In our mechanistic schemes of electric charging represented in Figure 3.12, it was suggested that head-group moieties of oil-soluble “nonionic” surfactants would drag some “ions” from their interaction counterpart water, which may sound somewhat counter-intuitive or proofless providing that these

significantly lipophilic surfactants are poorly soluble or dispersible in aqueous phases. Here, we represent some evidences for ionization of these surfactants in the presence of their interaction partner water. We employed the surfactant PIBS-C in this subsection.

5.2.1. Polarity of Surfactant Moieties

As discussed in Chapter 2, the oil-borne nonionic surfactants have some polarity, which essentially make these molecules to be “amphiphilic”.¹⁷⁻¹⁹ The interfacial activity of oil-borne surfactants could be qualitatively appreciated by observing the decrease in the measured interfacial tension of oil phase with (immiscible) polar phases.¹⁰ Taking one step forward, we proposed a pragmatic way of parameterizing the surfactant-mediated solution polarity with an acidity (γ_i^+) and a basicity (γ_i^-), by combining the experimental interfacial tensiometry and a surface thermodynamic theory of van Oss, Chaudhury, and Good (vOCG).¹⁹ The γ_i^+ and γ_i^- values of the PIBS-C solutions were obtained in a range of surfactant concentration, and the results are summarized in Figure 2.8 and 2.9. The increasing basicity of solutions (with no systematic increase in acidity) upon the addition of surfactants reflects in a semi-quantitative way that these surfactants may behave effectively as bases (electron donors or proton acceptors) at interfaces with a polar phase, although the solution parameters themselves are not intrinsic material properties but adaptive ones effective only at interfaces with a polar phase.¹⁹

5.2.2. Electric Charging of O/W Interfaces Mediated by the Nonionic Surfactant

A direct proof for the ionization of these surfactants' basic moieties can be shown by measuring the electrophoretic mobility of the surfactant-stabilized oil-in-water (o/w) emulsion droplets. Although these lipophilic surfactants are scarcely soluble or dispersible in water, they can be introduced into a large volume of aqueous phase by emulsifying a small volume of oil phase containing these surfactants. We added a 1 mL of hexane-based PIBS-C solution with a surfactant concentration 100 mM, into a 9 mL of DI water in a glass vial, and homogenized them at 30000 rpm for 1 min using a homogenizer (IKA Ultra-Turrax® T10 basic). As further diluting the stock emulsion into aqueous phases by a volume fraction 0.6%, the emulsion droplets kept dispersed and did not separate back at least for 6 hours, with hydrodynamic diameters (d_H) below 1 μm .

We measured the electrophoretic mobility of o/w emulsion droplets using phase analysis light scattering (PALS) and found that the oil surfaces were positively charged in a wide range of pH values (Figure 5.1). Providing that “pristine” surfaces of hydrophobic oil droplets tend to be negatively charged,²⁰⁻²³ this result indicates that the surfactant polar moieties have truly basic nature and they were likely to attract protons “pinned” at the o/w surfaces, even though the large lipophilic portion makes the overall surfactant molecules scarcely soluble/dispersible in aqueous bulk (Figure 5.2).

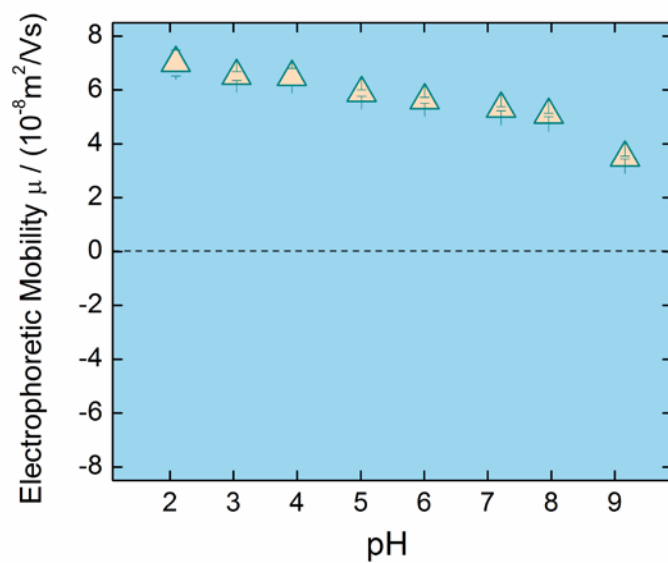


Figure 5.1. Electrophoretic mobility of the o/w emulsion droplets, stabilized by the surfactant PIBS-C, in a range of pH values.

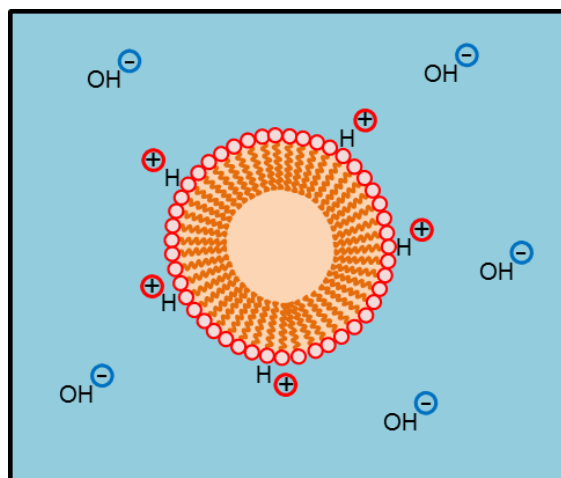


Figure 5.2. Schemes of the o/w emulsion droplets, positively charged by the surfactant PIBS-C “pinned” at the o/w interfaces.

5.2.3. Electric Charging of W/O Interfaces Mediated by the Nonionic Surfactant

These lipophilic nonionic surfactants were readily soluble in nonpolar phases, and at high surfactant concentrations (above ~ 2 mM), formed inverse micelles with an average solvodynamic diameter (d_s) ~ 3 nm.¹⁶ Even though one might imagine only a simple head-to-head adhesion for this self-assembly, we pointed out in previous Chapters that this process is likely to involve water molecules as bridges between the surfactant heads (Figure 3.12),⁵ providing that the complete removal of water molecules would be experimentally unrealistic.^{6,9-10,16,24-25} From such perspective, this process is essentially an inverted case of the oil-in-water system represented in the previous section, *i. e.* a water-in-oil system. Although the amount of the dispersed (water) phase in the order of 50 ppm¹⁶ is numerically very small, with no intended addition, we nonetheless note that its number concentration (or even the number concentration of water in pure alkanes) exceeds the typically reported total charge concentration in nonpolar surfactant solutions.^{12,14}

In Chapter 3, we observed the increase in electric conductivity in nonpolar media upon the addition of this surfactant (Figure 3.17);¹⁶ the viability of these phenomena may be simply appreciated by the classical charge fluctuation theory.²⁶⁻²⁹ However, we also observed systematically negative electrophoretic mobility (Figure 3.9),¹⁶ as we implemented electrophoretic light scattering on particle-free solutions of this surfactant, which cannot be easily described by any existing model. This observation indicated that the size of negatively charged micellar ions would be significantly larger than positive ions, scattering the incident light more strongly, and allowing for their selective detection (providing that the number of oppositely charged ions would be same, as dictated by

electro-neutrality, and formation of multi-valent ions would be energetically disfavored as dictated by the charge fluctuation theory²⁶⁻²⁹).

We demonstrated this size asymmetry in terms of i) intra-micellar donor-acceptor interaction between the basic surfactant head moieties and micelle-imbedded moisture, and ii) inter-micellar exchange of charged surfactants (Figure 3.12).¹⁶ We calculated polar work of adhesion at the interfaces³⁰ between water and surfactant solutions, *i. e.* the (intra-micellar) w/o interfaces, and found that the adduct formation of surfactant solutions' donor sites with water's acceptor sites (Figure 3.14) dominated the reverse case (Figure 3.15). As the heterolysis of these donor-acceptor adducts³¹ happened by expulsion of individual surfactant molecules or inter-micellar molecular exchange in a dynamic equilibrium state³²⁻³⁶ (Figure 3.12), therefore, it is likely that the micelle-remaining water phases are negatively charged and the expelling surfactant polar moieties are positively charged. As a consequence, on average, the larger water-swollen micellar ions would tend to be negatively charged and drier (less-swollen and smaller) micellar ions be positively charged, which explains why we could observe some size asymmetry between the oppositely charged micellar ions in these surfactant solutions.

Indeed, this propensity of charge transfer at the w/o interfaces would have been predicted by observing charging of the o/w interfaces shown in the previous section. As the surfactant molecules were "pinned" at the o/w interfaces, not effectively diffusing out into the aqueous continuous phase, the polar moieties charged the dispersed (oil) phase positively as a consequence of their polar interaction with water (Figure 5.2). For the inverted case shown in the current section, *i. e.* the w/o interfaces, the polar interaction and propensity of charged transfer between the two phases would be identical, but the

dispersed (aqueous) phase could be negatively charged as the positively charged surfactants would now “diffuse out” into the nonpolar continuous phase, becoming counter-ions.

Our scheme is against some typical (simplified) models where an identical (discrete) size of inverse micelles were assumed^{7,9-12,14} and water molecules, implicitly assumed to be equally distributed over the inverse micelles, were considered only a polar “pool” which “supports” some ionization processes. It suggests that inverse micelles, although often characterized with a single (mean) solvodynamic size, would have a size distribution^{12,36} in a dynamic equilibrium state, along which the micelles’ wetness may also fluctuate.¹⁶ Moreover, it considers water not only as a polar pool but also as a “component” which “reacts” with surfactant.

For further validation of this concept, we added an excess amount of water into the surfactant solutions, with a molar water-to-surfactant ratio 50:1, and monitored the change in electrical properties of the solutions. As applying sonication, water molecules were initially dispersed by surfactants, making the continuous phase highly turbid. After a couple of days, a significant volume of water phase settled down and the continuous phase became “clear” surfactant solutions.

As implementing the electrophoretic light scattering on these water-saturated surfactant solutions, we did observe that the negative signal of electrophoretic mobility for micellar ions was generally enhanced (Figure 5.3), which is consistent to our suggested charging pathway (Figure 3.12 and Figure 5.4).

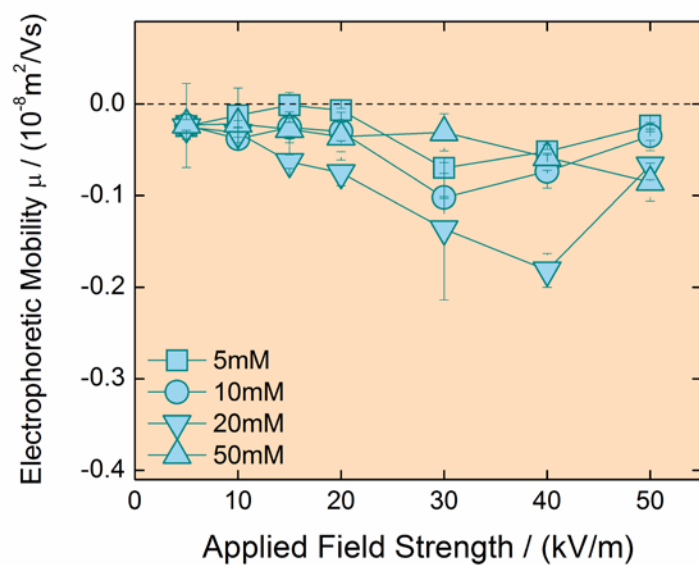


Figure 5.3. The field dependent electrophoretic mobility in the water-saturated PIBS-C/hexane solutions.

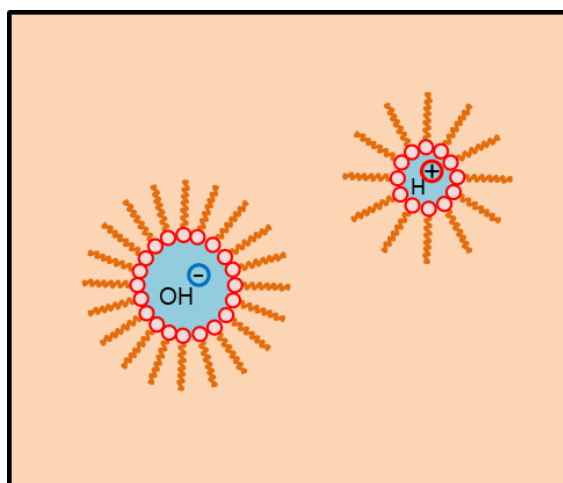


Figure 5.4. Schemes of the oppositely charged w/o emulsion droplets, created by i) intramicellar donor-acceptor interaction between water and surfactant polar moieties and ii) inter-micellar exchange of surfactant molecules.

The electric conductivity in these water-saturated solutions was also significantly enhanced, indicating the enhanced ionization process in these solutions, as we expected. It is notable that unlikely the dry solutions, the electric conductivity is now *linearly* dependent on the surfactant concentration, which is similar to the trend reported for water-in-oil emulsion systems²⁶⁻²⁹ (with the water added intentionally) and nonpolar solutions of some commercial surfactant products^{7,9-12} (possibly with full of chargeable impurities as well as absorbed moisture). Also, we note that such linear concentration dependence of electric conductivity is consistent to what the simplified scheme of micelle disproportionation model, *i. e.* $M + M \rightleftharpoons M^+ + M^-$, would predict.⁹⁻¹⁰ This may reveal that the disproportionation model has been derived for highly “contaminated” systems where the ionization processes were likely to be more effective than drier or purer systems and were limited only by the surfactant,¹⁰ one reactant of the intra-micellar polar interaction. The sub-linear concentration dependence of electric conductivity in dry surfactant solutions shown in previous Chapters might reflect that the solutions transformed into more “impurity-limited” systems as water-to-surfactant molar ratio decreases at higher surfactant concentrations. The enhanced formation of “ion-pairs” than the dissociated ions at high surfactant concentrations, suggested by Duhkin and co-workers,^{8,37} might essentially describe the same phenomena, *i. e.* the decreased efficiency of ionization processes.

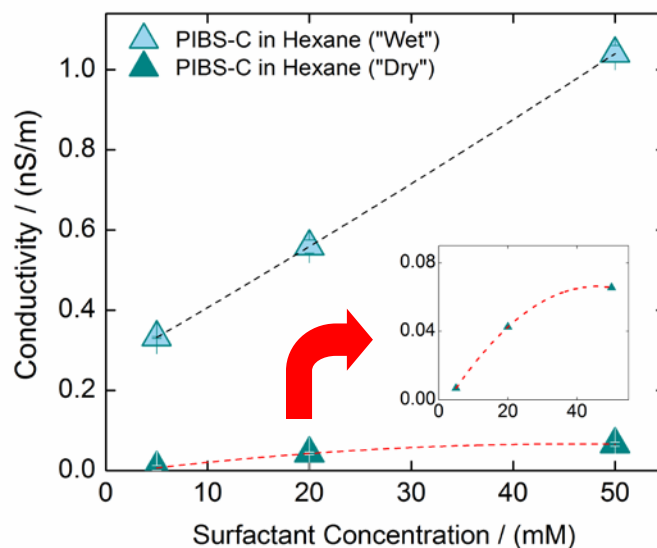


Figure 5.5. Electric conductivity of “dry” and “wet” hexane solutions of the surfactant PIBS-C, represented as a function of surfactant concentration. The inset shows a magnified plot for the dry solutions.

5.3. Surface Charging by Preferential Adsorption of Micelle “Ions”

In previous Chapters, we suggested that surface charging is likely a consequence of interplays between multiple surface charging pathways, which cannot be described by a simple acid/base balance between surfaces and surfactants or their direct polar interactions.¹⁵

The primary complexity arises from the fact that the “polarity” or “acid/base properties” of surfaces could be characterized with those of “particle bulk” or “specific surface functionality”, depending on moisture content in the system. It was

experimentally shown that the surface charge was correlated with either definition of surface polarity in a system dependent manner.¹⁵

The other complexity is associated with the difficulty of appreciating the contribution of chemically-driven micelle ion adsorption to the surface. By seeing the "monopolar basic" surfaces' entropic acquisition of chemically disfavored micelle anions in previous Chapters, we somewhat speculated that micelle cations might have also adsorbed to the surfaces in a competitive manner, via chemically-driven ion (cations) – dipole (surfaces) interactions.¹⁶ Strictly speaking, however, the exact contribution (or existence) of this chemically-driven micelle cation adsorption was difficult to be recognized being isolated from the charge transfer via direct acid-base interaction of monopolar basic surfaces with (electrically neutral) surfactants.

By investigating the surface charging behavior of amphoteric silica particles in the presence of the "dry" surfactant PIBS-C, we will show that surface charging can truly be mediated by other means than any direct charge transfer acid-base interaction of surface component with electrically neutral surfactants. We will show that the polar work of adhesion of surfactant with water (at the intra-micellar interfaces) still dominates that with the hydrophilic silica surface, indicating that the micelle ions primarily generated in the liquid bulk are likely to influence net surface charging significantly by adsorbing to the surfaces as another "acid" and "base" components. By arguing that the asymmetric adsorption state of micelle ions reflected in the surface charging behavior is not likely a consequence of the entropic preference for larger micelle anions, we will appreciate the contribution of micelle ion adsorption driven by some chemical preference of the particle bulk, in terms of ion-dipole interaction.

5.3.1. Polarity of the Silica Particle Surface

We can define the polarity of the solid silica surface in two different ways, to compare it with the polarity of surfactant solutions.

First, we measured the electrophoretic mobility of silica particles in aqueous environment with a range of pH (Figure 5.6 and 5.7). The particles were negatively charged at high pH values above 5, whereas the magnitude of negative charge decreased at low pH values reaching an isoelectric point between pH 2 – 3, which is consistent to the literature.³⁸ Comparing Figure 5.6 with Figure 5.1 with the aqueous pH values as “reference points”, it is inferred that the solid silica surface is chemically more “acidic” than the oil surface decorated with (basic) polar moieties of surfactants since the solid surface was more negatively charged than the oil/surfactant surface via polar interaction with the reference aqueous phases.

Based on the demonstrations in Chapter 4, this aqueous charging behavior of the solid surface is likely to reflect the acid/base properties of its (hydroxyl, –OH) functional groups³⁸ which would be effectively solvated in “wet” environments. If particle charging in nonpolar dispersions would be mainly caused by the acid-base interaction of the surface functional groups and surfactant polar moieties, the particles would be negatively charged according to the traditional acid-base particle charging mechanism.^{11,32,38}

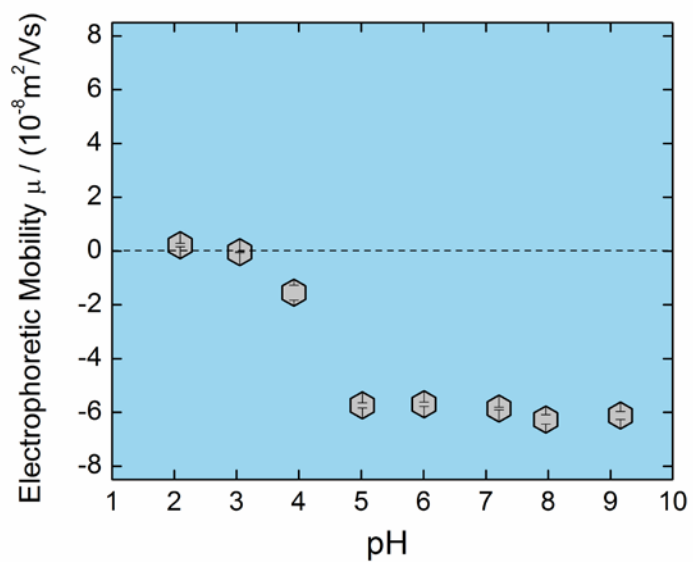


Figure 5.6. Electrophoretic mobility of the silica particles in aqueous phases in a range of pH values.

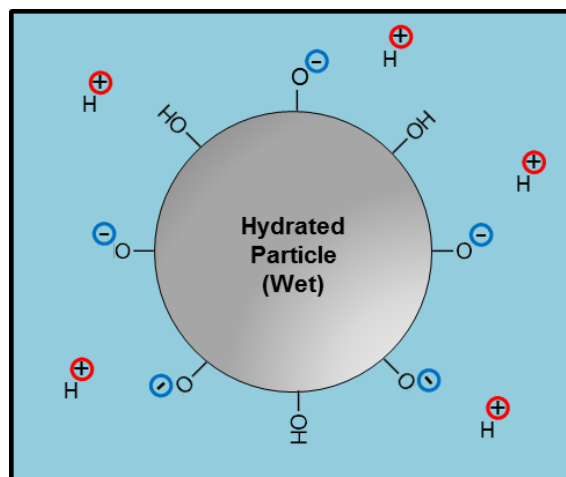


Figure 5.7. Schemes of the charged silica particles with hydroxyl functional groups effectively solvated and ionized in aqueous phases.

The polarity of silica surfaces can also be characterized with the acidity (γ_s^+) and basicity (γ_s^-) parameters in the framework of vOCG theory,^{30,39-40} and the literature values are shown in Table 5.1.⁴⁰

Table 5.1. Acid (γ_s^+) and base (γ_s^-) parameters of the solid silica surface (in mJ/m²).⁴⁰

Solid	Component Parameters (mJ/m ²)	
	Acidity (γ_s^+)	Basicity (γ_s^-)
Glass	1.97	40.22

Since the characterization is conducted for “dry” surfaces (not immersed in aqueous environments), these parameters are more likely to reflect the dry properties of particle bulk than the aqueous acid/base chemistry of surface functional groups, according to the demonstrations in Chapter 4. The finite γ_s^+ and γ_s^- values shown in Table 5.1 indicate that the silica surface has an amphoteric character different than monopolar basic surfaces such as PMMA and PS.³⁹⁻⁴⁰ We note that the significantly larger numerical magnitude of γ_s^- than γ_s^+ might not indicate that the surface is inherently more basic than acidic.^{19,40} As demonstrated in Chapter 2, it has been pointed out that the direct comparison between γ_s^+ and γ_s^- might be meaningless since the reference scale of the vOCG model was developed with an initial assumption $\gamma_{Water}^+ = \gamma_{Water}^-$,³⁰ which requires further validation. Also, the values of γ_s^- for other materials generally tend to be larger than those of γ_s^+ within the adopted reference scale. It has, therefore, been

suggested that only comparisons between the acidity parameters (or basicity parameters) of different materials should be made.⁴⁰

However, this somewhat arbitrary initial assumption does not affect the calculation of polar work of adhesion, $W_{12}^{AB} = -2(\gamma_1^+ \gamma_2^-)^{1/2} - 2(\gamma_1^- \gamma_2^+)^{1/2}$, since an arbitrary factor $a = \gamma_{Water}^+ / \gamma_{Water}^- \neq 1$, based on which the acid/base parameters of two materials 1 and 2 would be obtained, should be cancelled calculation of W_{12}^{AB} .³⁹ We note the manner we use the theory for predicting a possible charge transfer between two interacting phases via their acid-base interactions is to compare each term of W_{12}^{AB} , not comparing between any single parameter of interacting species. Figure 5.8 and 5.9 show the magnitude for $-2(\gamma_S^+ \gamma_{L_1}^-)^{1/2}$ and $-2(\gamma_S^- \gamma_{L_1}^+)^{1/2}$, which are corresponding to the free energy gain by the solid surface (S) acid sites' forming adduct with surfactant solution (L_1) basic sites and the reverse case, calculated using the parameters shown in Table 5.1 and Figure 2.8 – 2.9. Intuitively, the charge transfer via donor-acceptor interaction would be proportional to the free energy benefit by forming donor-acceptor adducts. The calculated results indicate that although the numerical basicity of this particle bulk is significantly larger than the acidity, the surface would be negatively charged via donor-acceptor interaction with predominantly basic (electrically neutral) surfactants, if such interaction would be the major contribution to surface charging.

Thus, with both types of definitions on the solid surface polarity, it is predicted that the surface would be negatively charged if the direct polar interaction between the surface and surfactant polar moieties would be the dominant surface charging pathway.

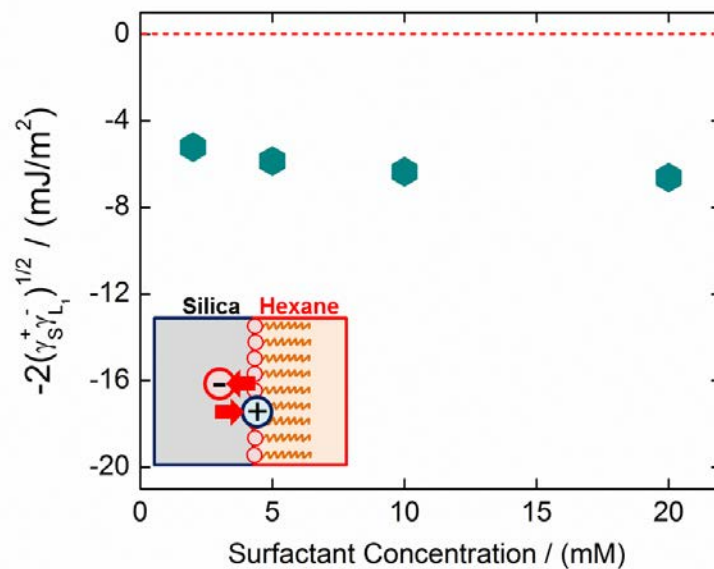


Figure 5.8. The adduct formation energy of the solid surfaces' acidic (electron acceptor or proton donor) sites with the surfactant solutions' basic (electron donor or proton acceptor) sites.

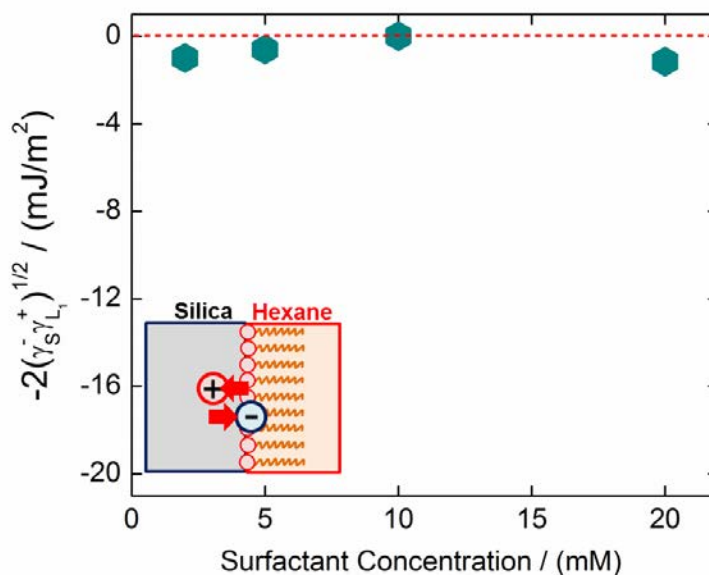


Figure 5.9. The adduct formation energy of the solid surfaces' basic (electron donor or proton acceptor) sites with the surfactant solutions' acidic (electron acceptor or proton donor) sites.

5.3.2. Surface Charging of the Silica Particles

We measured the electrophoretic mobility of charged silica particles in nonpolar dispersions containing the surfactant PIBS-C. Similar to previous Chapters, we observed a non-monotonic field dependence of the particle mobility in a range of the applied field strength from 2.5 kV/m to 50 kV/m (Figure 5.10), and extrapolated the field dependent mobility to zero field strength to infer the particles' equilibrium surface charging state in the absence of external electric fields ("zero-field mobility", Figure 5.11). Even though both predictions based on the two types of definitions on the surface polarity indicated that the surface would be negatively charged via direct charge transfer polar interactions with (electrically neutral) surfactants, we found that the net surface charge had a positive sign. This straightforwardly reveals that there exists another surface charging pathway than the "charge creation" by direct charge transfer polar interaction (Figure 5.12).^{11,32,38}

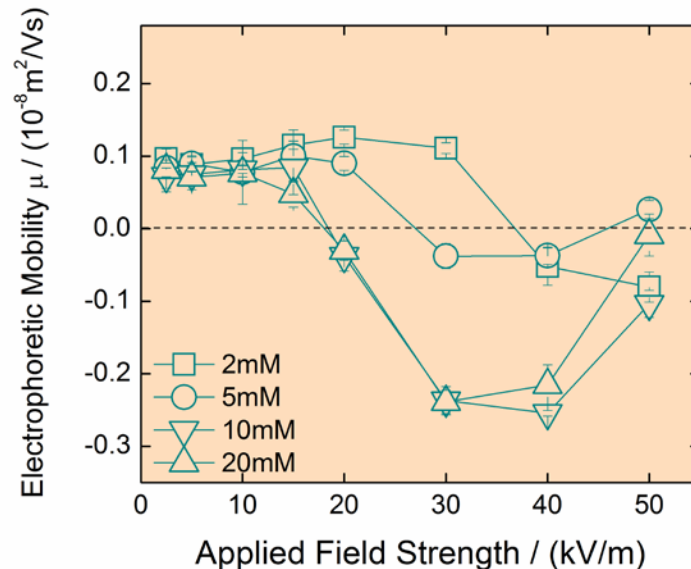


Figure 5.10. The field dependent electrophoretic mobility of the charged silica particles in hexane-based dispersions of the surfactant PIBS-C, in the range of applied field strength between 2.5 kV/m to 50 kV/m.

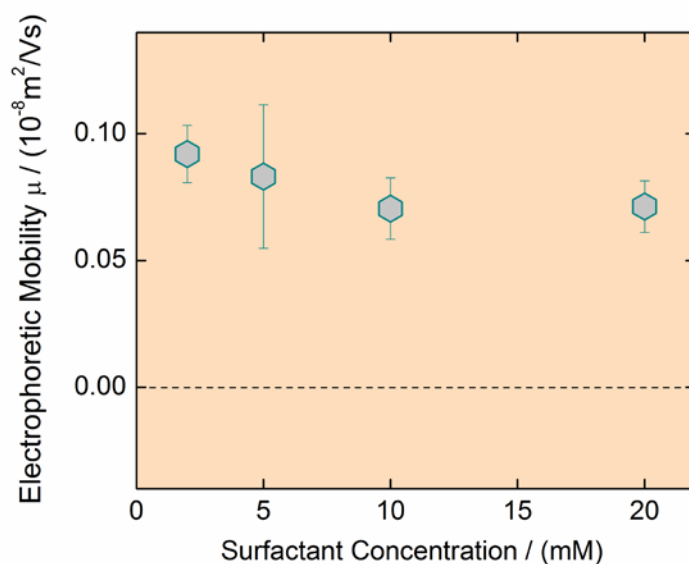


Figure 5.11. The zero-field electrophoretic mobility of the charged silica particles in hexane-based dispersions of the surfactant PIBS-C, represented as a function of surfactant concentration.

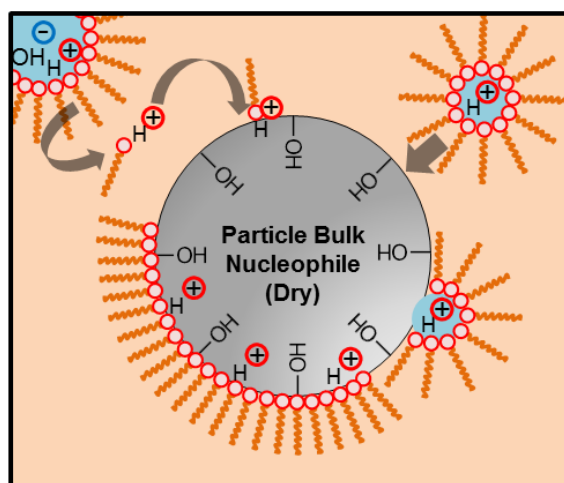


Figure 5.12. Schemes of the charged silica particles in nonpolar dispersions containing the surfactant PIBS-C. No evidence found for direct charge transfer polar interaction between the particle (bulk and functional groups) and surfactant.

As demonstrated in previous Chapters, the “charge acquisition” by micelle ion adsorption^{8-9,16,41-45} is a reasonably possible surface charging pathway rather than the direct polar interaction with electrically neutral surfactants. We note that even though the silica surface (Table 5.1) is significantly more polar than some hydrophobic polymer surfaces (Table 3.1 and 4.1), the total polar work of adhesion of surfactants with this surface (Figure 5.8 and 5.9) is still smaller than that with water (Figure 3.14 and 3.15). We also note that the total surface area of water phase, created as water molecules in the order of 50 ppm¹⁶ are dispersed by inverse micelles with a nanometer-size core, would readily exceed the surface area of micrometer-size particles (with a concentration diluted for electrophoresis). Therefore, the ionization process is likely to happen primarily in the liquid bulk via water-surfactant polar interactions, and the resulted micelle ions are likely to influence particle surface charging by adsorbing to the surface as another “acid” and “base” components.⁴⁶

For the asymmetric adsorption state of the oppositely charged micelle ions where the micelle cations dominated the anions, we point out that such asymmetry might not have been driven by the surface’s entropic preference¹⁶ for micelle cations since the size of micelle cations was smaller than micelle anions. We may possibly attribute this asymmetric adsorption state to somewhat chemical preference of the silica surface for the cations. The preference of the silica surface for the cations may indicate that the significantly larger basicity parameter (γ_s^-) of this surface than the acidity parameter (γ_s^+),⁴⁰ even though the validity of their direct comparison is under debate, might capture some real (nucleophilic) nature of the dry particle bulk.^{30,39} Unfortunately, we currently have no (quantitative) theoretical framework to describe this kind of (micelle) ion –

(surface) dipole interaction. However, we do evident that there is a contribution to surface charging, which is not the direct polar interaction of any surface component, particle bulk or functional groups, with electrically neutral surfactants, which is neither the entropy-driven adsorption of micelle ions.

5.4. Charging Agent “Amphiphiles” Other than the Molecular Surfactants

In previous Chapters, we repeatedly stressed that the presence of moisture, as a polar pool wherein charges can reside, would play a significant role in ionization process in nonpolar media. Electric charging of nonpolar liquids is not essentially a “magic”, such as a conduction of a mixture of non-conducting materials,³⁷ but a consequence of having locally high dielectric environments where ionization process can be facilitated.^{10,16}

We nonetheless note that the mere addition of water, with no surfactants, do not increase the electric conductivity significantly, because the polar water molecules do not tend to suspend in nonpolar media by themselves – the added aqueous phase immediately separates back from the nonpolar phase, since mixing of two phases is energetically disfavored process.

Therefore, a “suspender” of moisture, which suspends itself in nonpolar media by having a sufficiently lipophilic portion in its structure and also supports moisture to be suspended by having, too, somewhat hydrophilic faces consisting of polar moieties, would be required, as a charging agent, to cause charge fluctuation in nonpolar media.

In principle, this hypothesis should not limit the type of charging agents to small molecular surfactants we have discussed so far throughout the previous Chapters. Any “amphiphiles” which have some hydrophilic compartments but are lipophilic enough to suspend stably in nonpolar media, mimicking the molecular surfactants with low hydrophilic – lipophilic balance (HLB) number, would possibly increase the electric conductivity in nonpolar media.

We show an example of such atypical charging agent amphiphiles in this subsection.

5.4.1. Oil-dispersible “Janus” Particles

Janus particles, named after the two-faced Roman god, are colloidal particles with two distinctly different sides or “faces”. Amphiphilic Janus particles, with one hydrophilic and one hydrophobic face, have attracted much attention, because they combine properties of ordinary colloid particles and of small molecular surfactants.⁴⁷⁻⁵⁰ Thanks to the asymmetric bi-compartmentalization of these particles, their amphiphilicity can be finely tuned by varying either the chemistry and wettability of two compartments⁵¹⁻⁵² or their geometry.^{50,53-57} The strategy here is analogous to the case of designing molecular amphiphiles, where the molecules’ affinity to water (or oil) is controlled by their HLB number or packing parameter.⁵⁸⁻⁵⁹ One should note that although the term “amphiphilic” suggests a simultaneous affinity for both polar and nonpolar phases, surfactants often show very selective partitioning between the two phases whose interface they populate, sometimes to the point of being soluble in one bulk phase only. For example, the molecular surfactants with high HLB number (or small packing

parameter) are predominantly hydrophilic and used in applications where they are dissolved in aqueous phases. Examples include common water-soluble surfactants such as sodium dodecyl sulfate (SDS), alkyl benzene sulfonates, or highly ethoxylated sorbitan esters (Tweens).⁶⁰⁻⁶¹ On the other hand, surfactants with low HLB number (or large packing parameter), such as sorbitan esters of the Span series or polyisobutylene succinimide dispersants (OLOA), are hydrophobic and lipophilic, and typically added to nonaqueous media, sometimes purely *dispersive*⁵⁹ non-polar liquids such as saturated hydrocarbons.^{17,19,60,62} When it comes to amphiphilic Janus particles, it is notable that the examples presented in the literature almost exclude the ones selectively dispersible in nonpolar phases; the majority of amphiphilic Janus particles are either primarily water dispersible or dispersible both in water and oils. To our knowledge, it has not yet been established to what extent Janus particles can mimic the behavior of lipophilic molecular surfactants in nonpolar solvents. In this thesis, particularly, whether such lipophilic Janus particles would promote electric charging in the nonpolar solvent is of primary interest.

5.4.2. Particle Synthesis via a Two-Step Seeded Emulsion Polymerization

The oil-dispersible Janus particles prepared here are dimers of two partially merged polymeric spheres, a shape that can be described as “snowman” or “dumbbell”-like.^{50,53-57} This type of Janus particles is considered attractive since it is possible to control independently the chemistry and size ratio of the two lobes, where both parameters significantly influence the particles’ amphiphilicity. Another considerable advantage of these Janus particles is that they can be synthesized at high-yield via seeded emulsion polymerization.⁵⁶

We prepared the oil-dispersible Janus snowman particles by following well-established procedures⁵³⁻⁵⁷ of two-step seeded emulsion polymerization procedure with a small chemical modification.

In synthesis of the first (hydrophilic) bulb of a dimer, an aqueous dispersion of linear polystyrene (PS) particles, spherical latexes with 99 nm in diameter, with a particle concentration 9.2 wt. % was mixed with a monomer mixture of styrene (St, Sigma Aldrich) and 3-(trimethoxysilyl)propyl acrylate (TMSPA, Sigma Aldrich) (84:16 in wt. %), and an initiator 2,2'-azobisisobutyronitrile (AIBN, Sigma Aldrich) (0.5 wt. % of the monomer mixture). The weight ratio of the monomer mixture to PS seed particles was 50:50. The PS seed particles in aqueous dispersion were swollen with the monomers for 12 hrs. The polymerization was then carried out at an elevated temperature (70 °C), which resulted in spherical hydrophilic bulbs with the surface consisting of trimethoxy silane functionalized PS, poly(St-*co*-TMSPA).

In order to grow the second (hydrophobic) bulb of the dimer, an aqueous dispersion of the spherical particles synthesized in the first step (hydrophilic bulbs) with a particle concentration 11.7 wt. % was mixed with an emulsion of a monomer mixture, consisting of styrene and isodecyl methacrylate (IDMA, Sigma Aldrich) (32:68 in wt. %), the initiator AIBN (0.5 wt. % of the monomer mixture), and an aqueous 1.6 wt. % polyvinyl pyrrolidone (PVP, $M_w \sim 40000$ g/mol, Sigma Aldrich) solution. The weight ratio of the monomer mixture to aqueous PVP solution was 12:88. The weight ratio of the monomer mixture to the hydrophilic bulb particles was 82:18. The hydrophilic bulb particles were swollen with the monomers for 12 hrs. The polymerization was then carried out at an elevated temperature (70 °C), which resulted in the second spheres,

consisting of random copolymer of St and IDMA, poly(St-*co*-IDMA), partially engulfing the first spheres.

The synthesized particles were washed with methanol (three times) and ethanol (three times) to remove the unreacted monomers and PVP, by centrifuging the suspensions, removing the supernatant, and redispersing the particles in the cleaning solvent alcohols via sonication. It was found that the stability of these hydrophobic particles in polar alcohols significantly reduced, as the dialysis proceeded with the water/alcohol soluble stabilizer PVP washed out, forming macroscopic aggregates rapidly after the sonication (typically after the 2nd wash with methanol). The particles were then washed five times with non-polar solvent hexane (VWR); unlike the case where the particles were attempted to disperse in alcohols, they were readily dispersed in hexane. After the dialysis, the particles were finally dispersed in hexane and the dispersions were diluted with a concentration of interest.

The morphology of the synthesized particles was characterized by scanning electron microscope (SEM), using Ultra60 Field Emission SEM (Carl Zeiss AG). A small volume of diluted particle dispersion was pipetted on the glass substrate and dried under ambient condition. The particles deposited on the glass slide were sputter-coated with small gold/palladium particles before characterization, to prevent charging. An accelerating voltage of 5 kV was used. Figure 5.13 shows a representative SEM image of the Janus snowman particles.

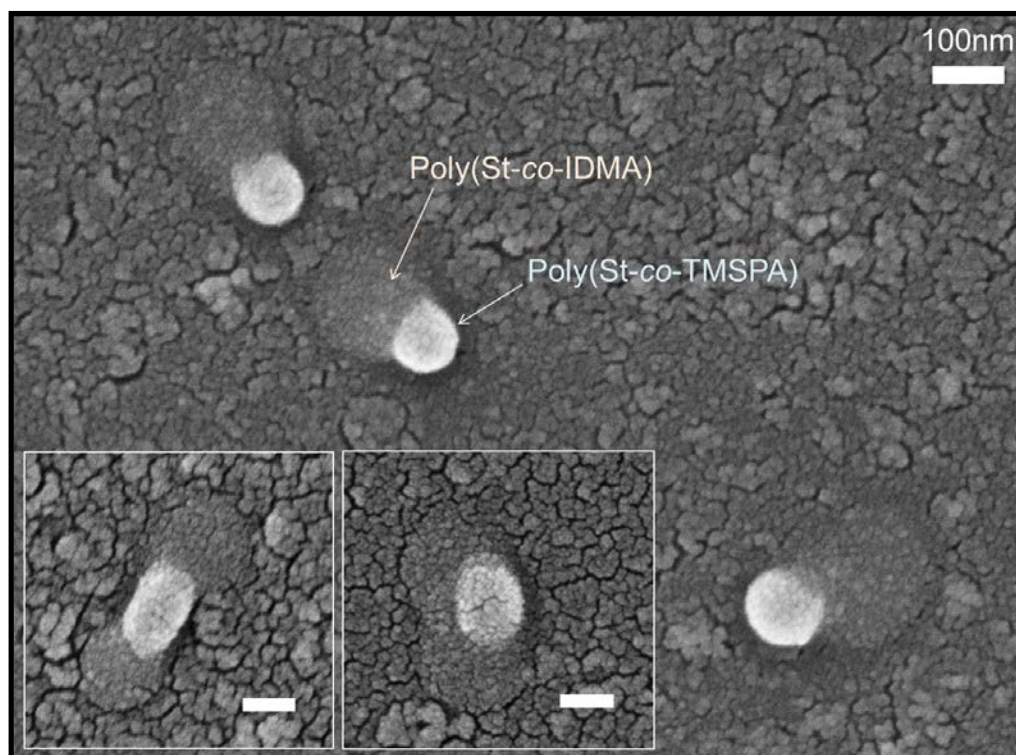


Figure 5.13. Oil-dispersible Janus snowman particles consisting of poly(St-co-TMSPA) (hydrophilic) and poly (St-co-IDMA) (hydrophobic) surfaces. The particles were deposited on the glass slide from a 20 ppm hexane dispersion and sputter-coated with small gold/palladium particles for SEM imaging. The (larger) hydrophobic lobes, which presumably swell in the alkane solution, are harder to discern in the images because of their weak contrast. The insets show examples of two associated snowman particles with their hydrophilic heads in contact. The scale bar represents a 100 nm.

5.4.3. Oil-Dispensibility of the Particles with a Co-Polymeric Hydrophobic Bulb

Our amphiphilic Janus snowman particle consists of two partially fused lobes, the hydrophilic lobe whose surface consists of a copolymer of styrene and 3-(trimethoxysilyl)propyl acrylate, and the hydrophobic lobe consisting of styrene and

isodecylmethacrylate. In previously reported similar procedures, pure PS was selected as the “hydrophobic” compartment of dimers.⁵³⁻⁵⁷ However, it should be noted that even the pure PS particles, without hydrophilic bulb, are not dispersible in nonpolar liquids without additives¹⁵ (Figure 5.14A). Therefore, the conventional Janus snowman particles or dumbbells generated by seeded emulsion polymerization, with PS as hydrophobic compartment, also cannot be dispersed in alkanes.

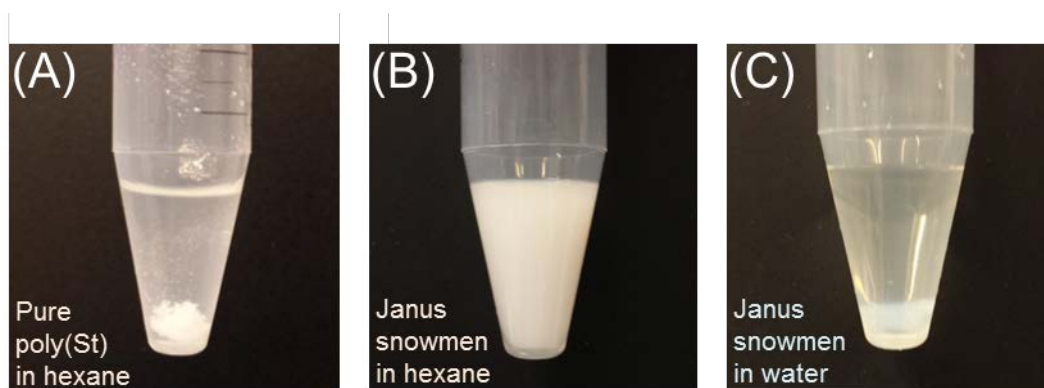


Figure 5.14. (A) Pure (linear) PS particles failing to disperse in hexane. (B) Lipophilic Janus snowman particles dispersed in hexane. (C) Lipophilic Janus snowman particles failing to disperse in water.

By contrast, the Janus snowmen particles prepared here, with a hydrophobic compartment made of (random) *copolymer* of alkylmethacrylate and styrene, are found to have excellent oil-dispersibility (Figure 5.14B).

We measured the solvodynamic diameter of these particles in hexane, using dynamic light scattering (DLS).⁶³⁻⁶⁴ For characterizing the diameter in nonpolar dispersions with *low* particle concentration (7 ppm, where the oil continuous phase looks almost clear), we used a ALV DLS/SLS-5022F (ALV-Laser Vertriebs GmbH) standard

goniometer system. A second order cumulant fit to the intensity autocorrelation function was used to obtain the solvodynamic diameter of particles. For the dispersions with *high* particle concentration (300, 1500, and 8600 ppm, where the oil continuous phase looks slightly turbid to completely milky), we employed 3D Cross Correlation DLS (3DDLS) technique to suppress undesired multiple scattering of light.⁶⁴ We use a 3D cross-correlation setup manufactured by LS Instruments. The laser wavelength is $\lambda = 632.8$ nm and scattered light is collected by two avalanche photodiode detectors mounted on a rotating goniometer. The measurements were taken at the scattering angle 20° to 140° in 10° increments, for 2 min (4 min at the highest conc.) at each angle.

The measured solvodynamic diameters at different particle concentrations are summarized in Table 5.2. Interestingly, the measured size (~ 400 nm) is roughly consistent with two or few associated snowman particles (such as the particle pairs shown in the insets of Figure 5.13). This size appears fairly independent of particle concentration, with no indication of the significantly larger aggregates commonly found in unstable dispersions, up to high concentrations (8600 ppm) where the dispersion looks milky.

Table 5.2. Solvodynamic diameter of the oil-borne particles in hexane measured by DLS.

Particle Concentration (ppm)	Solvodynamic Diameter (nm)	Measurement Method
7	403	DLS
300	414	3DDLS
1500	400	3DDLS
8600	397	3DDLS

5.4.4. Interfacial Activity of the Oil-Borne Particles with Water (Hydrophilicity)

Our Janus snowman particles have poor water-dispersibility (Figure 5.14C), unlike many Janus particles that are either primarily water dispersible or dispersible both in water and oils. In this regard they resemble the selectively oil-soluble surfactants often used as dispersants in nonpolar solvents. We note that the poor water solubility of such surfactants and their consequent retention in nonpolar media upon contact with water can be advantageous in their practical applications,¹⁹ and that the strong bias for nonpolar phases does not prevent these surfactants from adsorbing at oil-water interfaces and reducing the interfacial tension.^{3,19,62}

The question arises whether such interfacial activity can also be observed for our oil-borne, water-indispersible Janus snowman particles. To answer this question, we measured the interfacial tension of hexane-based snowman particle dispersions with water, using drop shape analysis. We used ramé-hart goniometer model-250 (ramé-hart) to carry out video image edge tracing of the pendent drop of oil phase at an inverted steel needle submerged in the surrounding aqueous phase. The interfacial tension between two immiscible phases was calculated based on the shape of pendant drop. Measurements were taken for longer than 20 min to measure the interfacial tension at equilibrium with particles saturated at the interface. Upon increasing the particle concentration, the (effective) interfacial tension between water and hexane dispersions steadily decreases from a value close to 50 mJ/m² in the absence of particles to a plateau value of ~31 mJ/m² for particle concentrations above 1000 ppm (Figure 5.15 and 5.16). The snowman particles thus adsorb at the oil-water interface with a collective adsorption energy large enough to substantially reduce the overall interfacial energy.

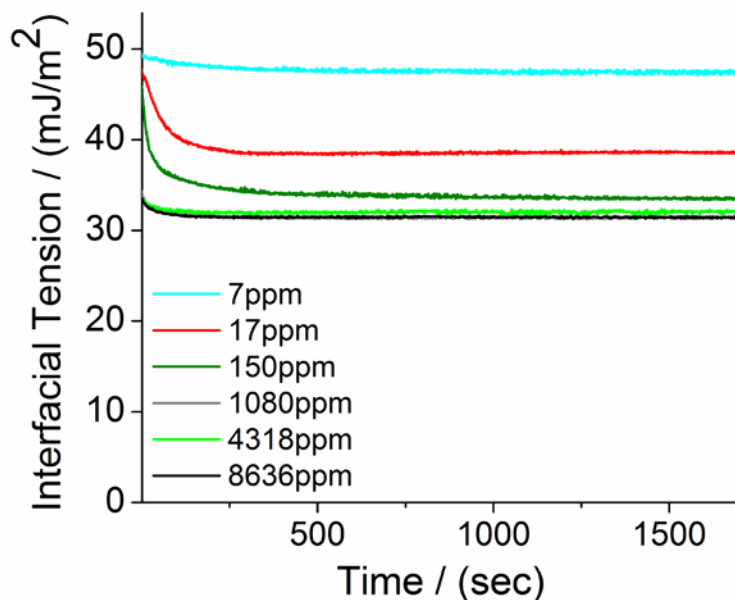


Figure 5.15. Time-dependent interfacial tension of water with hexane-based dispersions of Janus snowman particles.

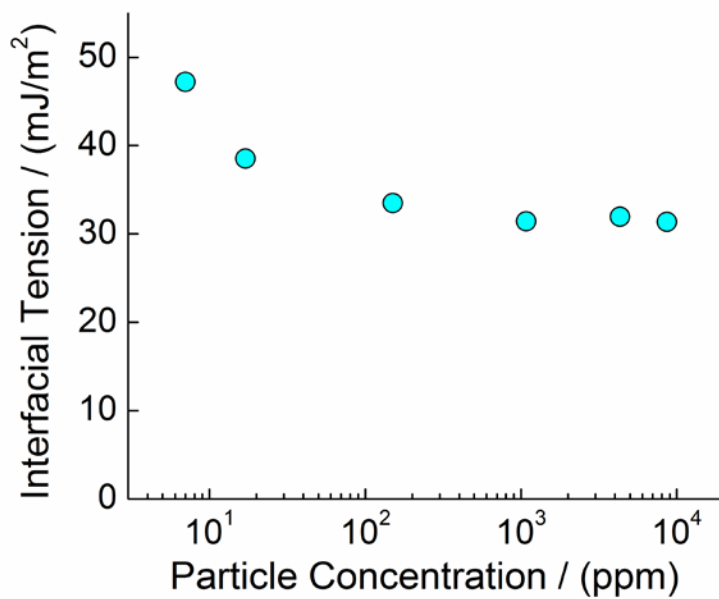


Figure 5.16. Equilibrium interfacial tension of water with hexane-based dispersions of Janus snowman particles (plateau values from Figure 5.15, represented as a function of particle concentration).

Given this *interfacial* activity,⁵⁰ one might expect that the lipophilic Janus snowman particles can stabilize w/o Pickering emulsions,⁶⁵⁻⁶⁶ as is indeed confirmed by emulsification experiments illustrated in (Figure 5.17). To prepare the colored w/o Pickering emulsion, we added 1 mL of DI water containing 0.01 wt. % Rhodamine B (Sigma Aldrich) and 2 mL of hexane containing 0.5 wt. % Janus snowman particles in a glass vial, and homogenized at 30000 rpm for 1 min using a homogenizer (IKA Ultra-Turrax® T10 basic).

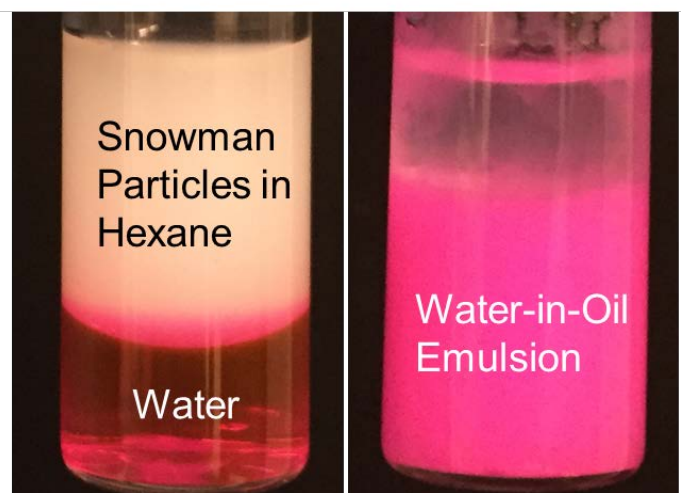


Figure 5.17. Formation of a water-in-oil (w/o) emulsion using oil-borne Janus snowman particles. Left: Water phase dyed with Rhodamine B (0.01 wt. %) and hexane based particle dispersion (white) prior to homogenization; Right: w/o emulsion with sedimented water droplets.

Interestingly, no pH dependence is found in performing the emulsification with these oil-borne Janus particles (Figure 5.18). This is in contrast to the emulsification performance of many particulate emulsifiers primarily dispersed in water, which can be affected strongly by the pH of the aqueous phase.^{20,22,57,67-69} The ubiquity of electric charges at particle-water interface⁶⁷⁻⁶⁸ and oil-water interface^{20,22,69} can cause water-borne particles to be repelled electrostatically from the interface unless the pH is adjusted appropriately. However, with the particles dispersed in the nonpolar phases, where low dielectric permittivity disfavors surface charging,⁷⁰⁻⁷¹ there is no pH-dependent electrostatic barrier to particle adsorption. The pH-insensitive emulsifier performance of the oil-dispersed snowman particles could be quite useful for applications in which pH-altering reactions are carried out inside the aqueous droplets.

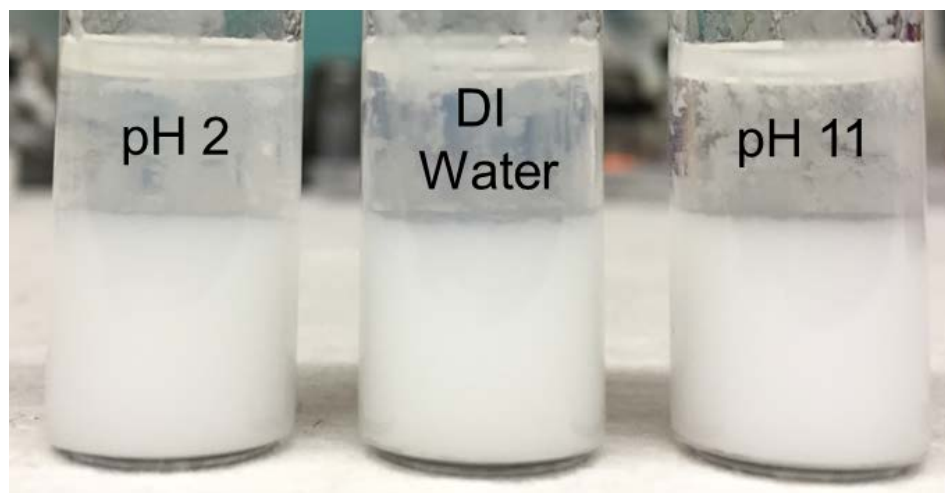


Figure 5.18. Stable emulsions produced at different pH with the Janus snowman particles.

5.4.5. Electric Charging of a Nonpolar Solvent Containing the Amphiphilic Particles

Throughout the previous sections, we confirmed that our snowman particles are sufficiently lipophilic to suspend stably in a nonpolar solvent and also somewhat hydrophilic reducing the energy cost of creating interfaces with the aqueous phase in nonaqueous phase, *i. e.* these particles, as amphiphiles, do the practically similar task as what lipophilic molecular surfactants do. The final question is whether these particles can also promote electric charging of the nonpolar solvent as we hypothesized.

We measured the electric conductivity of hexanes containing the snowman particles using the nonaqueous conductivity probe DT-700 (Dispersion Technology, Inc.), which we used for measuring the conductivity of surfactant solutions, and the result is shown in Figure 5.19.

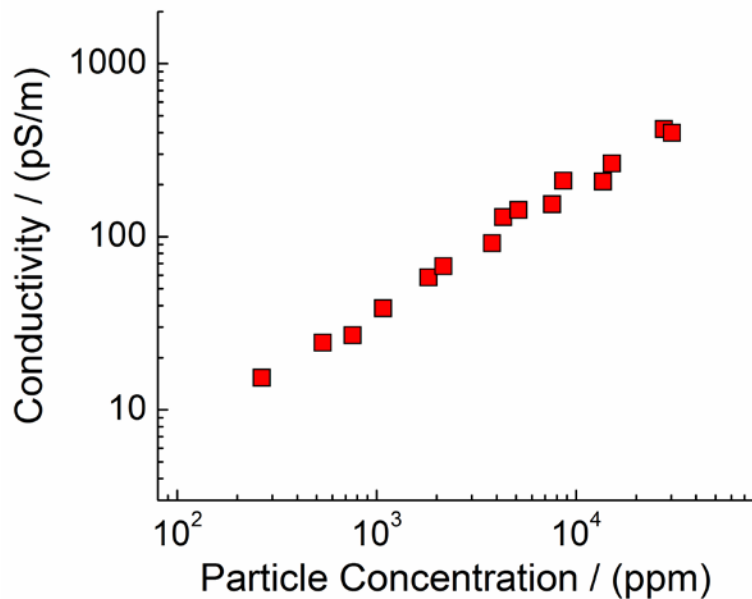


Figure 5.19. Electric conductivity of hexane involving Janus snowman particles, as a function of particle concentration (in pS/m).

In the investigated range of particle concentration, we clearly observed the increase in electric conductivity of the fluid, which is almost linearly dependent on the particle concentration. This linear concentration dependence of electric conductivity is distinguished from the typical square-root concentration dependence related to the dissociation of weak electrolyte ($AB \rightleftharpoons A^+ + B^-$),⁵⁹ *i. e.* the observed electric charging phenomena cannot simply be attributed to dissociation of some ionizable surface moieties.

We note that the linear concentration dependence of (small) electric conductivity is similar to what we observed for the surfactant solution saturated with moisture (Figure 5.5). A possible explanation for generation of electric conductivity is that the particles, with somewhat hydrophilicity, increased the moisture content in nonpolar phase by reducing the energy cost of such process (as revealed by the decrease in the interfacial tension of water with the nonpolar solvent containing the particles), which is equivalent to creating locally high dielectric environments where charges can reside with their ionization energy effectively reduced. This is essentially the same task as what the oil-borne molecular surfactants, as amphiphiles, do in the nonpolar continuous phase by forming inverse micelles with hydrophilic cores.

We measured the water content in hexanes containing the particles with volumetric Karl Fischer titration, using TitroLine KF titrator (SCHOTT), and the result is shown in Figure 5.20. As we expected, the total moisture content in the nonpolar phase increased systematically along with the addition of these amphiphilic particles.

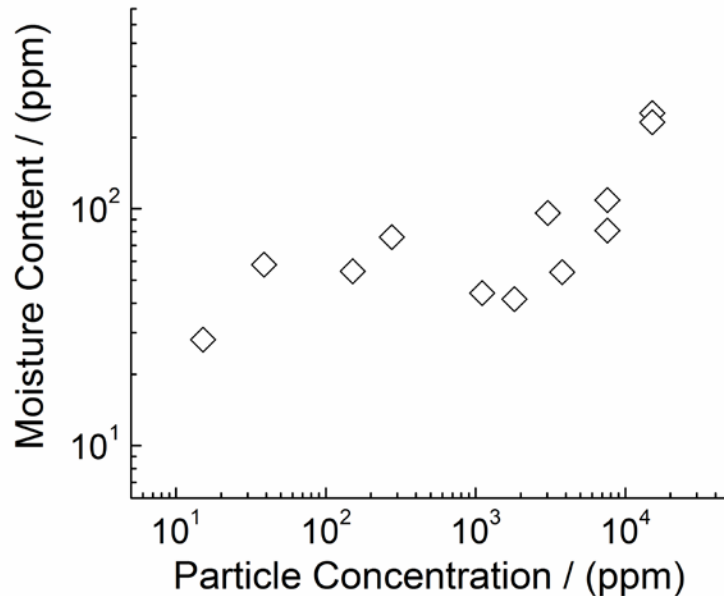


Figure 5.20. Moisture content in hexane involving Janus snowman particles, as a function of particle concentration (in ppm).

We also performed electrochemical impedance spectroscopy (EIS) for a dodecane-based dispersion of the same particles.¹² The sample was sandwiched between two electrodes of glass coated with 100 nm thick layer of indium tin oxide (ITO, Sigma-Aldrich), apart by a 250 μm polycarbonate spacer. A VersaSTAT 3 potentiostat (Princeton Applied Research), equipped with a Low Current Interface (LCI), powered the cell, a two electrode circuit, by short-circuiting the reference electrode terminal of the potentiostat to the terminal of the counter electrode.¹² The Nyquist plot of the measured real and imaginary impedance is shown in Figure 5.21 and the frequency response of the

real and imaginary part is shown in Figure 5.22 and 5.23. We note that the shape of spectra is qualitatively similar to those for nonpolar solutions of the commercial surfactant OLOA11000, where the measured electric current was attributed to the electrophoretic motion of charge carrier inverse micelles in the capacitor cell.¹² As the measured fluid resistance (R_f) within the capacitor, for the dodecane sample with the highest particle volume fraction (equivalent to 30303 ppm in mass for the hexane-based sample, shown in Figure 5.19), was converted into the electric conductivity (σ) by $\sigma = d / A_f R_f$ with d for the distance between two electrodes and A_f for the area of the two plates wet by the fluid, the calculated σ was 500 ± 30 pS/m, which is in the same order of magnitude with the measured σ using the conductivity probe DT 700.

Thus, the two electrical measurements in different geometries show the viability of electric conduction in nonpolar media in the presence of the solid particle amphiphiles, supporting our hypothesis. We expect some potential applications of this finding, in development of electrorheological fluids or lab-on-chip devices, with extensions of the synthesis procedure, *e. g.* labeling with fluorescent dyes.

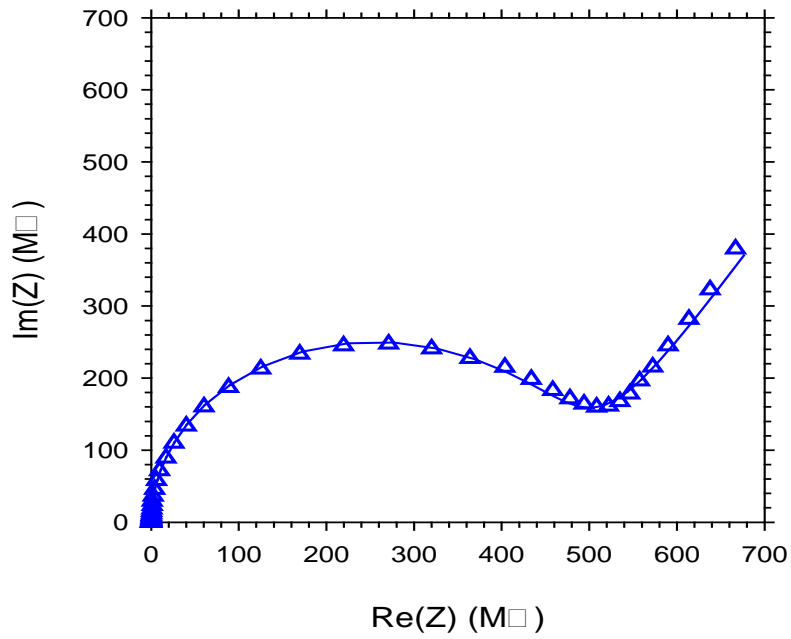


Figure 5.21. Nyquist plot of impedance data for the dodecane sample containing the Janus snowman particles. The data was taken at frequencies from 10^3 Hz to 10^{-2} Hz.

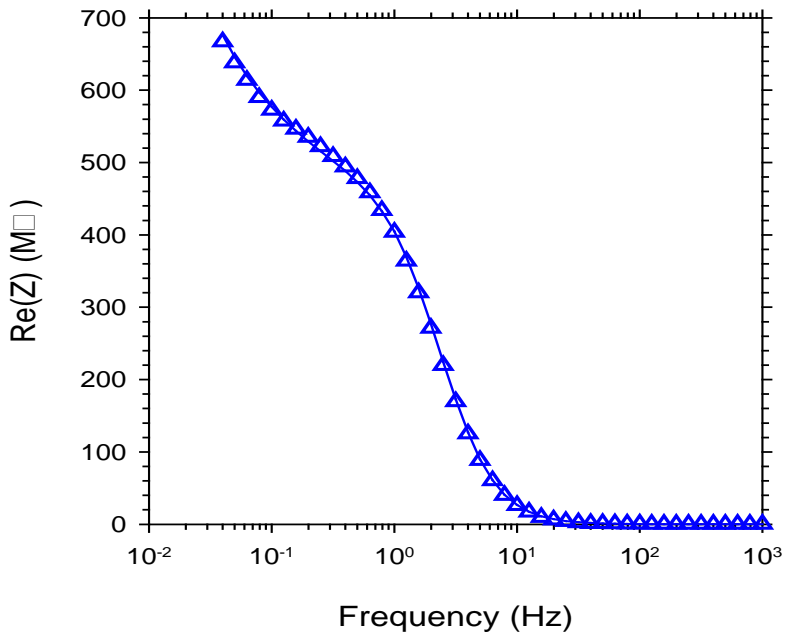


Figure 5.22. Semi-log Bode plot of the real impedance.

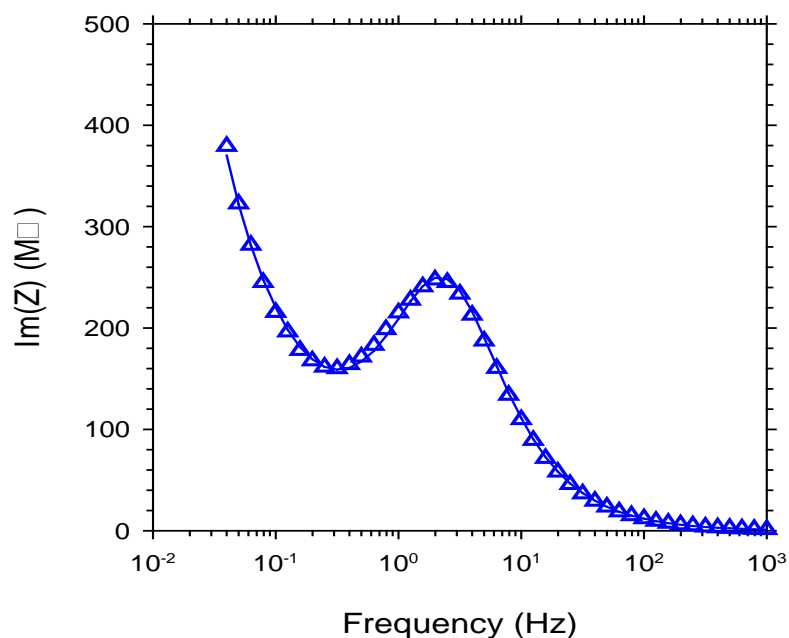


Figure 5.23. Semi-log Bode plot of the imaginary impedance.

5.5. References

1. Gunstone, F. D.; Padley, F. B. *Lipid Technologies and Applications*; Dekker; New York, 1997.
2. Rieger, M.; Rhein, L. D. *Surfactants in Cosmetics*, 2nd ed.; Dekker; New York, 1997.
3. McClements, D. J. *Food Emulsions: Principles, Practices, and Techniques*, 2nd ed.; CRC Press; Boca Raton, 2004.
4. Fegyver, E.; Meszaros, R. The Impact of Nonionic Surfactant Additives on the Nonequilibrium Association Between Oppositely Charged Polyelectrolytes and Ionic Surfactants. *Soft Matter* **2014**, *10*, 1953-1962.
5. Morrison, I. D. Electric Charges in Nonaqueous Media. *Colloids Surf., A* **1993**, *71*, 1-37.

6. Smith, G. N.; Eastoe, J. Controlling Colloid Charge in Nonpolar Liquids with Surfactants. *Phys. Chem. Chem. Phys.* **2013**, *15*, 424-439.
7. Kim, J.; Anderson, J. L.; Garoff, S.; Schlangen, L. J. M. Ionic Conduction and Electrode Polarization in a Doped Nonpolar Liquid. *Langmuir* **2005**, *21*, 8620-8629.
8. Dukhin, A. S.; Dukhin, S. S. How Non-Ionic “Electrically Neutral” Surfactants Enhance Electrical Conductivity and Ion Stability in Non-Polar Liquids. *Electrophoresis* **2005**, *26*, 2149-2153.
9. Roberts, G. S.; Sanchez, R.; Kemp, R.; Wood, T.; Barlett, P. Electrostatic Charging of Nonpolar Colloids by Reverse Micelles. *Langmuir* **2008**, *24*, 6530-6541.
10. Guo, Q.; Singh, V.; Behrens, S. H. Electric Charging in Nonpolar Liquids Because of Nonionizable Surfactants. *Langmuir* **2010**, *26*, 3203-3207.
11. Poovadorom, S.; Berg, J. C. Effect of Particle and Surfactant Acid-Base Properties on Charging of Colloids in Apolar Media. *J. Colloid Interface Sci.* **2010**, *346*, 370-377.
12. Yezer, B.; Khair, A. S.; Sides, P. J.; Prieve, D. C. Use of Electrochemical Impedance Spectroscopy to Determine Double-Layer Capacitance in Doped Nonpolar Liquids. *J. Colloid Interface Sci.* **2014**, *449*, 2-12.
13. Espinosa, C.E.; Guo, Q.; Singh, V.; Behrens, S. H. Particle Charging and Charge Screening in Nonpolar Dispersions with Nonionic Surfactants. *Langmuir* **2010**, *26*, 16941-16948.
14. Parent, M. E.; Yang, J.; Jeon, Y.; Toney, M. F.; Zhou, Z.-L.; Henze, D. Influence of Surfactant Structure on Reverse Micelle Size and Charge for Nonpolar Electrophoretic Inks. *Langmuir* **2011**, *27*, 11845-11851.
15. Guo, Q.; Lee, J.; Singh, V.; Behrens, S. H. Surfactant Mediated Charging of Polymer Particles in a Nonpolar Liquid. *J. Colloid Interface Sci.* **2013**, *392*, 83-89.
16. Lee, J.; Zhou, Z.-L.; Behrens, S. H. Mechanisms of Particle Charging by Surfactants in Nonpolar Dispersions. *Langmuir*, accepted. DOI: 10.1021/acs.langmuir.5b02875
17. Texter, J. *Reactions and Synthesis in Surfactant Systems*; CRC Press: New York, 2001.
18. Asadov, Z. H.; Tantawy, A. H.; Zarbaliyeva, I. A.; Rahimov, R. A.; Ahmadova, G. A. Surfactants Based on Palmitic Acid and Nitrogenous Bases for Removing Thin Oil Slicks from Water Surface. *Chem. J.* **2012**, *2*, 136-145.
19. Lee, J.; Zhou, Z.-L.; Behrens, S. H. Characterizing the Acid/Base Behavior of Oil-Soluble Surfactants at the Interface of Nonpolar Solvents with a Polar Phase. *J. Phys. Chem. B* **2015**, *119*, 6628-6637.

20. Marinova, K. G.; Alargova, R. G.; Denkov, N. D.; Velev, O. D.; Petsev, D. N.; Ivanov, I. B.; Borwankar, R. P. Charging of Oil-Water Interfaces Due to Spontaneous Adsorption of Hydroxyl Ions. *Langmuir* **1996**, *12*, 2045-2051.
21. Beattie, J. K.; Djerdjev, A. M. The Pristine Oil/Water Interface: Surfactant-Free Hydroxide-Charged Emulsions. *Angew. Chem. Int. Ed.* **2004**, *43*, 3568-3571.
22. Zangi, R.; Engberts, J. B. F. N. Physisorption of Hydroxide Ions from Aqueous Solution to a Hydrophobic Surface. *J. Am. Chem. Soc.* **2005**, *127*, 2272-2276.
23. Kudin, K. N.; Car, R. Why Are Water-Hydrophobic Interfaces Charged? *J. Am. Chem. Soc.* **2008**, *130*, 3915-3919.
24. Kemp, R.; Sanchez, R.; Mutch, K. J.; Bartlett, P. Nanoparticle Charge Control in Nonpolar Liquids: Insights from Small-Angle Neutron Scattering and Microelectrophoresis. *Langmuir* **2010**, *26*, 6967-6976.
25. Hsu, M. F.; Dufresne, E. R.; Weitz, D. Z. Charge Stabilization in Nonpolar Solvents. *Langmuir* **2005**, *21*, 4881-4887.
26. Eicke, H. F.; Borkovec, M.; Das-Gupta, B. J. Conductivity of Water-In-Oil Microemulsions: A Quantitative Charge Fluctuation Model. *J. Phys. Chem.* **1989**, *93*, 314-317.
27. Hall, D. G. Conductivity of Microemulsions: An Improved Charge Fluctuation Model. *J. Phys. Chem.* **1990**, *94*, 429-430.
28. Kallay, N.; Chittofrati, A. Conductivity of Microemulsions: Refinement of Charge Fluctuation Model. *J. Phys. Chem.* **1990**, *94*, 4755-4756.
29. Kallay, N.; Tomic, M.; Chittofrati, A. Conductivity of Water-In-Oil Microemulsions: Comparison of the Boltzmann Statistics and the Charge Fluctuation Model. *A. Colloid Polym. Sci.* **1992**, *270*, 194-196.
30. van Oss, C. J.; Chaudhury, M. K.; Good, R. J.; Interfacial Lifshitz-van der Waals and Polar Interactions in Macroscopic Systems, *Chem. Rev.* **1988**, *88*, 927-941.
31. Labib, M. The Origin of the Surface Charge on Particles Suspended in Organic Liquids. *Colloids. Surf.* **1988**, *29*, 293-304.
32. Fowkes, F. M.; Pugh, R. J. Steric and Electrostatic Contributions to the Colloidal Properties of Nonaqueous Dispersions. *ACS Symposium Series* **1984**, *240*, 331-354.
33. Halperin, A.; Alexander, S. Polymeric Micelles: Their Relaxation Kinetics. *Macromolecules* **1989**, *22*, 2403-2412.

34. Lund, R.; Willner, L.; Stellbrink, J.; Lindner, P. Richter, D. Logarithmic Chain-Exchange Kinetics of Diblock Copolymer Micelles. *Phys. Rev. Lett.* **2006**, *96*, 068302.
35. Choi, S.-H.; Lodge, T. P.; Bates, F. S. Mechanism of Molecular Exchange in Diblock Copolymer Micelles: Hypersensitivity to Core Chain Length. *Phys. Rev. Lett.* **2010**, *104*, 047802.
36. Robinson, B. H.; Toprakcioglu, C.; Dore, J. C. Small-Angle Neutron-Scattering Study of Microemulsions Stabilised by Aerosol-OT. *J. Chem. Soc., Faraday Trans.* **1984**, *80*, 13-27.
37. Dukhin, A.; Parlia, S. Ions, Ion Pairs and Inverse Micelles in Non-Polar Media. *Curr. Opin. Colloid Interface Sci.* **2013**, *18*, 93-115.
38. Gacek, M. M.; Berg, J. C. Investigation of Surfactant Mediated Acid-Base Charging of Mineral Oxide Particles Dispersed in Apolar Systems. *Langmuir* **2012**, *28*, 17841-17845.
39. van Oss, C. J.; Giese, R. F.; Wu, W. On the Predominant Electron-Donicity of Polar Solid Surfaces. *J. Adhesion* **1997**, *63*, 71-88.
40. Pizzi, A.; Mittal, K. L. *Handbook of Adhesive Technology*; CRC Press; New York, 2003.
41. Kitahara, A.; Satoh, T.; Kawasaki, S.; Kon-No, K. Specific Adsorption of Surfactants Containing Mn or Co on Polymer Particles Revealed by Zeta-Potential in Cyclohexane. *J. Colloid Interface Sci.* **1982**, *86*, 105-110.
42. Smith, P. G.; Patel, M. N.; Kim, J.; Milner, T. E.; Johnston, K. P. Effect of Surface Hydrophilicity on Charging Mechanism of Colloids in Low-Permittivity Solvents. *J. Phys. Chem. C* **2007**, *111*, 840-848.
43. Kemp, R.; Sanchez, R.; Mutch, K. J.; Bartlett, P. Nanoparticle Charge Control in Nonpolar Liquids: Insights from Small-Angle Neutron Scattering and Microelectrophoresis. *Langmuir* **2010**, *26*, 6967-6976.
44. Smith, G. N.; Alexander, S.; Brown, P.; Gillespie, D. A. J.; Grillo, I.; Heenan, R. K.; James, C.; Kemp, R.; Rogers, S. E.; Eastoe, J. Interaction between Surfactants and Colloidal Latexes in Nonpolar Solvents Studied Using Contrast-Variation Small-Angle Neutron Scattering. *Langmuir* **2014**, *30*, 3422-3431.
45. Smith, G. N.; Grillo, I.; Rogers, S. E.; Eastoe, J. Surfactants with Colloids: Adsorption or Absorption? *J. Colloid Interface Sci.* **2015**, *449*, 205-214.
46. Della Volpe, C.; Siboni, S. Acid-Base Surface Free Energies of Solids and the Definition of Scales in the Good-van Oss-Chaudhury Theory. *J. Adhesion Sci. Technol.* **2000**, *14*, 235-272.

47. de Gennes, P. G. *Soft Matter. Rev. Mod. Phys.* **1992**, *64*, 645-648.
48. Jiang, S.; Granick, S.; Schneider, H. J. *Janus particle synthesis, self-assembly and applications*; Royal Society of Chemistry; London, 2012.
49. Walther, A.; Müller, A. H. E. Janus Particles: Synthesis, Self-Assembly, Physical Properties, and Applications. *Chem. Rev.* **2013**, *113*, 5194-5261.
50. Kumar, A.; Park, B.J.; Tu, F.; Lee, D. Amphiphilic Janus Particles at Fluid Interfaces. *Soft Matter* **2013**, *9*, 6604-6617.
51. Roh, K.-H.; Martin, D. C.; Lahann, J. Biphase Janus Particles with Nanoscale Anisotropy. *Nat. Mater.* **2005**, *4*, 759-763.
52. Suzuki, D.; Tsuji, S.; Kawaguchi, H. Janus Microgels Prepared by Surfactant-Free Pickering Emulsion-Based Modification and Their Self-Assembly. *J. Am. Chem. Soc.* **2007**, *129*, 8088-8089.
53. Mock, E. B.; Bruyn, H. D.; Hawke, B. S.; Gilbert, R. G.; Zukoski, C. F. Synthesis of Anisotropic Nanoparticles by Seeded Emulsion Polymerization. *Langmuir*, **2006**, *22*, 4037-4043.
54. Kim, J.-W.; Larsen, R. J.; Weitz, D. A. Synthesis of Nonspherical Colloidal Particles with Anisotropic Properties. *J. Am. Chem. Soc.* **2006**, *128*, 14374-14377.
55. Kim, J.-W.; Lee, D.; Shum, H. C.; Weitz, D. A. Colloid Surfactants for Emulsion Stabilization. *Adv. Mater.* **2008**, *20*, 3239-3243.
56. Park, J.-G.; Forster, J. D.; Dufresne, E. R. High-Yield Synthesis of Monodisperse Dumbbell-Shaped Polymer Nanoparticles. *J. Am. Chem. Soc.* **2010**, *132*, 5960-5961.
57. Tu, F.; Lee, D. Shape-Changing and Amphiphilicity-Reversing Janus Particles with pH-Responsive Surfactant Properties. *J. Am. Chem. Soc.* **2014**, *136*, 9999-10006.
58. Tsonchev, S.; Schatz, G. C.; Ratner, M. A. Hydrophobically-Driven Self-Assembly: A Geometric Packing Analysis. *Nano Lett.* **2003**, *3*, 623-626.
59. Israelachvili, J. N. *Intermolecular and Surface Forces*, 3rd ed.; Academic Press; Oxford, 2011.
60. Griffin, W. C. Classification of Surface-Active Agents by "HLB" *J. Soc. Cosmet. Chem.* **1949**, *1*, 311-326.
61. Eastoe, J.; Nave, S.; Downer, A.; Paul, A.; Rankin, A.; Tribe, K. Adsorption of Ionic Surfactants at the Air-Solution Interface. *Langmuir* **2000**, *16*, 4511-4518.

62. Won, Y.-Y.; Meeker, S. P.; Trappe, V.; Weitz, D. Effect of Temperature on Carbon-Black Agglomeration in Hydrocarbon Liquid with Adsorbed Dispersant. *Langmuir* **2005**, *21*, 924-932.
63. Berne, B. J.; Pecora, R. *Dynamic light scattering*; John-Wiley & Sons; New York, 1976.
64. Schatzel, K. Suppression of Multiple Scattering by Photon Cross-Correlation Techniques. *J. Mod. Opt.* **1991**, *38*, 184-1865.
65. Pickering, S. U. Emulsions. *J. Chem. Soc.* **1907**, *91*, 2001-2021.
66. Aveyard, R.; Binks, B. P.; Clint, J. H. Emulsions Stabilised Solely by Colloidal Particles. *Adv. In Colloid Interface Sci.* **2003**, *100*, 503-546.
67. Tcholakova, S.; Denkov, N. D.; Lips, A. Comparison of Solid Particles, Globular Proteins and Surfactants as Emulsifiers. *Phys. Chem. Chem. Phys.* **2008**, *10*, 1608-1627.
68. Wang, H.; Singh, V.; Behrens, S. H. Image Charge Effects on the Formation of Pickering Emulsions. *J. Phys. Chem. Lett.* **2012**, *3*, 2986-2990.
69. Vacha, R.; Rick, S. W.; Jungwirth, P.; de Beer, A. G. F.; de Aguiar, H. B.; Samson, J.-S.; Roke, S. The Orientation and Charge of Water at the Hydrophobic Oil Droplet-Water Interface. *J. Am. Chem. Soc.* **2011**, *133*, 10204-10210.
70. Van der Hoeven, P. C.; Lyklema, J. Electrostatic Stabilization in Non-Aqueous Media. *Adv. Colloid Interface Sci.* **1992**, *42*, 205-277.
71. Berry, R. S.; Rice, S. A.; Ross, J. *Physical chemistry*, 2nd ed.; Oxford University Press; Oxford, 2000.

CHAPTER 6

CONCLUDING REMARKS

In this thesis, we introduced our novel approaches to achieve a better understanding on surfactant-mediated particle charging mechanisms in nonpolar dispersions, and represented several important mechanistic insights obtained by implementing such approaches. Also, we introduced a new type of solid particle charging agent amphiphile, developed based on the knowledge we gained from our mechanistic investigation with the molecular charging agent surfactants.

In Chapter 2, we pointed out that there has been no established way to characterize the acid/base (donor/acceptor) strength of oil-borne surfactants, even though such properties have often been hypothesized as important parameters determining the particles' surface charging behavior. Therefore, no validation of the traditional hypothesis on particle charging mechanisms (via acid-base interactions of the surfactants with particles) has been allowed, either. Here, we proposed a simple method of characterizing the Lewis acid/base behavior of oil-soluble nonionic surfactants at the interface of nonpolar solvents with a polar phase, by combining the tensiometric experiments and surface thermodynamic theory. This method allowed for characterizing the acid/base behavior of surfactants formally in the same unit ($[=] \text{ mJ/m}^2$) as the other condensed matters including polar solids and liquids, which was useful for estimating the propensity of charge transfer via acid-base interactions of surfactants with the other polar condensed surfaces.

In Chapter 3, we attempted to address the chronic ambiguities of the past studies on particle charging mechanisms, where only few widely dissimilar surfactant types were focused, by investigating surface charging behavior (of a model colloid particle) mediated by a series of well-purified custom surfactants under “minimal” structural variations. We synthesized and purified the three PIBS surfactants differing chemically in only one single electronegative atom of their polar head moieties, and used these surfactants to cause and investigate surface charging of PMMA colloids in hexanes. In an attempt to interpret the observed surface charging in the framework of acid-base interactions associated with the surfactants, using the surfactant solutions’ acid/base parameters characterized with the method introduced in Chapter 2, we found that some surface charging behavior should be attributed to asymmetric adsorption of “micellar ions”, which are created by the acid-base interaction of surfactants with the third polar species “moisture”, rather than the direct charge transfer acid-base interaction of surfactants with the surface. By showing the acid-base interaction of the surfactants with moisture is energetically more beneficial than that with the solid surface, and showing that the total surface area of nanoscale (intra-micellar) aqueous phase essentially surpassed the surface area of microscale colloids, we stressed that the micellar ions originated from the water-surfactant acid-base interaction are likely to influence net surface charging as ionic “acid” and “base” components. Besides the “chemical” preference of the solid for a certain sign of micellar ions in terms of ion-dipole interaction, we suggested that “entropic” preference could cause some asymmetric adsorption state of the oppositely charged micellar ions where the adsorption of larger micelle anions dominated the smaller micelle cations. This size asymmetry between micelle cations and anions was demonstrated in terms of the intra-micellar charge transfer acid-base interaction and inter-micellar exchange of the charged surfactants molecules, and was corroborated by implementing electrophoretic light scattering on particle-free surfactant solutions.

In Chapter 4, we chose a series of colloidal particles with their surface properties under systematic variations, {PMMA-sulfate, PS-sulfate, PS-carboxyl, PS-amidine}, and observed their surface charging mediated by one of our custom surfactants (PIBS-N) and a commercial surfactant product (OLOA11000). The surface polarity of these particles was “defined” by measuring their aqueous charging behavior, which was likely to reflect the acid/base chemistry of specific “functional groups”, and by measuring the vOCG acidity/basicity parameters likely reflecting the polarity of dry “particle bulk”. We experimentally proved that net surface charging of the particles was not universally determined by a simple acid-base balance between particle surface (by any definition) and surfactants as the traditionally suggested acid-base particle charging mechanism would predict. For “dry” systems containing our custom surfactant, the relative surface charging of the particles was correlated with the nucleophilicity of particle bulk, irrelevant to the acid/base character of specific functional groups shown in the aqueous (wet) environments. This might reflect the role of polar interaction of “particle bulk” with electrically neutral surfactants (with subsequent charge transfer) or charged micelle ions, as a surface charging pathway in nonpolar media. For “wet” systems containing the commercial surfactant product, where the moisture content was measured to be significantly larger than the system containing the commercial surfactant, we found “some” evidence for ionization of surface functional groups, as “a contribution” to net surface charging. Comparing the two systems reveals that the surface polarity can be “adaptive” to system components (such as the moisture content), and therefore, it is unlikely that every surface charging phenomenon is universally predicted by a simple polar interaction of the surfactant with either particle bulk or surface functional groups. Also, the contribution of micellar ions’ asymmetric adsorption to the surface further complicates the resulted net surface charging properties. The fact that all these monopolar basic particles (including the one functionalized with amidine group) were “negatively” charged strongly indicated that the contribution of entropic adsorption of micelle anions,

originated from water-surfactant acid-base interaction, would also be significant in determining the net surface charging behavior. Thus, it seems more reasonable to view the surfactant-mediated surface charging phenomena as a consequence of interplays between multiple charging pathways, rather than a reaction product regulated by simple acid/base balances between the particle and surfactant moieties.

In Chapter 5, some atypical concepts of the proposed mechanistic schemes were reviewed and further supported by additional experimental results. In the first subsection of this Chapter, the “ionizability” of water-insoluble, “nonionic” surfactant PIBS-C was experimentally proven by measuring the electrophoretic mobility of oil droplets stabilized by this surfactant in aqueous phase. In the second subsection, we verified the existence of micelle ions’ asymmetric adsorption which is not driven by the entropic reason, by investigating the charging behavior of amphoteric silica surfaces in the presence of the dry surfactant PIBS-C. The result suggested that the dry particle bulk may have a significant surface nucleophilicity as proposed by the classical Lewis acid/base theory, which has been debated for a long while. In the final subsection, we developed a solid particle amphiphile that was sufficiently lipophilic to suspend itself in nonpolar phase and also somewhat hydrophilic increasing the moisture content therein. We found that this particle, by suspending locally high dielectric environments (moisture as a polar pool), promoted the electric conduction of nonpolar phase. This finding indeed supports back our initial hypothesis on the importance of moisture in electric conduction of nonpolar liquids.

We expect our findings on the underlying mechanisms of the particle charging phenomena will be an important fundamental guideline based on which a smarter strategy can be made in practical formulation of a further complicated system. By knowing that the physicochemical properties of micellar ions, created by the polar interaction of the third species with surfactants, could influence the particle charging behavior, an operator

would choose their co-solutes (for specific functions, usually in order to increase the dispersion stability) more carefully and investigate the ionization behavior associated with such co-solutes independently to appreciate their possible influence on particle charging. Also, by knowing that a net surface charging is a consequence of interplays between multiple charging pathways, the operator may want to engineer the polarity of particle surfaces more deliberately in terms of dry particle bulk and specific functional groups, and find the surfactant type which suitably controls the wetness of the system to activate either type of particle polarity.

For interpretation of more complicated systems, we recommend our general strategy to solve the problems by defining the physicochemical properties of the relevant system parameters (in a more quantitative way with some compatibility between the interacting species, if possible) and precisely controlling/varying such parameters by a subtle increment. For further elucidation of the complicated mechanisms, we recommend implementing experimental investigations accompanying, too, computational chemistry-based approaches, to capture the detailed molecular-level pictures behind the apparent charging phenomena.